Mercury TMDL Development for the Willamette River Basin (Oregon) – Technical Support Document

December 16, 2019

PREPARED FOR

Oregon Department of Environmental Quality
and
U.S. Environmental Protection Agency, Region 10

PREPARED BY

Tetra Tech
One Park Drive, Suite 200
PO Box 14409
Research Triangle Park, NC 27709
Tel 919-485-8278
Fax 919-485-8280
tetratech.com

The primary authors of this report are: Jonathan Butcher, Michelle Schmidt, and Mark Fernandez, Tetra Tech, Inc., Research Triangle, NC

CONTENTS

TABLES

FIGURES

(This page left intentionally blank.)

Acronyms and Abbreviations

ac	acre
ANOVA	analysis of variance
BCE	Before Common Era
BLU	bluegill (*Lepomis macrochirus*)
BMF	biomagnification factor
BMP	best management practice
C	carbon
CAR	common carp (*Cyprinus carpio*)
CDL	Cropland Data Layer
CE	Common Era
CF	unit conversion factor
CL	confidence limit
CMAQ	Community Multiscale Air Quality model
CSO	combined sewer overflow
csv	comma-separated variable format file
CTT	cutthroat trout (*Oncorhynchus clarki*)
CWA	Clean Water Act
DEQ	Department of Environmental Quality
df	degrees of freedom
dHg[II]	dissolved ionic mercury
dMeHg	dissolved methylmercury
DMA	Designated Management Agencies
DMR	Discharge Monitoring Report
DOM	dissolved organic matter
dTHg	dissolved total mercury
ECDMS	Environmental Contaminants Database Management System (U.S. Fish and Wildlife Service)
ECSI	Oregon DEQ Environmental Cleanup Site Information
EIA	effective impervious area
EMAP	Environmental Monitoring and Assessment Program (U.S. EPA)
EMMMA	Environmental Mercury Mapping, Modeling, and Analysis (USGS)

EVT	USFS LANDFIRE existing vegetation layer
FTable	HSPF “functional table” for representing stage-storage-discharge relationships
FWM	Food Web Model
g	gram
GPM	gallons per minute
Hg	mercury
Hg[0]	non-ionic elemental mercury
Hg[II]	ionic inorganic mercury
HgS	mercuric sulfide (cinnabar)
HRU	hydrologic response unit
HSG	hydrologic soil group
HSPF	Hydrologic Simulation Program – FORTRAN
HUC	Hydrologic Unit Code (USGS)
HUC8	8-digit Hydrologic Unit Code
Kw	Kruskal-Wallis statistic
kg	kilogram
LA	load Allocation for nonpoint source
lb	pound
LMB	largemouth bass (*Micropterus salmoides*)
LSS	largescale sucker (*Catostomus macrocheilus*)
MDL	method detection limit
MeHg	methyl mercury (particulate and dissolved)
mg/L	milligrams per liter
MLE	maximum likelihood estimator
MS4	Municipal Separate Storm Sewer System
ng/L	nanograms per liter
NLCD	National Land Cover Database
NPDES	National Pollutant Discharge Elimination System
NPM	northern pikeminnow (*Ptychocheilus oregonensis*)
NRCS	Natural Resources Conservation Service
OAR	Oregon Administrative Rules
ODEQ	Oregon Department of Environmental Quality
ODOT	Oregon Department of Transportation

OLS	ordinary least squares regression
P-value	probability value
PGE	Portland General Electric
POTW	publicly owned treatment works
PQL	practical quantitation limit
QAPP	Quality Assurance Project Plan
QA/QC	Quality Assurance/Quality Control
R^2	squared correlation coefficient (fraction of variance explained)
RBT	rainbow trout (*Oncorhynchus mykiss*)
RM	river mile
ROS	regression on order statistics
SD	standard deviation
SE	standard error
SIC	Standard Industrial Classification
SMB	smallmouth bass (*Micropterus dolomieui*)
SO_4	sulfate
TC	fish tissue criterion target concentration
THg	total mercury (particulate and dissolved, all forms)
TL	trophic level
TL_n	target level for species n.
TMDL	Total Maximum Daily Load
tMeHg	total methyl mercury
TRI	Toxics Release Inventory
UGB	urban growth boundary
USEPA	U.S. Environmental Protection Agency
USFS	U.S. Forest Service
USGS	U.S. Geological Survey
WLA	Wasteload Allocation for permitted point source
WLS	weighted least squares regression
WRB	Willamette River Basin
µg	microgram
Ω	Mercury Translator relationship (“omega”)

(This page left intentionally blank.)

1.0 INTRODUCTION

This report describes the development of technical analyses in support of Mercury TMDL development for the Willamette River Basin (WRB) in Oregon. The work was performed under contract to Tetra Tech from U.S. Environmental Protection Agency (USEPA), Region 10. All work was conducted in accordance with an approved Quality Assurance Project Plan (Tetra Tech, 2017).

The Oregon Department of Environmental Quality (ODEQ) developed the Willamette Mercury TMDL in 2006 (ODEQ, 2006). That TMDL must now be revised to reflect Oregon's new fish tissue criterion for mercury and to incorporate additional data collected since 2006. The introductory statements in ODEQ (2006) regarding mercury pollution in the WRB remain fully relevant today:

> *Mercury is a naturally occurring element found in cinnabar deposits and areas of geothermal activity. In Oregon, mercury was mined commercially and used extensively in gold and silver amalgamation (Brooks, 1971; Park and Curtis, 1997). Mercury has been used historically in fungicide formulations and can still be found in many commercial products including fluorescent lights, thermometers, automobile switches and dental amalgam. Mercury is also naturally present in trees and fossil fuels such as coal, natural gas, diesel fuel and heating oil. The mercury present in these fuel sources is released into the atmosphere upon combustion. This atmospheric mercury can be transported great distances…*
>
> *Mercury can be present in various physical and chemical forms in the environment (Ullrich et al., 2001; USEPA, 2001b). The majority of the mercury found in the environment is in the form of inorganic or elemental mercury but these forms of mercury can be converted to organic or methylmercury by sulfate-reducing bacteria. Methylmercury production is affected by a host of physical and chemical factors including temperature, redox potential, dissolved oxygen levels, organic carbon, sediment particle size, alkalinity, sulfate concentration and pH. Methylmercury, once formed, represents the most bioaccumulative form of mercury in fish tissue and the most toxic form of mercury for human consumers (USEPA, 2001a). Methylmercury is a potent neurotoxin that has the potential to cause permanent damage to the brain, kidney, and developing fetus (ATSDR, 1999). Effects on brain functioning may cause irritability, shyness, tremors, changes in vision or hearing and memory problems. Children are known to be more sensitive than adults to mercury intoxication…*
>
> *The primary route of human exposure to mercury is via the consumption of fish or seafood containing elevated levels of mercury (USEPA, 2001a).*

1.1 PROBLEM DEFINITION

The WRB consists of 12 HUC8 watersheds, entirely within the state of Oregon (Figure 1-1). Starting in 1998, ODEQ began identifying various waterbodies in the WRB as impaired by elevated levels of mercury in fish tissue. This earlier work culminated in the development of a Total Maximum Daily Load (TMDL) for mercury in the WRB (ODEQ, 2006). A TMDL is a means for recommending controls needed to restore and maintain the quality of water resources (USEPA, 1991). TMDLs represent the total pollutant loading that a waterbody can receive without violating water quality standards.

Figure 1-1. Willamette River Basin

The 2006 TMDL target was based on ODEQ's fish tissue consumption criterion for protection of human health, which at the time was 0.35 mg/kg (wet weight) methylmercury (MeHg). (The 2006 TMDL used a target of 0.30 mg/kg (wet weight) to provide an additional margin of safety.) The criterion was subsequently revised (first proposed in 2004 but not approved by USEPA until 2011) to 0.040 mg/kg (wet weight) MeHg (Oregon Administrative Rules [OAR] 340-041-8033, Table 40). Oregon has also promulgated water column criteria for the protection of aquatic life of 2.4 µg/L (acute) and 0.012 µg/L (chronic) total mercury (THg) (OAR 340-041-8033, Table 30). The chronic water column criterion is equivalent to 12 ng/L.

Table 1-1 shows the water quality assessments relative to mercury for the WRB from Oregon's 2012 Integrated Report (http://www.deq.state.or.us/wq/assessment/rpt2012/results.asp), the latest Integrated Report that has been approved by USEPA. Those waters currently assessed as requiring a TMDL (Category 5) are shown in Figure 1-2. Waters for which mercury impairments were addressed by the 2006 TMDL are indicated in the last column of Table 1-1. Several segments that were listed in Category 5 in the WRB after the completion of the 2006 TMDL are also addressed in this revised TMDL.

Table 1-1. Waterbody Segments Assessed for Mercury in the Willamette River Basin in 2012

Record ID	Segment ID	Name	Miles	HUC 8	Assessed	Affected Use	Category	2006 TMDL
21153	37	Amazon Diversion Canal (A3 Drain)	0 to 3.9	17090003	2010	Fishing	5	X
25050	1387	Beaver Creek	0 to 8.3	17080001	2012	Aquatic life	2	
25057	1395	Kelly Creek	0 to 4.8	17080001	2012	Aquatic life	2	
25085	1426	Fairview Creek	0 to 1.7	17090012	2012	Aquatic life	2	
25150	1515	Johnson Creek	0 to 23.7	17090012	2012	Aquatic life	2	
25202	1593	Fanno Creek	0 to 13.9	17090010	2012	Aquatic life	3	
7717	1640	Zollner Creek	0 to 7.8	17090009	1998	Drinking water; Resident fish and aquatic life; Anadromous fish passage	2	
25304	1699	Beaverton Creek	0 to 9.8	17090010	2012	Aquatic life	2	
26019	1744	Yamhill River	0 to 11.2	17090008	2012	Human health	5	
17028	1774	Coast Fork Willamette River	0 to 31.3	17090002	2012	Aquatic life	3	X
6773	1775	Coast Fork Willamette/ Cottage Grove Reservoir	28.5 to 31.3	17090002	2012	Resident fish and aquatic life; Anadromous fish passage; Drinking water	5	X
17061	1782	Mill Creek	0 to 25.7	17090007	2004	Aquatic life; Human health	3	
6774	1786	Row River/ Dorena Lake	7.3 to 11.9	17090002	2012	Drinking water; Resident fish and aquatic life; Anadromous fish passage	5	X

Record ID	Segment ID	Name	Miles	HUC 8	Assessed	Affected Use	Category	2006 TMDL
17099	1789	Pringle Creek	0 to 6.2	17090007	2004	Aquatic life; Human health	3	
17280	1839	Oak Creek	0 to 21.6	17090003	2004	Aquatic life; Human health	3	
17289	1843	Santiam River	0 to 12	17090005	2004	Aquatic life; Human health	3	
6796	1844	South Yamhill River	0 to 18.1	17090008	1998	Resident fish and aquatic life; Anadromous fish passage; Drinking water	3B	
7716	1890	Muddy Creek	0 to 56.1	17090003	1998	Resident fish and aquatic life; Anadromous fish passage; Drinking water	2	
7719	2651	Middle Fourth Lake		17090003	1998	Drinking water; Resident fish and aquatic life; Anadromous fish passage	3B	
25111	9073	Kelly Creek	0 to 3.6	17090012	2012	Aquatic life	2	
25137	9125	Clackamas River	0 to 83.2	17090011	2012	Human health	5	
25155	9181	Tualatin River	0 to 80.7	17090010	2012	Human health	5	
16507	9340	Laying Creek	0 to 14.4	17090002	2004	Aquatic life; Human health	3	
16513	9345	Brice Creek	0 to 15.5	17090002	2004	Aquatic life; Human health	3	
25228	9383	Multnomah Channel	0 to 21.7	17090012	2012	Human health	5	
16981	9624	Middle Fork Willamette River	0 to 82.2	17090001	2012	Aquatic life	3	
25384	9624	Middle Fork Willamette River	0 to 82.2	17090001	2012	Human health	5	
25386	9644	Coast Fork Willamette River	0 to 38.8	17090002	2012	Human health	5	X
17074	9669	Row River	0 to 20.8	17090002	2012	Aquatic life	2	
25408	9712	McKenzie River	0 to 84.8	17090004	2012	Human health	5	
17174	9721	Dennis Creek	0 to 1.4	17090002	2012	Aquatic life; Human health	5	X
25417	9732	East Fork Dairy Creek	0 to 21.5	17090010	2012	Aquatic life	2	
17252	9780	Calapooia River	0 to 78	17090003	2004	Aquatic life; Human health	3	
25470	11894	Santiam River	0 to 26.2	17090005	2012	Human health	5	
16463	12101	Willamette River	0 to 186.6	17090003 17090007 17090012	2004	Aquatic life; Human health	3	

Record ID	Segment ID	Name	Miles	HUC 8	Assessed	Affected Use	Category	2006 TMDL
25195	12101	Willamette River	0 to 186.6	17090003 17090007 17090012	2012	Human health	5	X
17029	12114	Coast Fork Willamette River	31.3 to 38.8	17090002	2012	Aquatic life; Human health	5	X
21152	12141	Amazon Creek Diversion Canal	0 to 6.6	17090003	2010	Fishing	5	X
25102	31157	Osburn Creek	0 to 5.8	17090012	2012	Aquatic life	2	
25696	31748	Lookout Creek	0 to 9.7	17090004	2012	Aquatic life	2	
25830	31806	North Santiam River	0 to 90	17090005	2012	Aquatic life	3	

Notes: Information from 2012 Integrated Report. Categories are 2: Attaining some criteria/uses; 3: Insufficient data; 3B: Insufficient data, potential concern; 5: Water quality limited, 303(d) list; TMDL needed.

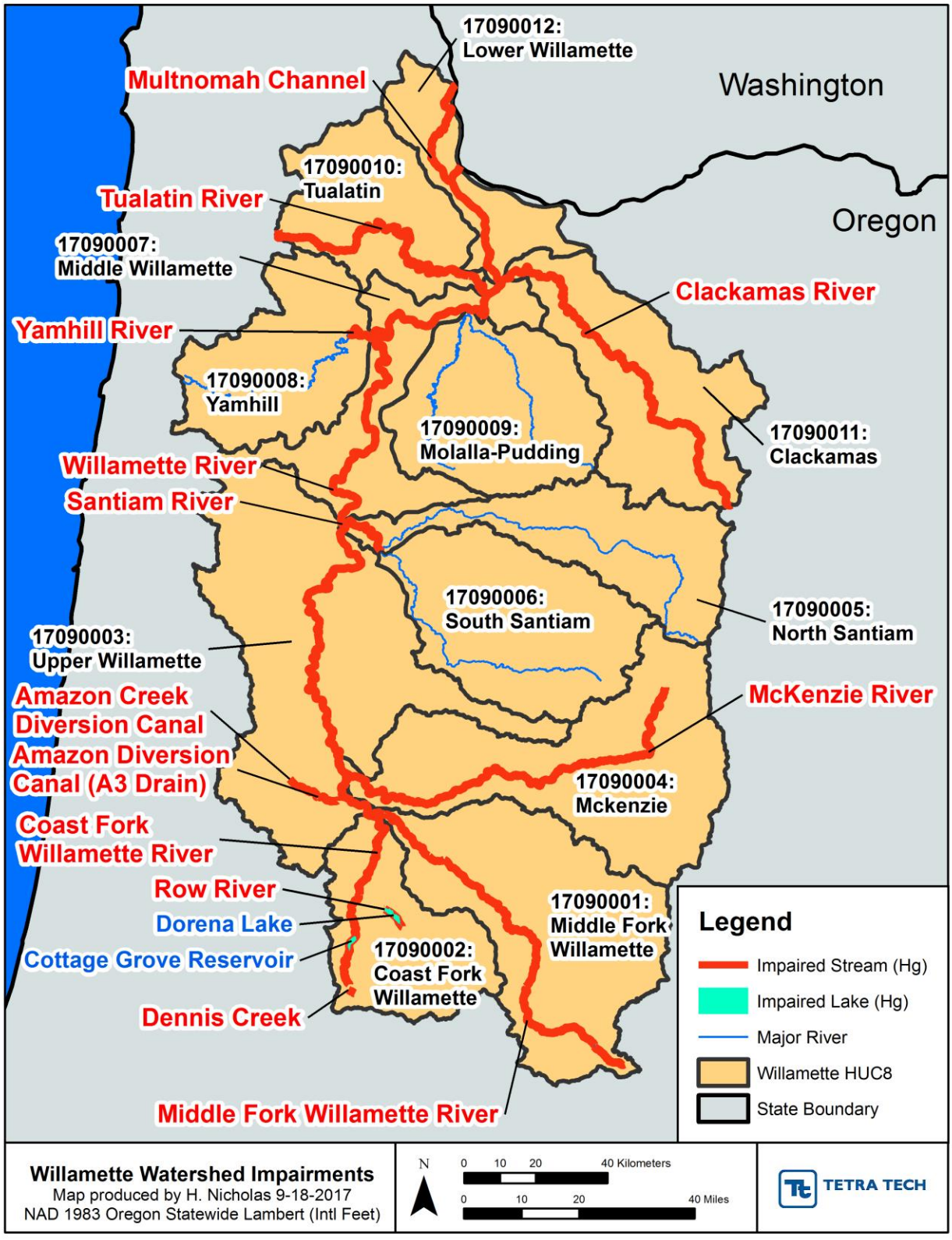

Figure 1-2. Mercury Impairments in the Willamette River Basin

The 2006 TMDL presents an interim solution and at several points suggests the need for additional data collection and refinements of the analytical approach. U.S. District Court proceedings regarding the 2006 TMDL brought by *Northwest Environmental Advocates vs. USEPA* (2017) resulted in a voluntary remand of the TMDL for reconsideration and revision. The order of Judge Hernandez on 4 April 2017 (document 149) stated that USEPA and Oregon must submit a revised TMDL within two years. This order also adopts the earlier findings of Magistrate Judge Acosta (document 133, 10/12/2016). Judge Acosta's findings highlighted DEQ and EPA statements that the revision will "require analysis of factors affecting mercury pollution, including potential multiple sources, bioaccumulation patterns, and changes in the types of mercury being released and transformed in the entire complex river system", and the existing modeling "must be revised and incorporate all the new data related to mercury that has been gathered since the first TMDL…" Judge Acosta's findings agree with EPA's commitment to apply the revised Oregon fish tissue criterion for protection of human health and suggested that the appropriateness of developing wasteload allocations for individual point sources and calculation of the TMDL in terms of a daily load be considered.

Thus, the mercury TMDL for the WRB must be revised under a court-ordered deadline. The updated TMDL builds upon the existing TMDL modeling analysis, while also making substantial improvements.

The primary goal of the TMDL is to achieve the Oregon criterion for fish tissue concentrations of MeHg. Mercury in higher trophic level fish is present largely as MeHg, which is a potent neurotoxin in humans and other vertebrates. MeHg also readily bioaccumulates in the food chain. Bioaccumulation starts with the uptake of dissolved-phase MeHg into the base of the aquatic food web via pelagic or benthic pathways. The amount of MeHg present in aquatic systems is related to the amount of mercury present and the factors affecting the methylation process. The food chain bioaccumulation depends on the exposure concentrations of dissolved MeHg (dMeHg)in the water column and sediment pore water. Concentrations of dMeHg are in turn attributed to the amount of external mercury loading and mercury transformation kinetics. The majority of the mercury found in the environment is in inorganic forms; but these forms can be converted to the organic form of MeHg by certain anaerobic bacteria, such as sulfate or iron reducers, among others. MeHg production rates are affected by a host of physical and chemical factors including temperature, redox potential, pH, and concentrations of dissolved oxygen (DO), organic carbon (C), and sulfate (SO_4).

Determining the TMDL linkage between the ultimate stressor (THg loads) and the management objective (attaining acceptable fish tissue concentrations of MeHg to protect human health) is complicated because of the many intervening kinetic and transport processes. MeHg is produced under anoxic conditions, which can occur within a river or within its watershed. Within a river, MeHg production mostly occurs within the sediment, with the quiescent water of backwater channels potentially having higher rates of methylation. Within a watershed, wetlands or areas with saturated soils can often provide important locations for MeHg production. The relative importance of internally produced (within the waterbodies and their sediments) or externally produced (within soils and groundwater prior to reaching waterbodies) sources of MeHg has not been assessed for the WRB. MeHg monitoring data are available primarily from the water column. The simplified conceptual framework used in this TMDL is that the long-term average MeHg concentration in the water column depends on THg concentrations in the sediment, which in turn depend on rates of THg loading from upstream. The complex transformations between different forms of mercury are not explicitly simulated; rather, they are approximated by an empirical relationship between observed MeHg and THg in the water column as described in the following sections.

1.2 Technical Approach

Estimation of the 2006 TMDL required an analysis of the linkage between mercury sources and impairments. The linkage analysis is complicated for mercury because the water quality criteria on which the assessments of impairment are based are in terms of the mercury concentration in fish tissue. The tissue concentration is the result of bioaccumulation in the food web, which primarily occurs for MeHg. In contrast, THg loading in the watershed occurs predominantly in the form of inorganic mercury (e.g., Eagles-Smith et al. 2016a).

1.2.1 2006 Technical Approach

The 2006 TMDL established limits on THg loads to attain the criterion for MeHg in fish. THg loads and MeHg tissue concentrations were related to one another through a linkage analysis that contained three model components (gray boxes) and four mercury pools (tan ovals), as summarized in Figure 1-3. Each model component provided a linkage between two mercury pools:

- The Food Web Model established the link between ambient mercury exposure (primarily as dMeHg but also including Hg[II]) and fish tissue concentrations.
- The Mercury Translator Model converted unfiltered THg concentrations in water to corresponding dMeHg and dissolved Hg[II] concentrations using empirical relationships.
- The watershed Mass Balance Model connected sources of THg load throughout the watershed to ambient THg concentrations and loads within the river network.

The physical, chemical, and biological processes that result in elevated MeHg in fish proceed from the bottom to the top of Figure 1-3, as indicated by the orange arrows. The TMDL analysis worked backward through the linkages. That is, it began at the top with a criterion concentration in fish, used the Food Web Model to determine the corresponding acceptable exposure concentration of dMeHg and Hg[II], and then used the Mercury Translator Model to convert this into a target for unfiltered THg in water. Finally, the Mass Balance model was used to attribute the unfiltered THg concentration target into a total loading capacity and loads associated with different sources of Hg.

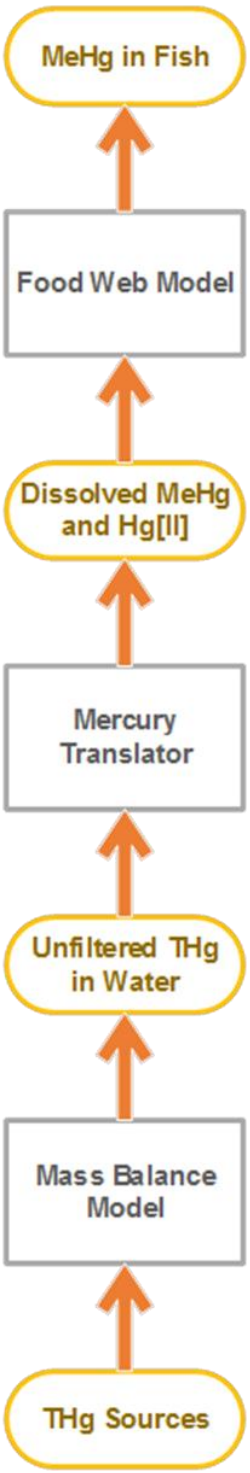

Figure 1-3. Components of the Willamette River Mercury TMDL Linkage Analysis

The primary tool for the TMDL linkage analysis was a probabilistic Food Web Model, which estimated the statistical distribution of THg and MeHg concentrations in different fish species as a function of ambient THg concentrations, bioenergetics of fish and prey species, and food web structure (Hope, 2003, 2006). The Food Web Model simulated bioaccumulation of both MeHg and inorganic mercury (Hg[II]) in fish. This required estimates of the ambient dissolved concentrations of both MeHg and Hg[II] in surface water. However, the majority of monitoring data available for TMDL analysis were measurements of THg. While THg in water is predominantly present as Hg[II], MeHg is a small fraction of THg – but it is only MeHg that biomagnifies through the food chain. Therefore, the second step in the linkage analysis was the application of a Mercury Translator Model to estimate dMeHg from unfiltered THg based on the ratio observed in a limited number of samples (ODEQ, 2006, p. 3-8). The Translator (referred to in the 2006 TMDL as Ω [omega]) consisted of a statistical distribution representing the ratio of dMeHg to THg that applied at all locations in the WRB.

The final component of the 2006 linkage analysis was a Mass Balance Model (Hope, 2005), which was used to (1) estimate the overall THg load in the WRB, and (2) estimate the fractions of this load attributable to different source categories. Whole-river THg load was calculated in two ways: from instream observations in the lower river and also from an analysis of THg sources and delivery. First, ODEQ used observations from the downstream reaches of the Willamette (River Mile [RM] 0) up to Eugene (RM 186.9) to establish a log-transformed and bias-adjusted regression relationship (e.g., non-linear rating curve) between THg concentration and flow in the lower river. Flows are gaged at only a few points, so the flow estimates corresponding to THg observations were themselves based on a regression against drainage area. The analysis suggested a mean annual loading rate of 126.8 kg/yr THg delivered at the mouth of the Willamette in Portland; however, the relationship between THg concentration and flow was weak, with an R^2 of 0.2046. Secondly, Hope (2005) estimated THg inputs from both point and non-point sources, modified by delivery ratios (Figure 1-4). The nonpoint sources loaded to the mainstem of the Willamette were analyzed in terms of direct deposition of Hg to water, runoff of atmospheric deposition to the land surface with associated delivery fractions, and soil erosion with associated delivery ratio assumptions. THg concentrations in soil were set to a single, fixed value, while erosion loss rates were based on typical rates by land use type provided by the Natural Resources Conservation Service (NRCS). The major mining source loads are reduced by settling of particulate material within Cottage Grove and Dorena Reservoirs, which was implicitly represented by using outflow concentrations from these reservoirs. Point source discharges were entered directly into the mainstem load without reduction. Some reduction in loads was assumed to occur during transport in the mainstem, but this was estimated only by difference. The results appeared to be in good agreement with the average annual THg loading estimate, with the difference (1.7 kg/yr) assumed to represent the net effects of sediment deposition and resuspension in the mainstem channel.

Attribution of total load to individual THg source types, as shown in Figure 1-4, allowed for the development of THg TMDL allocations. The apparent agreement between mass balance load estimates obtained from the downstream rating curve and load estimates obtained from the source analysis appears somewhat forced as it is largely dependent on the assumptions for THg delivery ratios (for atmospheric deposition) and sediment delivery ratios (for soil erosion). Hope (2005) notes regarding the Mass Balance Model, “these estimates…should be seen as only an initial view of mercury movement in the Basin. A more elaborate mass balance model would be a valuable tool to estimate or predict the outcome of alternatives…”

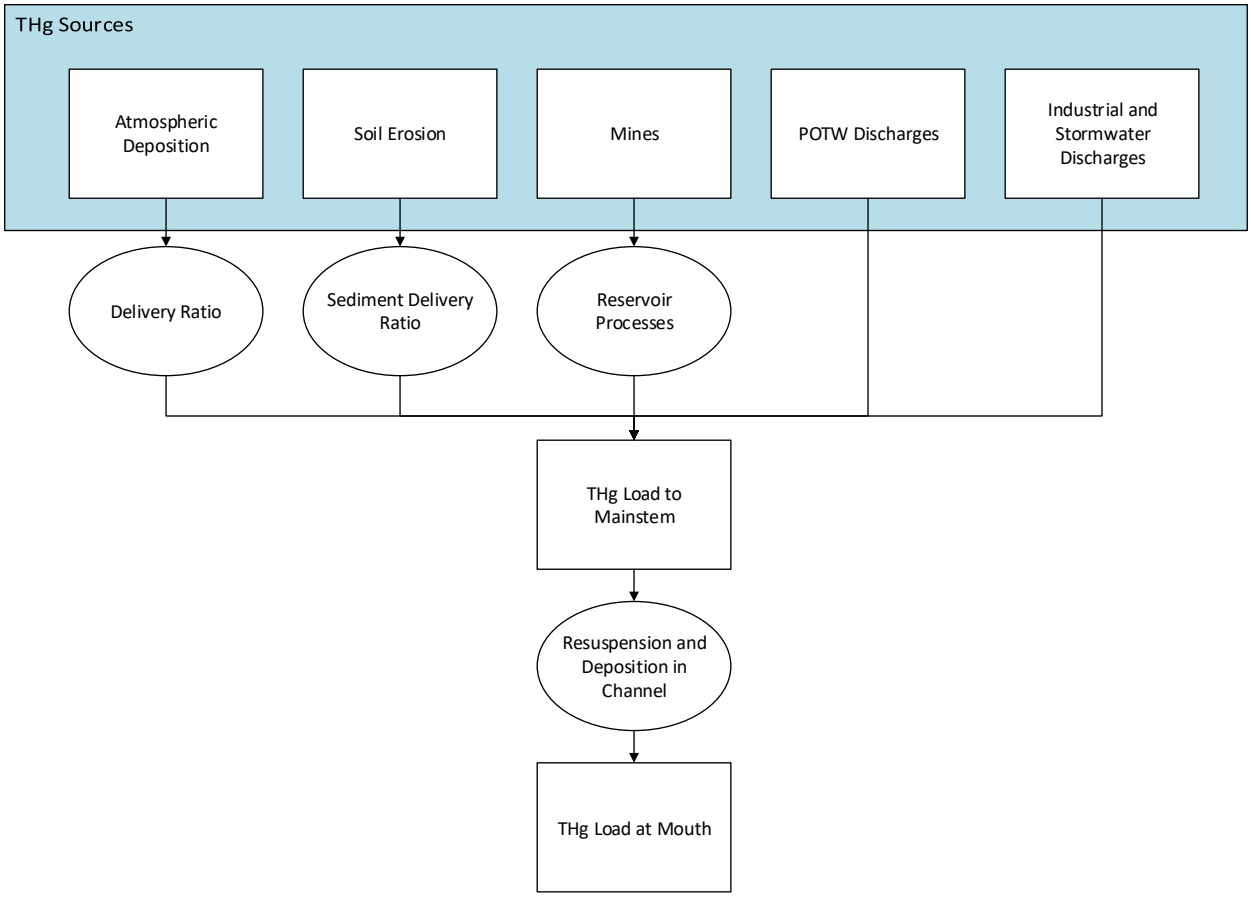

Figure 1-4. THg Mass Balance Model for the 2006 TMDL

1.2.2 Revised Technical Approach

The technical approach for the update of the TMDL, as described in the QAPP (Tetra Tech, 2017), builds upon the approach used in the 2006 TMDL and summarized above, but incorporates a series of updates, expansions, and refinements of the existing TMDL analysis models. An updated Food Web Model is used to link the new fish tissue criteria for mercury to corresponding estimated water column concentrations of dMeHg and Hg[II]. An empirical Mercury Translator Model is used to convert the dissolved water column concentrations to corresponding THg concentrations and loads, but is revised to incorporate the wealth of new data collected since 2006. Finally, the revised Mass Balance Model approach builds upon more recent data and is enhanced with information from an existing watershed model of flow and sediment transport in the WRB. These components are described in further detail in the following sections.

2.0 DATA SOURCES

We relied on mercury monitoring data provided by the ODEQ, USEPA, the United States Geological Survey (USGS), and Clean Water Services (CWS). These data sources are summarized in Table 2-1. Monitoring records included water column (THg and MeHg in dissolved and total forms), fish tissue, and sediment samples collected from the mainstem, tributaries, and lakes in the WRB.

The TMDL revision uses only data collected from 2002 onward for THg and MeHg concentrations in water and sediment due to improvements in sampling and analytical procedures compared to earlier data. For some fish species, data on tissue concentrations of THg from prior to 2002 are used in the analysis if sufficient later data were not available.

Table 2-1. Summary of Mercury Data Sources for the Phase II TMDL Analysis

Origin	Data Provider	Sampling Medium	Sample Dates
2006 TMDL Fish Data (Fish_Data_AppendixB_of_TMDL_2003.xls)	ODEQ	Fish tissue	7/8/2003 – 9/2/2003
2008 Fish Sample Records from the ODEQ Laboratory (Will fish Hg 2008.xlsx)	ODEQ	Fish tissue	8/20/2008 – 10/28/2008
Ambient Water Quality Monitoring System (AWQMS; ODEQ retrieved the data, completed the quality control (QA/QC) review, and provided the AWQMS data in R files)	ODEQ	Water column	1/10/2013 – 12/6/2017
ARRA Willamette Mercury Monitoring Project (Willamette Mercury TMDL 2010 data.xls)	ODEQ	Water column, fish tissue, and sediment	8/23/2010 – 10/1/2010
Black Butte Mine Storm Sampling (BBM_CDM_updated.xls.xlsx)	USEPA	Water column	1/7/2013 – 1/19/2017
Clean Water Services Monitoring Data (CWS provided the data to ODEQ through personal communication, ODEQ completed the quality control (QA/QC) review, and provided the data in R files)	CWS	Water column	3/5/2012 – 10/8/2019
Cottage Grove Analytical Reports (CottageGrove_SamplingReports [multiple files])	ODEQ	Fish tissue	6/2/2005 – 8/8/2005
Cottage Grove Reservoir Monitoring (CGR_data_updated_1.xls.xlsx)	USEPA	Water column	3/8/2013 – 11/24/2014
DEQ Laboratory LASAR Database (Compilation of multiple sampling organizations) (Willy_Hg_DEQ_lab_database.xlsx)	ODEQ	Water column, fish tissue, and sediment	8/14/2002 – 3/30/2009
DEQ Toxics Monitoring Program (WillyHgTissue.xlsx)	ODEQ	Fish tissue	8/20/2008 – 10/1/2010
USEPA R10 Columbia River Basin Mercury Database (crbfish12_20_11_maintained_by_HelenRueda.xlsx)	USEPA	Fish tissue	7/8/1969 – 12/7/2010*
NLA Lake Fish Tissue Mercury Data (WQX_fishdata_final.xlsm)	USEPA	Fish tissue	4/16/2014 – 10/17/2014
Portland Harbor Superfund Mercury Data (multiple zip files from Water Quality Portal retrieved by EPA)	USEPA	Water column and fish tissue	6/25/2002 – 9/5/2008
USGS Mercury Data for Cottage Grove Lake and Coast Fork Willamette (All NWIS USGS Data.xlsx)	USEPA	Water column and sediment	7/13/1992 – 9/30/2014*

USGS Willamette River Mercury Sampling (2011 Willamette River Fish Hg_for EPA.xlsx; willamette water query for EPA.xlsx)	USGS	Fish tissue and water column	7/8/2011 – 8/26/2011

* Water column and sediment THg data prior to 2002 are not used in the TMDL analyses. See notes regarding usability of the USEPA R10 Mercury Database. There is overlap of samples between the various DEQ databases.

2.1 MERCURY DATABASE DEVELOPMENT

Available data were compiled into a comprehensive database consisting of Microsoft Excel™ workbooks. Two versions of each data file were maintained, an original copy of each data file as it was received from ODEQ, USEPA, or USGS and a processing version. Relevant comments from the agency that provided the data, processing notes, and station information were added to the processing workbooks. Additional fields useful for tracking and filtering the data, such as waterbody type for water column samples (e.g. stream or reservoir), were incorporated. A global nomenclature scheme was developed and used to establish consistency in field and variable names across the datasets. Samples marked as below the detection limit were maintained as received with associated flags. Duplicate samples, identified by matching date, station, parameter, and closest time if needed, were averaged. Both long and wide data formats were used in the original workbooks. To facilitate development of the database, all workbooks in long format were converted to wide format. The processed workbooks were then exported as comma-separated variable (csv) files, read into the R statistical environment (R Core Team, 2017), stitched together using a full outer join, and exported as a compiled csv. The resulting database files are available electronically.

Special notes are required for the USEPA Region 10 Mercury Database. This database is a secondary compilation of fish tissue THg data from numerous other sources throughout the Columbia River Basin, some of which are not now readily available, but most of which are from prior to 2002. Unfortunately, QC evaluation revealed that some of the data had become mis-sorted, such that length and weight, and, in a few cases, fish species names, are not always correctly associated with fish tissue THg data. This problem appears to be most prevalent in the copy of the ODEQ TMDL data that had been transferred to this database, where there are frequent instances of physically implausible length-weight combinations. The discrepancies were revealed by comparing the database against the 2003 sampling results published in Hope (2006). Many of the sort errors appear to involve fish samples where the same laboratory sample identification number was assigned to a large group of fish samples. However, there are also other unexplainable errors, such as two Portland Harbor fish samples that are cited as being derived from the publication *Arsenic, Mercury, and Selenium in Fish Tissue from Idaho Lakes and Reservoirs: A Statewide Assessment*, but do not appear therein (https://www.deq.idaho.gov/media/639760-arsenic_mercury_fish_tissue_report_0508.pdf). Certain other samples also appear to have incorrect attributions. The scrambling of samples was present in the original version of this database supplied by EPA (crbfish12_20_11.xlsx, transmitted by email from Leigh Woodruff, U.S. EPA to Jonathan Butcher, Tetra Tech, 9/13/2017).

Based on these QC findings, Tetra Tech determined that the USEPA Region 10 Mercury Database was not suitable for use. Fortunately, most of the data contained therein were from before 2002 or available in other databases with more direct retrieval from the primary quality assured source (e.g., the Portland Harbor Superfund data). There are two datasets included in crbfish12_20_11.xlsx that contain data in or after 2002 and can be confirmed from other sources. These are samples from the USGS EMMMA (Environmental Mercury Mapping, Modeling, and Analysis; https://emmma.usgs.gov/datasets.aspx) database and the U.S. Fish and Wildlife Service ECDMS database (Environmental Contaminants

Database Management System, https://ecos.fws.gov/ecdms4/), both of which primarily address trout species in their Oregon samples. EMMMA data are derived from a number of sources, but for Oregon primarily represent fish tissue samples from the EPA EMAP (Environmental Monitoring and Assessment Program). The EMMMA data were downloaded and used directly to augment the other fish tissue samples for the Willamette. The ECDMS data can be queried by site via a map interface, but are not readily available in bulk. We therefore performed checks of data from individual sites against the ECDMS data mirror with crbfish12_20_11.xlsx and determined that these data were reproduced without error – perhaps because there are unique sample identifiers associated with each entry.

Finally, for several fish species where it was desirable to examine pre-2002 tissue data due to a shortage of later data, we relied on the compilations contained in FWM spreadsheets used for the approved 2006 TMDL rather than re-querying potentially corrupted data from the crbfish12_20_11.xlsx file.

2.2 Mercury Data for TMDL Update

The WRB is comprised of 12 HUC8s (refer to Figure 1-1), many of which contain streams that are listed as impaired for elevated concentrations of mercury (Figure 1-2). Over 13,000 sample records collected after 2002 were provided by ODEQ, USEPA, and USGS. However, on review of the data, some of these records turned out to be duplicates, from outside of the WRB, or ancillary measures not directly relevant to the TMDL modeling (e.g., dry weight tissue results, concentrations in individual organs of fish). Data counts for 2002-2019 are summarized in (Figure 2-1) according to the following conventions:

- Only data from within the WRB are tabulated.
- Only unique records are shown.
- Biotic tissue mercury data is summarized for fish only, including removal of mollusk and crustacean samples incorrectly listed as “fish”.
- For fish tissue samples, only wet weight analyses of fillets or whole body samples are counted. Samples where the tissue type is not indicated are assumed to fall into these categories (fillet or whole body).
- Counts of fish tissue samples include both juveniles and adults.
- Composite fish tissue samples are counted as single observations.

Mercury sampling efforts have primarily been concentrated along the mainstem Willamette, corresponding to the Lower, Middle, and Upper Willamette HUC8s (17090012, 17090007, and 17090003). The combined count of samples collected in these three HUC8s after 2002 is 5,464, following the tabulation conventions shown above. Sampling efforts have also been focused in the Coast Fork Willamette HUC8 (17090002), which receives drainage from mercury-contaminated historic mining sites. As the primary health concern for mercury is exposure through elevated fish tissue concentration, a majority of the mercury sampling that has been conducted in the basin was for fish tissue concentrations.

Substantial amounts of additional data have been collected since the 2006 TMDL, which used observations through 2003 only. Efforts to collect additional data began shortly after the TMDL was published. The temporal distribution of samples from 2002 to present used to update the food web, translator, and mass balance models is shown in Figure 2-2.

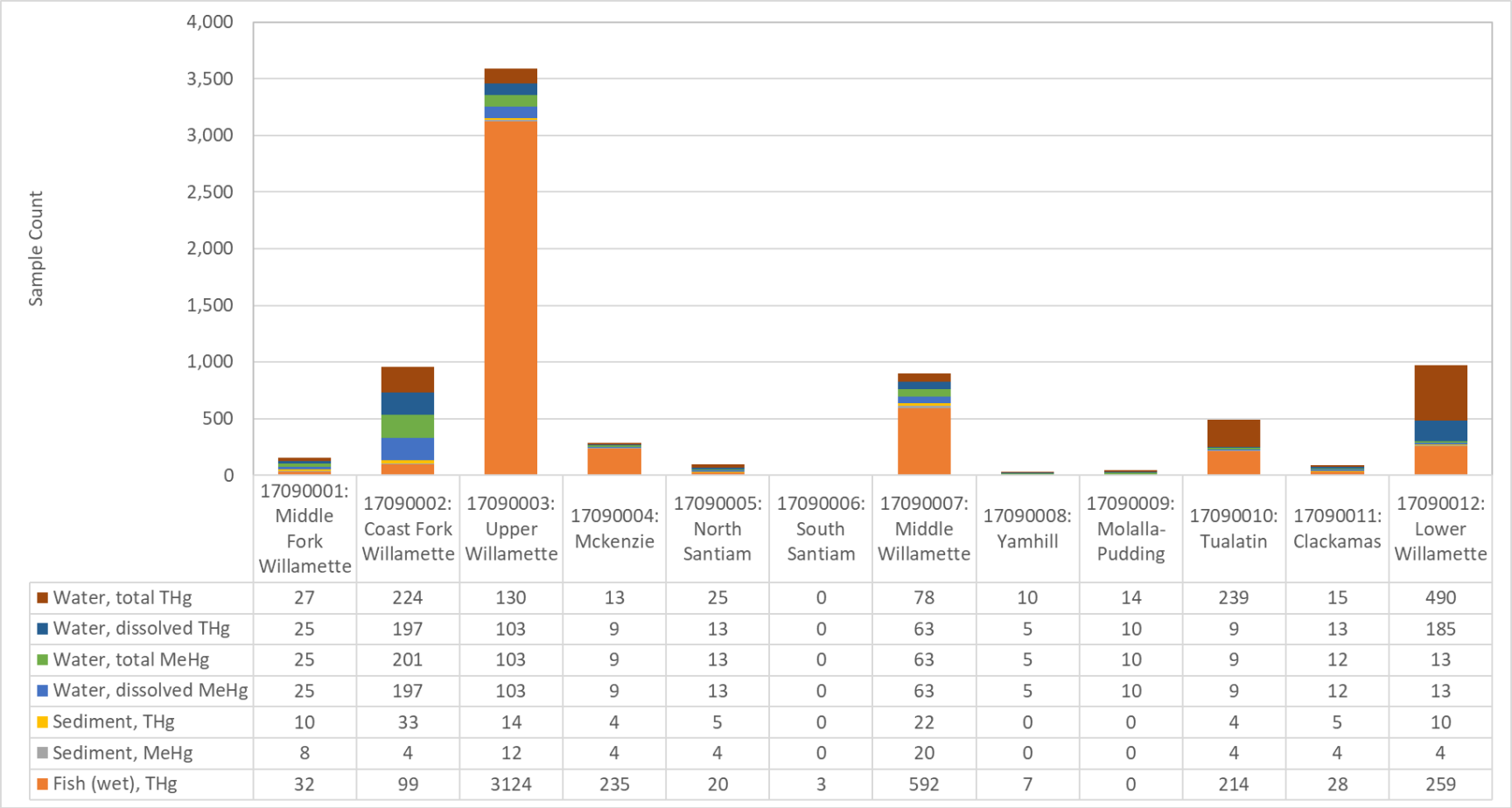

	17090001: Middle Fork Willamette	17090002: Coast Fork Willamette	17090003: Upper Willamette	17090004: Mckenzie	17090005: North Santiam	17090006: South Santiam	17090007: Middle Willamette	17090008: Yamhill	17090009: Molalla-Pudding	17090010: Tualatin	17090011: Clackamas	17090012: Lower Willamette
Water, total THg	27	224	130	13	25	0	78	10	14	239	15	490
Water, dissolved THg	25	197	103	9	13	0	63	5	10	9	13	185
Water, total MeHg	25	201	103	9	13	0	63	5	10	9	12	13
Water, dissolved MeHg	25	197	103	9	13	0	63	5	10	9	12	13
Sediment, THg	10	33	14	4	5	0	22	0	0	4	5	10
Sediment, MeHg	8	4	12	4	4	0	20	0	0	4	4	4
Fish (wet), THg	32	99	3124	235	20	3	592	7	0	214	28	259

Figure 2-1. Mercury Sampling Data Availability for HUC8s in the Willamette River Basin

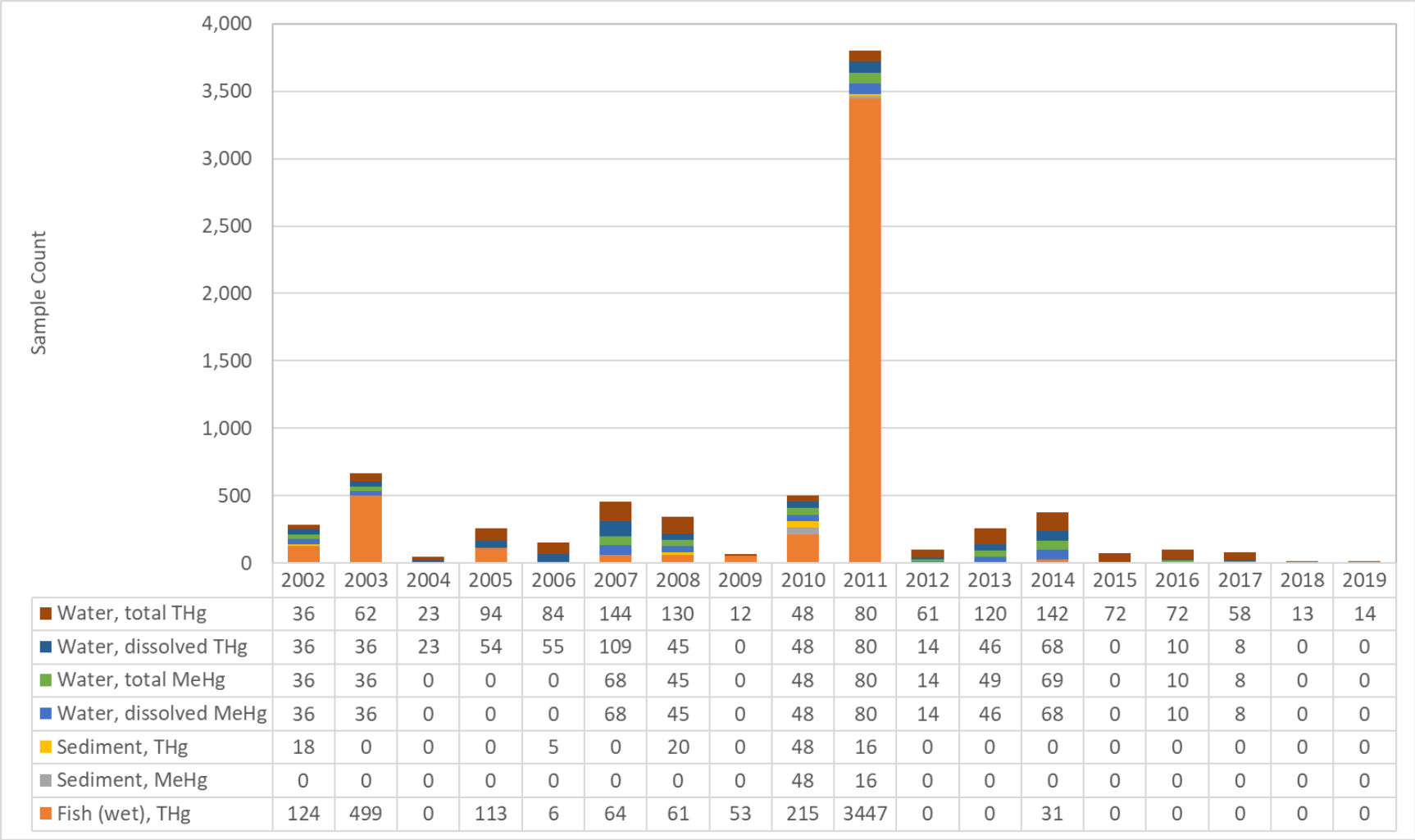

	2002	2003	2004	2005	2006	2007	2008	2009	2010	2011	2012	2013	2014	2015	2016	2017	2018	2019
Water, total THg	36	62	23	94	84	144	130	12	48	80	61	120	142	72	72	58	13	14
Water, dissolved THg	36	36	23	54	55	109	45	0	48	80	14	46	68	0	10	8	0	0
Water, total MeHg	36	36	0	0	0	68	45	0	48	80	14	49	69	0	10	8	0	0
Water, dissolved MeHg	36	36	0	0	0	68	45	0	48	80	14	46	68	0	10	8	0	0
Sediment, THg	18	0	0	0	5	0	20	0	48	16	0	0	0	0	0	0	0	0
Sediment, MeHg	0	0	0	0	0	0	0	0	48	16	0	0	0	0	0	0	0	0
Fish (wet), THg	124	499	0	113	6	64	61	53	215	3447	0	0	31	0	0	0	0	0

Figure 2-2. Temporal Distribution of Mercury Samples in the Willamette River Basin

(This page left intentionally blank.)

3.0 FOOD WEB MODEL

To support the development of updated surface water THg concentration target levels for the WRB, the existing 2006 mercury food web model (FWM; Hope, 2006) was updated and recalibrated using new water quality and fish tissue data for the watershed. The content and creation of this dataset is documented in the *Willamette River Basin Mercury Data Summary* (Schmidt, 2018). Updating the 2006 FWM consisted of three steps: 1) converting the 2006 FWM from Excel with Crystal Ball add-in format to R format, 2) updating a subset of the FWM input distributions using the Willamette dataset, and 3) calibrating the updated FWM. The development process for the updated FWM is described below.

3.1 MODEL CONVERSION

The 2006 FWM (Hope, 2006) was developed using Microsoft Excel™ and the Crystal Ball™ application. Crystal Ball is proprietary Monte Carlo simulation software that works alongside Excel through a Crystal Ball tab on the Excel ribbon. The FWM input distributions and the number of samples were entered via the Crystal Ball tab, while the model formulae were entered in Excel. A Monte Carlo model works by taking thousands of samples from specified statistical distributions (e.g., normal or log-normal) as inputs, running those samples through the model formulas, and producing thousands of trial outputs for each model endpoint of interest. The outputs are then aggregated, typically using the median value, with percentiles (e.g., 5th and 95th) reported to quantify the uncertainty in the results. A Monte Carlo model is a stochastic process where the inputs are random draws from their specified distributions. As such, each run of a Monte Carlo model will produce different results, although pseudo-random number generator seeds can be set to maintain reproducibility.

ODEQ requested that the FWM be transferred from an obsolete version of Crystal Ball to the R statistical platform (R Core Team, 2017). The package “mc2d” (Pouillot and Delignette-Muller, 2010) was used to perform the Monte Carlo simulation. The number of samples was set to 10,000. Latin hypercube sampling was set for all the Monte Carlo draws, as was done in the 2006 FWM. Correlation between body weight and age was set to one for invertebrates, as specified in the 2006 TMDL Appendix B.

ODEQ provided what was stated to be the final version of the 2006 FWM. The FWM input parameters are specified in Table 3 of the 2006 TMDL Appendix B (Hope, 2006) as well as in the Excel/Crystal Ball file, which in turn differs from the peer-reviewed version presented in Hope (2003). There were some mostly minor discrepancies between the parameters in the 2006 TMDL Appendix B Table 3 and the received Excel/Crystal Ball file (see Table 3-2). In general, we used the Excel/Crystal Ball values where discrepancies existed. One notable exception is that there was an evident error on the Hg2Paths worksheet of the Excel workbook in which the adult carp (CAR) section cells I215:I240 reference CAR juvenile values instead of CAR adult values. This reference was repaired. A detailed analysis of the discrepancies is provided in Fernandez (2017).

The main outputs from the FWM are biomagnification factors (BMFs) and estimated fish tissue mercury concentration distributions. These are combined with the Mercury Translator Model (Section 4.0) to estimate surface water THg target levels. For each output, the FWM calculates taxon-specific estimates for eight fish species. The output from the R version of the FWM was compared to the 2006 FMW output documented in the 2006 TMDL Appendix B Tables 7, 8, and 9. The values will not be identical due to the stochastic nature of the FWM and use of a different random number generator in R. Further minor differences are likely associated with the discrepancies between the Excel/Crystal Ball package and the

parameter values documented in Appendix B of the 2006 TMDL. The output from the R version of the FWM was found to be similar to the 2006 FWM output, with resulting THg target values within 10 percent of those presented in Hope (2006), with the exception of calculations regarding carp (CAR), where an error was present in the 2006 model setup, as noted above. The presence of these minor discrepancies is not a major concern because the input distributions for the FWM have been updated and the results recalibrated.

3.2 Updating the Distributions

Inputs for a Monte Carlo model are sampled from a specified statistical distribution, as opposed to being set to constant values. A statistical distribution consists of two parts: the distribution form (e.g., normal or log-normal) and the distribution sufficient statistics (e.g., mean and standard deviation values). Together, a distribution describes the pattern and frequency of possible values to be used in the modeling process.

The distributions for a Monte-Carlo model are selected based on published studies or are fit to observed data. The updated Willamette database provided new data that were used to re-fit some of the FWM input distributions, including surface water mercury concentration and adult fish length. The database for fitting these distributions was first filtered to use only data collected in or after year 2002, and data for adult fish measurements (as opposed to juvenile fish observations). The 2006 TMDL Appendix B Table 4 specifies the range of adult fish length for each species of interest. These range values were used to filter the database for adult fish samples only. For several species with limited post-2002 data, the length and body weight distributions were left as specified in the 2006 TMDL. Table 3-1 lists the FWM fish biometric inputs and indicates whether they were updated from the 2006 model. Some input distributions were not updated due to lack of new data. Figure 3-1 displays the observed and FWM histograms from one of the fish species (NPM) for example.

Fish tissue THg concentration data from sites directly associated with legacy mining operations (e.g., the local creeks associated with Black Butte mine tailings described in Section 5.3.4) were also omitted for the FWM analysis (only) as these sites are likely to exhibit extreme and highly variable mercury concentrations and atypical food webs. Fish tissue THg concentration data from fillet fish samples were applied because fillets are the primary component consumed by humans.

Distributions of both dMeHg and dHg[II] in water were updated based on extensive new data collection. The water chemistry data included censored (below detection limit) observations. To account for this, the distribution was estimated using the imputed values calculated using a robust regression on order statistics (ROS) method (see discussion of methods for censored data in Section 4.1.3 on the Mercury Translator model below). Monitoring data from sites associated with legacy mining contamination (e.g., Black Butte Mine tailings area) were also removed for both water chemistry and fish length variables in the Food Web Model.

The R package "fitdistrplus" (Delignette-Muller and Dutang, 2015) was used to fit the univariate distributions. The appropriate distribution family for each variable was selected based on observed and theoretical cumulative distribution function (CDF) plots. The following distributions were evaluated for each stochastic variable in the updated FWM:

- Normal, log-normal, and inverse normal
- Gamma and inverse gamma
- Weibull and inverse Weibull
- Logistic

Table 3-1. Fish Species in the Food Web Model and Identification of Updated Distributions

Fish Species	Length	Body Weight
Northern Pikeminnow (NPM)	Updated	Updated
Largemouth Bass (LMB)	Updated	Updated
Smallmouth Bass (SMB)	Updated	Updated
Largescale Sucker (LSS)	Updated	Updated
Common Carp (CAR)	Not updated	Not updated
Rainbow Trout (RBT)	Not updated	Not updated
Cutthroat Trout (CTT)	Not updated	Not updated
Bluegill (BLU)	Not updated	Not updated

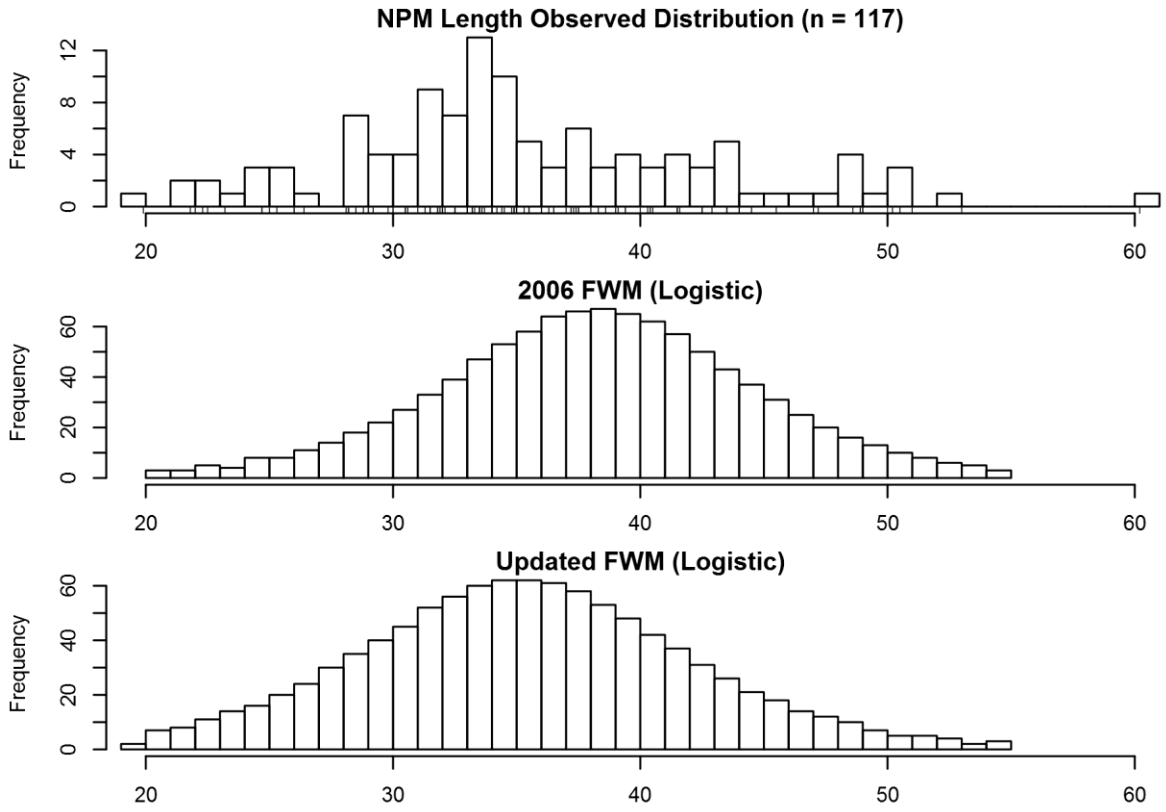

Figure 3-1. Histograms of NPM fish length (cm) for observed data (top), 2006 FWM (middle), and updated FWM (bottom).

The FWM calculates adult fish bodyweight as a nonlinear power function of length:

$$BW = a * L^b$$

where *BW* is body weight (g), *L* is length (cm), and *a* and *b* are estimated parameters (see Hope (2006), Appendix B, Equation 16). The weight formula applies to both juvenile and adult fish, and the parameters for a given species are the same for juveniles and adults. The parameters *a* and *b* were re-fit to observed paired fish length and fish weight data for NPM, LMB, SMB, and LSS. See Figure 3-2 for an example plot for adult NPM, which shows that the additional newer data resulted in only small changes in the relationship.

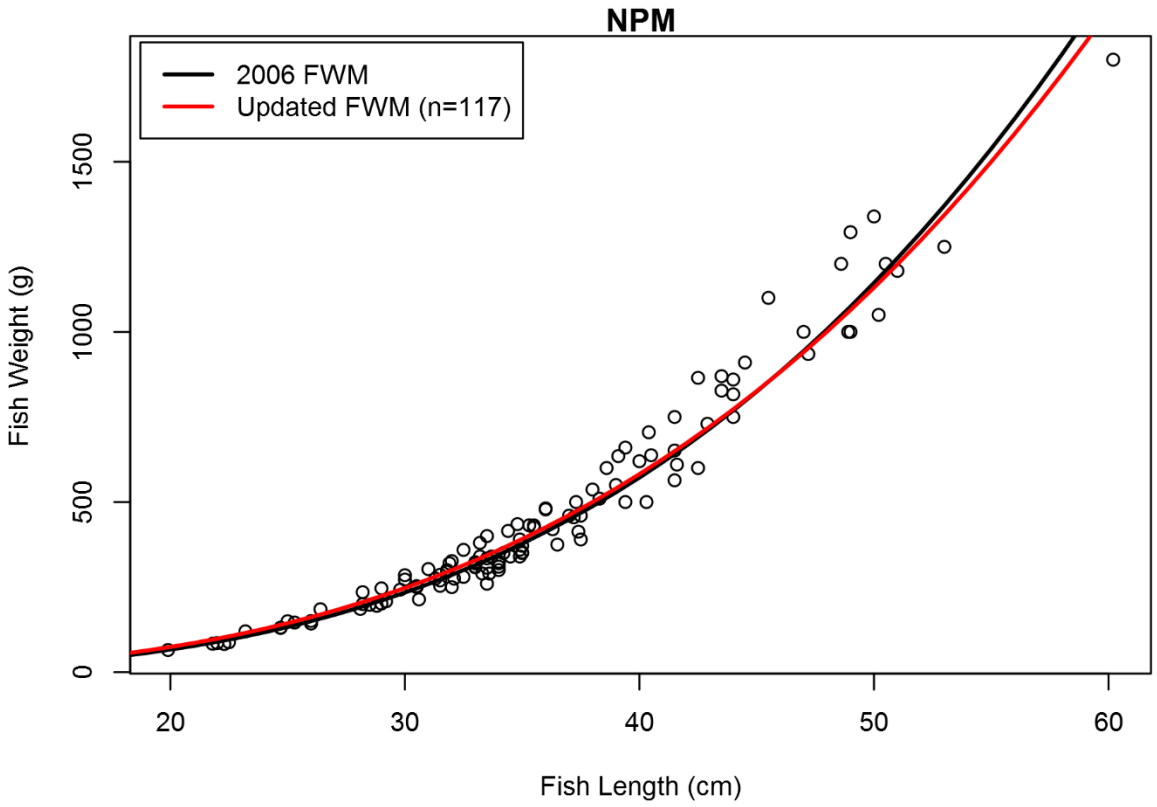

Figure 3-2. Plot of Paired Adult NPM Weight and Length Observations, with FWM Fits

3.3 Initial Model Calibration

Initial calibration of the updated FWM followed the process described in TMDL Appendix B for the 2006 FWM. We used only 2002 and later adult fish data for the higher trophic level species for which many new samples are available (NPM, LMB, SMB, LSS); however, we used all available fish data for this step, including fish data from prior to 2002, to ensure sufficient sample size to calibrate for CAR, RBT, CTT, and BLU. The updated FWM model was calibrated using 1) observed adult fish tissue concentrations and 2) observed adult fish lengths. First, plots of FWM estimated and observed fish tissue concentration CDFs were overlaid. FWM parameters were then adjusted to minimize the differences between the modeled and observed median CDF values. See Figure 3-3 for an example CDF plot. The right-hand side of this figure shows the calibrated distribution for cutthroat trout and is read as follows: A fish tissue concentration of 0.2 mg/kg on the x-axis, for example, corresponds to a cumulative distribution fraction of about 80 percent on the y-axis. This indicates that 80 percent of adult cutthroat trout are expected to

have a tissue concentration of 0.2 mg/kg or less, while the remaining 20 percent are expected to have a tissue concentration of greater than 0.2 mg/kg.

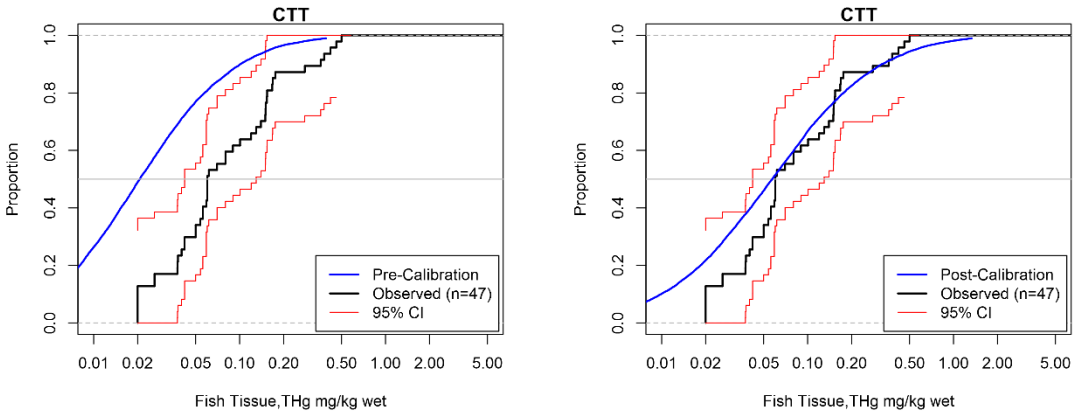

Figure 3-3. Pre- (left) and Post- (right) Calibration Plots for Fish Tissue Mercury Concentration of Cutthroat Trout (CTT)

Second, the relationship between fish tissue mercury concentration and fish length was reviewed. The fits from these two models were overlaid on a scatterplot of the observed data points and compared. The calibration process was repeated for each of the eight fish species. During calibration, the number of adjusted parameters was kept to a minimum necessary to achieve a reasonable fit (see Table 3-2 for a list of updated parameters).

While the initial calibration effort did reproduce the medians, the model fit was not fully satisfactory for upper trophic level fish. In particular, the tails of the CDF were not well matched for northern pikeminnow (NPM) and largemouth bass (LMB) and the predicted 95th percentiles of the distributions for these two species (7.34 mg/kg for LMB and 5.79 mg/kg for NPM) were significantly greater than any observed fish tissue concentrations in the WRB. Therefore, some additional modifications of the FWM structure were investigated, as described in the next section. Final calibration plots for all species are provided below in Figure 3-5.

3.4 FWM Modifications

Several efforts were pursued to address and improve fit of the fish CDFs. We first changed the calibration approach to attempt to align observations and predictions for the entire CDF, while ensuring that the median remained within the 95th percentile confidence limits of the observed CDF. We then tested optimizing additional parameters that had not been treated as calibration variables in the previous effort.

1. The MeHg elimination rate (Hope, 2006, equation 17) is specified as $\ln k_{2(ME)} = c \cdot T - d \cdot lnBW + e - f$, where *T* is surface water temperature, *BW* is body weight, and *a, b, c*, *d, e,* and *f* are parameters. Distributions were previously specified for the parameters based on literature values from Trudel and Rasmussen (1997). We tested varying these specifications.
2. Food ingestion rate (Hope, 2006, equation 19) was previously specified using the model of Gobas (1993) with fixed coefficients: $IR = (0.022 \cdot BW^{0.85})(\exp(0.06 \cdot T))$. We investigated and adopted the approach of specifying the two BW parameters in this

equation as species-specific constants *i* and *j* that could be adjusted during the calibration process: $IR = (i \cdot BW^{j})(\exp(0.06 \cdot T))$.

These changes alone did not greatly improve the FWM's ability to fit the tails of the CDFs for higher trophic level fish.

The problems in fitting the tails of the CDF primarily reflect an over-estimation of the predicted variance of the fish tissue concentration distributions. Analysis of the sources of this variance indicated that it was largely driven by the specification of the distribution of MeHg exposure concentrations. While the concentration distribution is based on observed data, there is a philosophical disconnect in that the FWM is constructed as a steady-state model, whereas the observed MeHg data are individual grab samples that represent points in time and not steady-state exposure concentrations. It is not surprising that the distribution of individual samples has a greater variance than the distribution of the central tendency of the exposure concentration over time; indeed, the latter should have lower variance according to the Central Limit Theorem (e.g., Helsel and Hirsch, 2002).

A partial solution to this issue was to change the exposure concentration input to the distribution of the local median, not individual grab samples. Medians are used rather than means because the distribution is expected to be right-skewed and is also censored by observations reported as below the detection limit. We defined local medians by aggregating the data to 62 approximate locations based on a search radius of 0.01 decimal degrees. This approach substantially reduces the over-estimation of variance in the fish mercury CDFs; however, it is likely that the variance in the exposure concentration distribution is still biased high due to the presence of aggregate locations with small sample sizes.

The modifications to the calibration process resulted in an excellent fit to fish CDFs at lower trophic levels, such as BLU and CTT. For the higher trophic level species, notably NPM and LMB, the revised approach gave an improved fit, but there still appeared to be over-estimation of the upper percentiles of the CDF, especially for NPM.

We also investigated whether the CDF fit for NPM and LMB could be further improved by evaluating the potential dependence of assimilation efficiency on body weight and by revising the elimination rate analysis for MeHg.

Hope's (2006) bioaccumulation model for Hg in the Willamette River Basin includes a food term (*f*) for each trophic level, expressed as

$$f = \frac{AE \cdot NIR \cdot NDF}{k_2}$$

where *AE* is the assimilation efficiency, *NIR* is the weight-normalized food intake rate, *NDF* is the dietary fraction normalized over all preferred food items, and k_2 is the toxicant elimination rate (day^{-1}). Although not explained by Hope, the underlying formulation is the differential equation

$$\frac{dC}{dt} = AE \cdot NIR \cdot NDF - k_2 \cdot C$$

where *C* is the tissue concentration at time *t*. A solution to this equation with $C = 0$ at $t = 0$ is

$$C = \frac{AE \cdot NIR \cdot NDF \cdot [1 - exp(-k_2 t)]}{k_2}$$

which converges to Hope's steady-state solution as *t* becomes large. The elimination rate (k_2) is formulated as a function of body weight and temperature, following Trudel and Rasmussen (1997). *AE* was assumed to be constant in the previous versions of the FWM.

Barber (2008) criticized food uptake models that are based on the assumption of constant values for both k_2 and *AE*, demonstrating that the apparent assimilation rate of a toxicant must decline over time and recommending that chemical *AE*s should be considered as a function of K_{OW} and the fish's body weight, growth, and feeding rates. Barber discusses more complex thermodynamic and diffusion-based formulations that are appropriate for analysis of laboratory exposure studies. He does not, however, consider the simple case where k_2 is not constant but is dependent on body weight, as in the Willamette Food Web Model. In the steady-state solution, only the ratio AE/k_2 is used, so making only one of these factors dependent on body weight and calibrating the result is likely to be sufficient

There appears to be little support in the more recent literature for a more complex representation of *AE* in steady-state bioaccumulation models. In theory, the uptake of MeHg should be associated with the uptake of protein because MeHg binds to sulfur in protein (Trudel and Rasmussen, 2006). The *AE* for protein is typically around 0.8; but lower values tend to emerge in calibration for bioaccumulation of MeHg – suggesting that the AE/k_2 ratio formulation is not optimal.

Trudel and Rasmussen (2006) also show that the overall biomagnification factor (BMF) should scale in accordance with $AE \cdot I/(E+G)$, where *I* is the total ingestion rate, *E* is the elimination rate, and *G* is the growth rate. Both *I* and *E* tend to scale with body mass with an exponent close to -0.2 (Trudel and Rasmussen, 1997); thus, body burden of MeHg will increase with body mass if growth decreases faster with body mass than the ingestion rate.

The formulation of Trudel and Rasmussen (2006) implies that the effective or apparent value of k_2 is $E + G$, so the k_2 parameter must represent both actual elimination and growth dilution of mercury burden – which is partially consistent with the empirical formulation used in the Willamette FWM, where apparent elimination is represented as a fitted function of temperature and body weight. Trudel and Rasmussen did not see a need to assume a non-constant *AE.*

Finally, a more recent study by Dang and Wang (2011) found no dependence of *AE* on fish size or weight.

The model developed by Hope takes the equation and default parameters for elimination rate from Trudel and Rasmussen's (1997) expression for *E*:

$$\ln(E) = c\,T - d\ + \ln(BW) + K$$

where *T* is temperature (°C) and *K* is a constant (represented as the sum of two terms). Thus, *E* varies as exp(*T*)/*BW*.

However, as seen above, the *effective* elimination rate should be represented as the sum of the true elimination rate and the growth rate, so *E* and k_2 are not equivalent. We therefore made the parameters for k_2 part of the calibration, as follows:

The growth rate can be expressed as

$$G = \gamma I - M$$

where γ is the fraction of ingested food that is assimilated and *M* is the total metabolic expenditure. *I* is a function of exp(*T*) and *BW* raised to a fractional power. *M* will also vary with *T* and is known to scale with *BW*, which affects both the base metabolic rate and the activity coefficient associated with foraging (Trudel and Rasmussen, 2006). If we assume the temperature dependence of *M* is similar to that of *I*, represented in the Gobas (1993) model as $\exp(0.06 \cdot T)$, this suggests that the effective elimination rate should have a form similar to the following:

$$k_2 = E + g \cdot \exp(0.06\,T) \cdot\ BW^h$$

where *E* is the elimination rate as specified in the 2006 model using Trudel and Rasmussen's (1997) formulation and the second term represents the growth dilution addition to the effective elimination rate. Here, *g* and *h* are additional parameters for the FWM. In sum, the literature suggests that the general representation of *AE* should not be modified, but that k_2 should be redefined to include a growth dilution term in addition to *E*.

Two other changes were made to FWM parameters based on literature review: First, fish length and age are related by a von Bertalanffy (1938) growth function:

$$L_t = L_\infty\ (1 - [exp(-K \cdot (t - t_0)])$$

where *L* is length (cm), *t* is age in years, and *K* is a parameter (yr^{-1}). Hope (2006) obtained the asymptotic length (L_∞) and *K* from www.fishbase.org; however, Hankin and Richards (ww) suggest that an appropriate value of *K* for NPM is 0.179, rather than the value of 0.100 in fishbase. We also re-assessed the predator-prey size ratio for NPM, which was previously set to a triangular distribution with maximum ratio of 0.275 for all fish other than LMB. Research reported by Zimmerman (1999) shows that the ratio for NPM is more likely in the range of 0.35 or greater.

3.5 Final Calibrated FWM

Results of the revised FWM CDF calibration adjustment are shown in Figure 3-4for all evaluated species (see species abbreviations in Table 3-1 above). The fit for NPM is not perfect but is reasonable and is not nearly as skewed as in the initial recalibration.

Figure 3-5 compares fish tissue concentrations versus length. Here, the orange triangles represent the observed data (2002 or later only for LMB, LSS, NPM, and SMB; all available data for BLU, CAR, CTT, and RBT), while the gray dots show the 10,000 stochastic Monte Carlo realizations for each fish species. A locally weighted regression (LOESS; Cleveland and Devlin, 1988) smoothed line is fitted through the post-calibration distribution and indicates a generally good quality of match to observed data. Note that the Y-axis is on a log-10 scale. A close-up of the post-calibration plot for NPM (Figure 3-6) shows that the LOESS fit to the Monte Carlo model output closely follows a LOESS fit to the observed post-2002 data.

Final distribution selections and parameter values for the calibrated FWM are provided in Table 3-2.

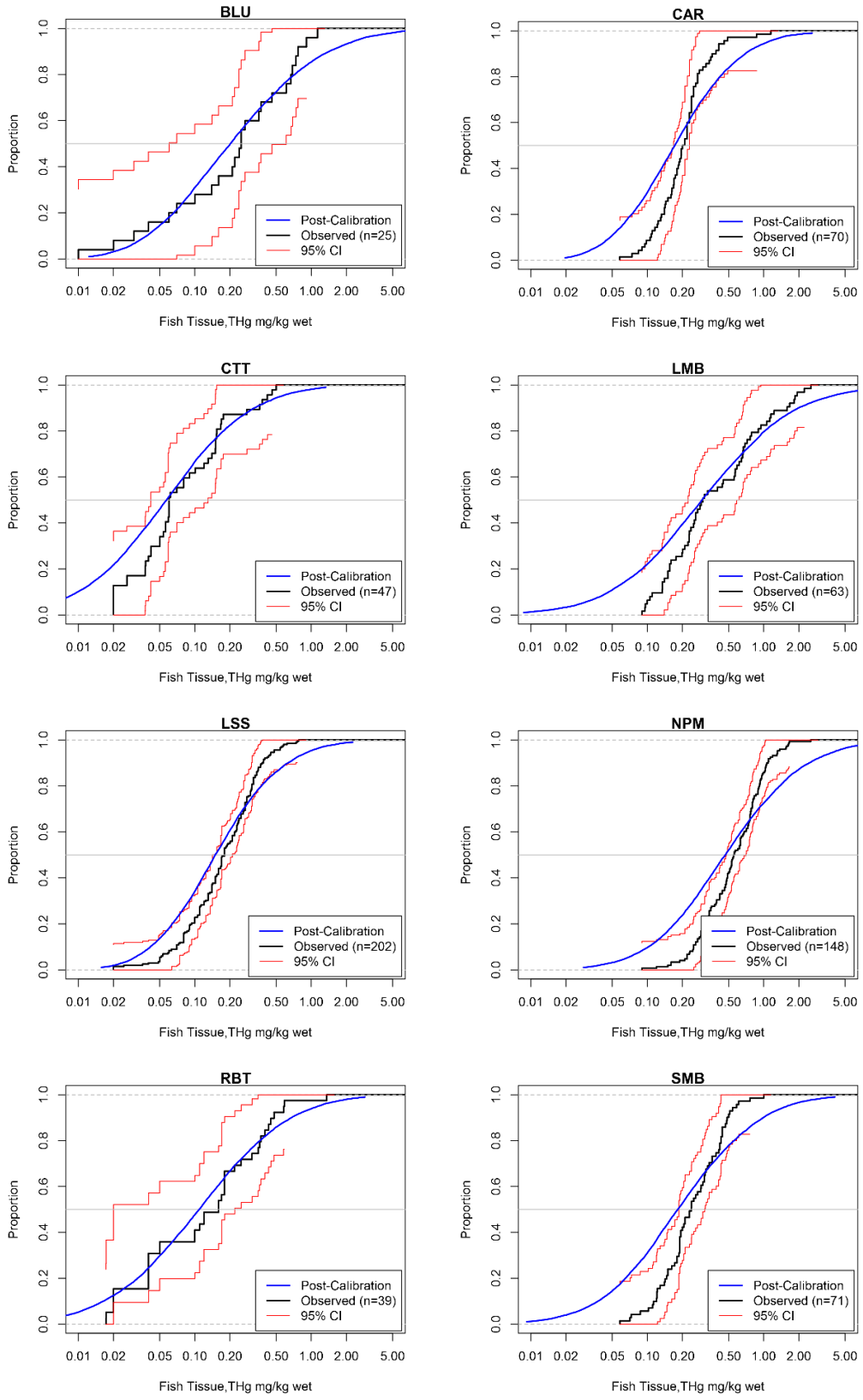

Figure 3-4. Post-calibration Plots for Fish Tissue Mercury Concentration CDFs

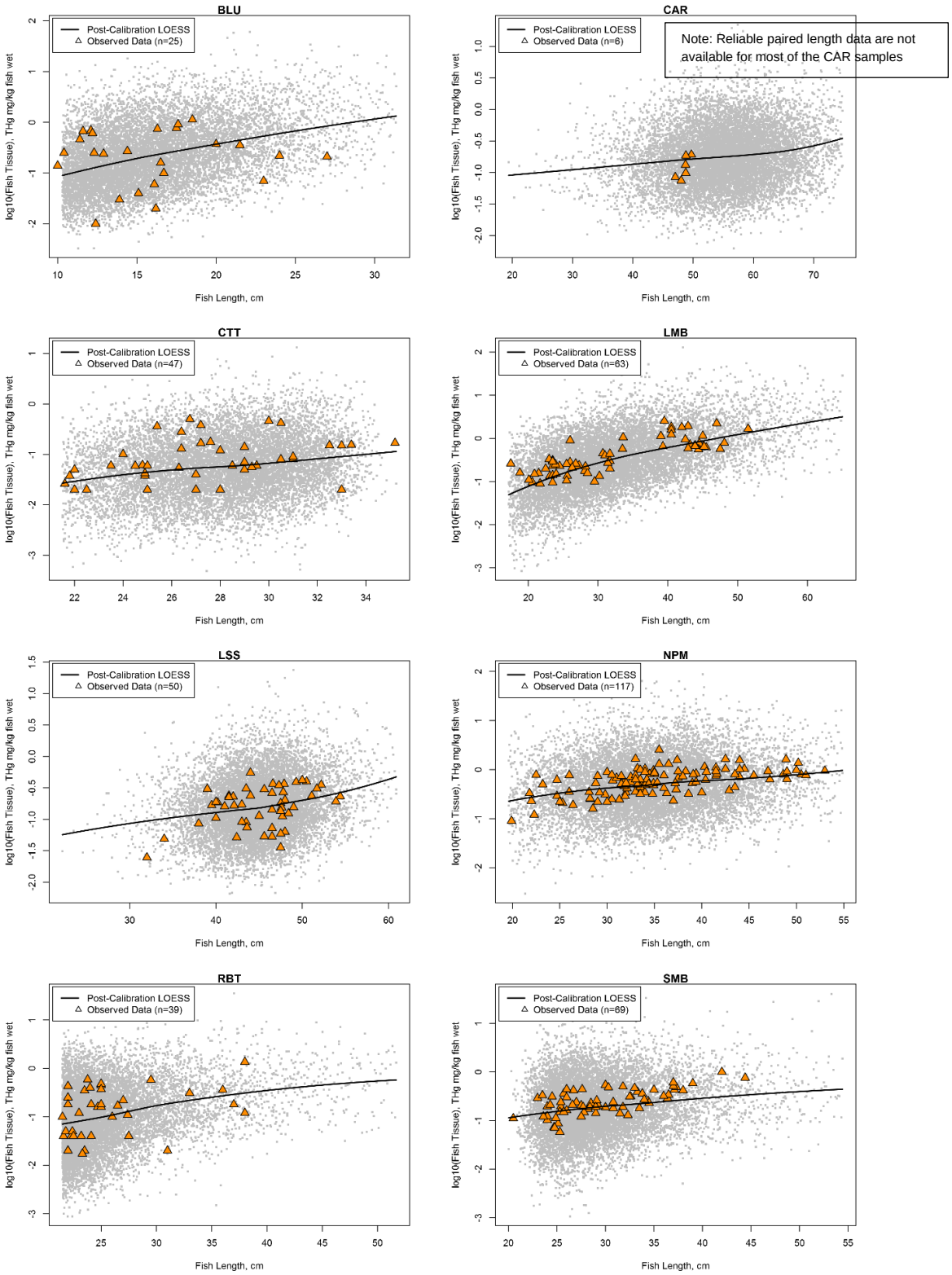

Figure 3-5. Post-Calibration Plots of Mercury Concentration versus Fish Length

Note: Orange triangles are observed data; gray points show the results of 10,000 Monte Carlo simulation runs.

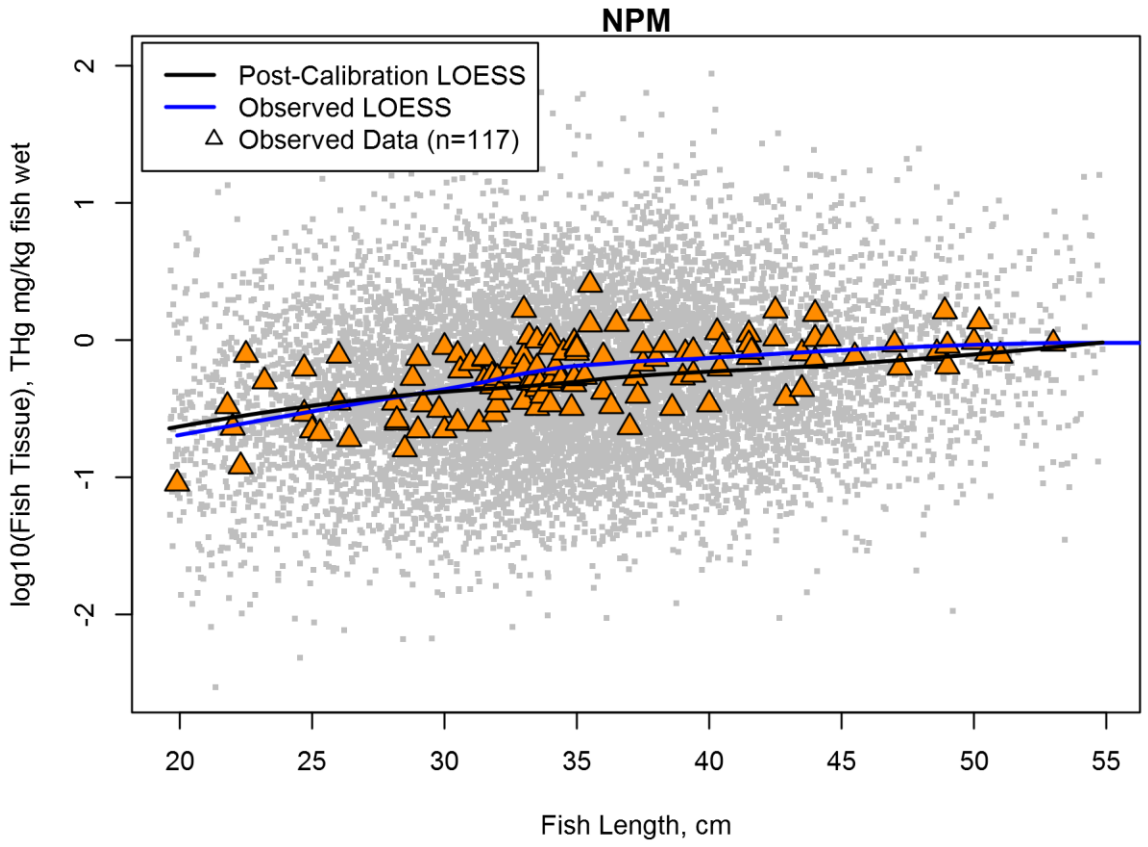

Figure 3-6. Post-Calibration Plot for Northern Pikeminnow

Note: Orange triangles are observed data; gray points show the results of 10,000 Monte Carlo simulation runs.

Table 3-2. List of Input Distribution Parameters for the 2006 FWM and the Updated FWM

Info		2006 FMW (TMDL App B Values)			Updated FWM		
Variable Name (in R code)	**Units**	**Distribution Name**	**Parameter Estimates**	**Updated During 2006 Calibration?**	**Distribution Name**	**Parameter Estimates**	**Change Notes**
Environmental Variables							
water_Hg2	ng/L	Lognormal[§]	mean=1.32, sd=1.45		Inverse Weibull	shape=1.962, scale=0.364	Distribution updated to new data
water_MeHg	ng/L	Lognormal	mean=0.06, sd=0.03		Inverse Gamma	shape=2.531, scale=0.053	Distribution updated to new data
HgTranslatorDistr	unitless	Lognormal	mean=0.056, sd=0.082, upper bound = 1		Normal	mean= 0.0161 sd=0.0006	See Section 4.3 for more information
water_Temp	°C	Triangular	6.0, 12.5, 22.0		Triangular	1.65, 5.9, 24.71	Distribution updated to new data
MeHg Bioconcentration Factor (BCF)							
BCF_MeHg_DET	L/kg	LogTriangular	2.50, 3.00, 3.50		LogTriangular	2.50, 3.00, 3.50	
BCF_MeHg_AQP	L/kg	LogTriangular	0.80, 2.15, 3.50		LogTriangular	0.80, 2.15, 3.50	
BCF_MeHg_PHY	L/kg	Triangular	3.50, 4.50, 5.50		LogTriangular	3.50, 4.50, 5.50	Parameters updated to match CB Excel file
BCF_MeHg_PER	L/kg	Triangular	3.50, 4.50, 5.50		LogTriangular	3.50, 4.50, 5.50	Parameters updated to match CB Excel file
BCF_MeHg_ZOO	L/kg	LogTriangular	2.45, 3.90, 5.40		LogTriangular	2.45, 3.90, 5.40	
BCF_MeHg_AQL	L/kg	LogTriangular	2.80, 3.40, 4.10		LogTriangular	2.80, 3.40, 4.10	
BCF_MeHg_AQC	L/kg	LogUniform	2.45, 5.40		LogUniform	2.45, 5.40	
BCF_MeHg_AQI	L/kg	LogTriangular	2.80, 3.15, 3.50		LogTriangular	2.80, 3.15, 3.50	
BCF_MeHg_AQM	L/kg	LogTriangular	3.00, 4.20, 5.40		LogTriangular	3.00, 4.20, 5.40	
BCF_MeHg_AQW	L/kg	LogTriangular	2.00, 2.65, 3.30		LogTriangular	2.00, 2.65, 3.30	
BCF_MeHg_MOST_FISH	L/kg	LogTriangular	3.00, 4.50, 6.00		LogTriangular	3.00, 4.50, 6.00	
BCF_MeHg_BLU	L/kg	LogTriangular	3.00, 6.50, 7.00	Yes	LogTriangular	3.00, 6.50, 7.00	
Ingestion Rate (IR)							
IR_BLU	unitless	Constant	i=0.022, j=0.85		Constant	i=0.070, j=0.85	Parameter updated during calibration
IR_CAR	unitless	Constant	i=0.022, j=0.85		Constant	i=0.080, j=0.55	Parameter updated during calibration
IR_CTT	unitless	Constant	i=0.022, j=0.85		Constant	i=0.008, j=0.85	Parameter updated during calibration
IR_LMB	unitless	Constant	i=0.022, j=0.85		Constant	i=0.015, j=1.0	Parameter updated during calibration
IR_LSS	unitless	Constant	i=0.022, j=0.85		Constant	i=0.082, j=0.85	Parameter updated during calibration
IR_NPM	unitless	Constant	i=0.022, j=1.0		Constant	i=0.0172, j=0.55	Parameter updated during calibration
IR_SMB	unitless	Constant	i=0.022, j=0.85		Constant	i=0.011, j=0.55	Parameter updated during calibration
IR_RBT	unitless	Constant	i=0.022, j=0.85		Constant	i=0.025, j=0.85	Parameter updated during calibration
MeHg Assimilation Efficiency (AE)							
AE_MeHg_ZOO	unitless	Triangular	0.20, 0.50, 0.80		Triangular	0.20, 0.50, 0.80	

Info		2006 FMW (TMDL App B Values)			Updated FWM		
Variable Name (in R code)	Units	Distribution Name	Parameter Estimates	Updated During 2006 Calibration?	Distribution Name	Parameter Estimates	Change Notes
AE_MeHg_AQL	unitless	Triangular	0.50, 0.73, 0.95		Triangular	0.50, 0.73, 0.95	
AE_MeHg_AQC	unitless	Uniform	0.50, 0.95		Uniform	0.50, 0.95	
AE_MeHg_AQI	unitless	Uniform	0.50, 0.95		Uniform	0.50, 0.95	
AE_MeHg_AQM	unitless	Triangular	0.50, 0.75, 0.95		Triangular	0.50, 0.73, 0.95	Parameters updated to match CB Excel file
AE_MeHg_AQW	unitless	Uniform	0.50, 0.95		Uniform	0.50, 0.95	
AE_MeHg_BLU	unitless	Triangular	0.45, 0.60, 0.95		Triangular	0.70, 0.75, 0.80	Distribution updated during calibration
AE_MeHg_RBT	unitless	Triangular	0.35, 0.50, 0.95	Yes	Triangular	0.55, 0.60, 0.65	Distribution updated during calibration
AE_MeHg_NPM	unitless	Triangular	0.40, 0.45, 0.50	Yes	Triangular	0.55, 0.60, 0.65	Distribution updated during calibration
AE_MeHg_LBM	unitless	Triangular	0.50, 0.55, 0.60	Yes	Triangular	0.70, 0.75, 0.80	Distribution updated during calibration
AE_MeHg_CAR	unitless	Triangular	0.10, 0.10, 0.30	Yes	Triangular	0.70, 0.75, 0.80	Distribution updated during calibration
AE_MeHg_LSS	unitless	Triangular	0.15, 0.25, 0.30	Yes	Triangular	0.70, 0.75, 0.80	Distribution updated during calibration
AE_MeHg_CTT	unitless	Triangular	0.20, 0.30, 0.50	Yes	Triangular	0.70, 0.75, 0.80	Distribution updated during calibration
AE_MeHg_SMB	unitless	Triangular	0.05, 0.10, 0.95	Yes	Triangular	0.68, 0.73, 0.78	Distribution updated during calibration
AE BW adjustment for all fish species	unitless	Not used			Constant	g = 5E-4, h = -1.30	Updated during calibration
MeHg Elimination Rate (k_2)							
ER_MeHg_ZOO	d-1	LogTriangular	-1.17, -0.69, -0.22		LogTriangular	-1.17, -0.69, -0.22	
ER_MeHg_AQL	d-1	LogTriangular	-1.48, -1.00, -0.52		LogTriangular	-1.48, -1.00, -0.52	
ER_MeHg_AQC	d-1	LogTriangular	-1.37, -1.06, -0.76		LogTriangular	-1.37, -1.06, -0.76	
ER_MeHg_AQI	d-1	LogUniform	-1.48, -1.00, -0.52		LogUniform	-1.48, -1.00, -0.52	
ER_MeHg_AQM	d-1	LogUniform	-3.00, -0.22		LogUniform	-3.00, -0.22	
ER_MeHg_AQW	d-1	LogUniform	-2.00, -0.22		LogUniform	-2.00, -0.22	
ER_MeHg_BLU	d-1	Normal	c(0.066, 0.019)*		Normal	c(0.066, 0.019)	
	d-1	Normal	d(0.22, 0.06)*	Yes	Normal	d(0.22, 0.06)	
	d-1	Normal	f(6.56, 0.45)*		Normal	f(7.0, 0.45)	Distribution updated during calibration
ER_MeHg_RBT	d-1	Normal	c(0.066, 0.019)*		Normal	c(0.066, 0.019)	
	d-1	Normal	d(0.20, 0.06)*	Yes	Normal	d(0.20, 0.06)	
	d-1	Normal	f(6.56, 0.45)*		Normal	f(7.0, 0.45)	Distribution updated during calibration
ER_MeHg_SMB	d-1	Normal	c(0.066, 0.019)*		Normal	c(0.066, 0.019)	
	d-1	Normal	d(0.30, 0.06)*	Yes	Normal	d(0.30, 0.06)	
	d-1	Normal	f(6.56, 0.45)*		Normal	f(5.8, 0.10)	Distribution updated during calibration
ER_MeHg_NPM	d-1	Normal	c(0.066, 0.019)*		Normal	c(0.066, 0.019)	
	d-1	Normal	d(0.28, 0.06)*	Yes	Normal	d(0.28, 0.06)	
	d-1	Normal	f(6.56, 0.45)*		Normal	f(5.8, 0.10)	Distribution updated during calibration

Info		2006 FMW (TMDL App B Values)			Updated FWM		
Variable Name (in R code)	Units	Distribution Name	Parameter Estimates	Updated During 2006 Calibration?	Distribution Name	Parameter Estimates	Change Notes
ER_MeHg_LMB	d-1	Normal	c(0.066, 0.019)*		Normal	c(0.066, 0.019)	
	d-1	Normal	d(0.18, 0.06)*	Yes	Normal	d(0.18, 0.06)	
	d-1	Normal	f(6.56, 0.45)*		Normal	f(7.0, 0.10)	Distribution updated during calibration
ER_MeHg_LSS	d-1	Normal	c(0.066, 0.019)*		Normal	c(0.066, 0.019)	
	d-1	Normal	d(0.54, 0.06)*	Yes	Normal	d(0.54, 0.06)	
	d-1	Normal	f(6.56, 0.45)*		Normal	f(7.0, 0.45)	Distribution updated during calibration
ER_MeHg_CTT	d-1	Normal	c(0.066, 0.019)*		Normal	c(0.066, 0.019)	
	d-1	Normal	d(0.20, 0.06)*	Yes	Normal	d(0.20, 0.06)	
	d-1	Normal	f(6.56, 0.45)*		Normal	f(7.0, 0.45)	Distribution updated during calibration
ER_MeHg_CAR	d-1	Normal	c(0.066, 0.019)*		Normal	c(0.066, 0.019)	
	d-1	Normal	d(0.55, 0.06)*	Yes	Normal	d(0.55, 0.06)	
	d-1	Normal	f(6.56, 0.45)*		Normal	f(5.8, 0.45)	Distribution updated during calibration
Hg[II] Bioconcentration Factor (BCF)							
BCF_Hg2_DET	L/kg	LogTriangular	2.50, 3.00, 3.50		LogTriangular	2.50, 3.00, 3.50	
BCF_Hg2_AQP	L/kg	LogTriangular	0.50, 1.65, 2.80		LogTriangular	0.50, 1.65, 2.80	
BCF_Hg2_PHY	L/kg	LogTriangular	2.90, 3.45, 4.00		LogTriangular	2.90, 3.45, 4.00	
BCF_Hg2_PER	L/kg	LogTriangular	2.90, 3.45, 4.00		LogTriangular	2.90, 3.45, 4.00	
BCF_Hg2_ZOO	L/kg	LogTriangular	3.40, 3.65, 3.90		LogTriangular	3.40, 3.65, 3.90	
BCF_Hg2_AQL	L/kg	LogTriangular	2.10, 3.20, 4.30		LogTriangular	2.10, 3.20, 4.30	
BCF_Hg2_AQC	L/kg	LogTriangular	2.00, 2.25, 2.50		LogTriangular	2.00, 2.25, 2.50	
BCF_Hg2_AQI	L/kg	LogTriangular	2.60, 3.25, 3.90		LogTriangular	2.60, 3.25, 3.90	
BCF_Hg2_AQM	L/kg	LogTriangular	2.30, 2.60, 2.90		LogTriangular	2.30, 2.60, 2.90	
BCF_Hg2_AQW	L/kg	LogTriangular	2.30, 2.78, 3.25		LogTriangular	2.30, 2.78, 3.25	
BCF_Hg2_FISH	L/kg	LogTriangular	0.70, 2.20, 3.70		LogTriangular	0.70, 2.20, 3.70	
Hg[II] Assimilation Efficiency (AE)							
AE_Hg2_ZOO	unitless	Triangular	0.50, 0.60, 0.90		Triangular	0.50, 0.60, 0.90	
AE_Hg2_AQL	unitless	Triangular	0.50, 0.60, 0.90		Triangular	0.50, 0.60, 0.90	
AE_Hg2_AQC	unitless	Triangular	0.50, 0.60, 0.90		Triangular	0.50, 0.60, 0.90	
AE_Hg2_AQI	unitless	Triangular	0.50, 0.60, 0.90		Triangular	0.50, 0.60, 0.90	
AE_Hg2_AQM	unitless	Triangular	0.01, 0.04, 0.12		Triangular	0.01, 0.04, 0.12	
AE_Hg2_AQW	unitless	Triangular	0.50, 0.60, 0.90		Triangular	0.50, 0.60, 0.90	
AE_Hg2_FISH	unitless	Triangular	0.112, 0.172, 0.264		Triangular	0.112, 0.172, 0.264	
Hg[II] Elimination Rate (k2)							
ER_Hg2_INVERTS	d-1	LogTriangular	-1.89, -0.89, 0.10		LogTriangular	-1.89, -0.89, 0.10	

Info		2006 FMW (TMDL App B Values)			Updated FWM		
Variable Name (in R code)	Units	Distribution Name	Parameter Estimates	Updated During 2006 Calibration?	Distribution Name	Parameter Estimates	Change Notes
Body Weight (BW)							
BW_ZOO	g	Triangular	1.4e-5, 3.3e-5, 7.6e-5		Triangular	1.4e-5, 3.3e-5, 7.6e-5	
BW_AQL	g	Triangular	4e-4, 6.25e-4, 9.8e-4		Triangular	4e-4, 6.25e-4, 9.8e-4	
BW_AQC	g	LogUniform	-1.00, 0.60		LogUniform	-1.00, 0.60	
BW_AQI	g	Triangular	4e-4, 6.25e-4, 9.8e-4		Triangular	4e-4, 6.25e-4, 9.8e-4	
BW_AQM	g	Estimate of mollusk weight not required as an estimated body-weight normalized intake rate was available					
BW_AQW	g	LogUniform	0.0023, 0.019		LogUniform	-2.63, -1.72	Parameters updated to match CB Excel file
BW_BLU	g	Deterministic	0.0500*L^2.8702		-	0.0500*L^2.8702	
BW_NPM	g	Deterministic	0.0060*L^3.1079		-	0.0110*L^2.9535	Distribution updated to new data
BW_LMB	g	Deterministic	0.0185*L^2.9920		-	0.0081*L^3.1864	Distribution updated to new data
BW_LSS	g	Deterministic	0.0175*L^2.8687		-	0. 0543*L^2. 5481	Distribution updated to new data
BW_CAR	g	Deterministic	0.0280*L^2.8289		-	0.0280*L^2.8289	
BW_RBT	g	Deterministic	0.0146*L^2.9748		-	0.0146*L^2.9748	
BW_CTT	g	Deterministic	0.0090*L^3.0044		-	0.0090*L^3.0044	
BW_SMB	g	Deterministic	0.0120*L^3.0570		-	0. 0303*L^ 2.7931	Distribution updated to new data
Food Intake Rate (IR)							
IR_ZOO	g/d	LogTriangular	-1.04, -0.56, -0.09		LogTriangular	-1.00, -0.56, -0.09	Parameters updated to match CB Excel file
IR_AQL	g/d	LogUniform	-1.00, -0.39		LogUniform	-1.00, -0.39	
IR_AQC	g/d	LogUniform	-1.00, -0.39		LogUniform	-1.00, -0.39	
IR_AQI	g/d	LogUniform	-1.00, -0.39		LogUniform	-1.00, -0.39	
IR_AQM	g/d	LogTriangular	-1.65, -1.525, -1.40		LogTriangular	-1.65, -1.525, -1.40	Central estimate based on 0.025 g/g/d as in Hope (2006)
IR_AQW	g/d	LogUniform	-1.00, -0.39		LogUniform	-1.00, -0.39	
Fish Length (L)							
L_BLU_j	cm	Uniform	1.0, 10.3		Uniform	1.0, 10.3	
L_NPM_j	cm	Uniform	1.0, 12.0		Uniform	1.0, 19.6	Updated based on Hankin and Richards (2000)
L_LMB_j	cm	Uniform	1.0, 17.2		Uniform	1.0, 17.2	
L_LSS_j	cm	Uniform	1.0, 22.3		Uniform	1.0, 22.3	
L_CAR_j	cm	Uniform	1.0, 18.8		Uniform	1.0, 18.8	
L_RBT_j	cm	Uniform	1.0, 21.5		Uniform	1.0, 21.5	
L_CTT_j	cm	Uniform	1.0, 21.5		Uniform	1.0, 21.5	
L_SMB_j	cm	Uniform	1.0, 16.2		Uniform	1.0, 19.0	Corrected to Hope (2006), Table 4

Info		2006 FMW (TMDL App B Values)			Updated FWM		
Variable Name (in R code)	**Units**	**Distribution Name**	**Parameter Estimates**	**Updated During 2006 Calibration?**	**Distribution Name**	**Parameter Estimates**	**Change Notes**
L_BLU_a	cm	Weibull	location=90.93, scale=76.80, shape=1.5869		Weibull	location=90.93, scale=76.80, shape=1.5869	
L_NPM_a	cm	Logistic	mean=38.3.00, scale=3.80		Logistic	location=34.470, scale=4.114	Distribution updated to new data
L_LMB_a	cm	Beta	a=6.50, b=6.50, scale=67.860		Inverse Normal	mean= 32.378, shape=374.486	Distribution updated to new data
L_LSS_a	cm	Logistic	mean=45.804, scale=3.01		Logistic	mean=44.958, scale=2.586	Distribution updated to new data
L_CAR_a	cm	Logistic	mean=55.441, scale=4.52		Logistic	mean=55.441, scale=4.52	
L_RBT_a	cm	Pareto	location=21.394, shape=5.61		Pareto	location=21.394, shape=5.61	
L_CTT_a	cm	Beta	a=16.26, b=4.65, scale=35.64		Beta	a=16.26, b=4.65, scale=35.64	
L_SMB_a	cm	Uniform	19.00, 41.00		Inverse Weibull	shape=7.612, scale=27.018	Distribution updated to new data
Lifespan							
T_ZOO	d	Uniform	10, 20		Uniform	10, 20	
T_AQL	d	Uniform	30, 360		Uniform	30, 360	
T_AQC	d	Uniform	30, 360		Uniform	30, 360	
T_AQI	d	Uniform	30, 360		Uniform	30, 360	
T_AQM	d	Uniform	30, 360		Uniform	30, 360	
T_AQW	d	Uniform	30, 360		Uniform	30, 360	
Predator - Prey Size Ratio (fish only)							
LMB	unitless	Normal	0.340, 0.028		Normal	0.340, 0.028	
NPM	unitless	Triangular	0.225, 0.25, 0.275		Triangular	0.275, 0.300, 0.325	Distribution updated during calibration
All other fish	unitless	Triangular	0.225, 0.25, 0.275		Triangular	0.225, 0.25, 0.275	

* c, d, and f refer to parameters in the methylmercury elimination rate equation, cT – d lnBW + e – f, where T is surface water temperature (°C), BW is fish body weight (g), and e is the acute/chronic exposure value (unitless) set to 0.73 (0.24 standard error for chronic, 0 for acute. g and h are additional terms added to the elimination rate equation as $g \cdot \exp(0.06\,T) \cdot BW^{h}$.

§ For the 2006 TMDL, Crystal Ball's default parameterization for the lognormal distribution uses the arithmetic mean and standard deviation, whereas R's default parameterization uses the mean of the logarithms (meanlog) and their standard deviation (sdlog). Lognormal parameter values were converted to meanlog and sdlog where needed for the updated FMW.

3.6 Discussion

The FWM is a steady-state approximation of a complex and dynamic reality. For each model realization, the FWM assumes that exposure concentrations are constant and that changes in rate parameters for mercury uptake and elimination can be predicted solely based on body weight and a constant water temperature selected from the range of median water temperatures throughout the WRB. In reality, neither exposure concentration nor water temperature are constant in time, nor are growth, uptake, and elimination rates, which are likely to vary by sex as well as season. These factors limit the ability of the FWM to exactly reproduce the tails of the observed fish tissue mercury CDFs.

As seen from the model experiments reported in Section 3.4, a primary factor controlling the tails of the CDF, especially for higher trophic level fish, is the specification of the distribution of exposure concentrations. For a steady-state model, the exposure concentrations should, in theory, be represented as the distribution of long-term means or medians across locations throughout the WRB. Existing MeHg water column monitoring data are insufficient to specify this distribution with accuracy – especially considering the large number of censored data. In addition, existing sampling is not evenly distributed across the WRB, and fish tissue samples are available from many more locations than MeHg samples, so the exposure concentration distribution is likely biased in relation to the fish tissue samples. At this time, these appear to be irreducible uncertainties in the FWM approach. Model calibration, however, ensures that the FWM represents the observed median and any discrepancy in the tails of the distribution will be of limited importance as the ultimate water column target and the resulting allocations are developed using the median results.

Another portion of the FWM that likely affects results is the specification of predator-prey relationships. One observation from the model calibration exercise is that LMB and NPM have rather different slopes to their fish tissue mercury CDFs, yet are specified as having essentially identical predator-prey matrices. Calibration experiments showed that a better fit for NPM could be obtained with AE greater than 1. This is not physically possible, and was therefore not used, but suggests that NPM are consuming a greater proportion of more contaminated prey species compared to LMB than is represented in the FWM.

Food habits of NPM have been the subject of a fair amount of study because they consume a significant number of juvenile salmonids. However, studies in the Columbia River system (e.g., Zimmerman, 1999; Naughton and Bennett, 2003) also suggest that even large NPM are likely to consume a significant amount of crayfish and other crustaceans. The FWM model, as currently designed, assumes that the likelihood of a given fish consuming higher trophic level prey is entirely a function of relative body weight (as estimated from length) and a uniform 0 – 1 probability of consumption of specific prey types as allowed in the predator-prey matrix. Better definition of these probabilities based on gut content analysis might help to better resolve the observed data. However, data do not appear to be available, nor is it within the current scope, to better refine predator-prey interaction probabilities in the FWM.

3.7 Food Web Model Results

For each Monte Carlo run, the FWM calculates estimates of BMFs and THg tissue concentration distributions for eight fish species. Because the output from the updated FWM is stochastic, the results are summarized using the median value, with 5th and 95th percentiles used to quantify uncertainty. Table 3-3 provides the final BMF estimates. Table 3-4 presents the updated fish tissue concentration distribution estimates. The 95th percentile estimates tend to be greater than the maximum observed

concentrations; however, the 90th percentile estimates are more consistent with the range of observed results.

Table 3-3. Updated FWM Biomagnification Factors (BMFs; L/kg) for Fish Tissue THg Concentrations (mg/kg wet weight) as a Function of Water Column dMeHg Concentration (mg/L)

Fish Species	Mean	Standard Deviation	5th %ile	Median	95th %ile
BLU	1.90E+07	3.99E+07	1.34E+06	7.76E+06	7.29E+07
CAR	9.67E+06	1.07E+07	1.92E+06	6.77E+06	2.68E+07
CTT	4.36E+06	7.84E+06	3.00E+05	2.23E+06	1.48E+07
LMB	2.93E+07	7.04E+07	1.40E+06	1.15E+07	1.06E+08
LSS	8.64E+06	9.72E+06	1.63E+06	5.97E+06	2.41E+07
NPM	3.40E+07	5.93E+07	3.48E+06	1.83E+07	1.08E+08
RBT	9.02E+06	1.68E+07	4.62E+05	4.30E+06	3.07E+07
SMB	1.34E+07	2.61E+07	1.18E+06	7.21E+06	4.35E+07

Table 3-4. Estimated FWM Fish Tissue THg Concentrations (mg/kg wet weight)

Fish Species	Mean	Standard Deviation	5th %ile	Median	90th %ile	95th %ile
BLU	0.66	2.02	0.03	0.20	1.42	2.49
CAR	0.33	0.65	0.03	0.17	0.69	1.06
CTT	0.15	0.38	0.01	0.06	0.32	0.54
LMB	1.00	3.17	0.03	0.29	1.98	3.70
LSS	0.30	0.61	0.03	0.15	0.63	0.96
NPM	1.16	3.00	0.07	0.47	2.47	4.10
RBT	0.30	0.87	0.01	0.11	0.67	1.14
SMB	0.46	1.26	0.02	0.18	0.98	1.58

Notes: The calculations for Table 3-3 and Table 3-4 include both lotic (river/stream) and lentic (lake/reservoir) samples consistent with the decision to create a single FWM for the entire WRB that matches the structure of Hope (2006). In Table 3-4, the mean and standard deviation are calculated across all fish lengths. About one quarter of the fish samples are from reservoirs, which in general tend to have elevated fish tissue concentrations compared to rivers and natural lakes (Willacker et al., 2016).

The definition of BMF used by Hope [a cumulative BMF] differs from the terminology used by USEPA (2001b), in which the BMF is defined as the relationship between one trophic level (TL) and the next lower trophic level. In USEPA's definition, the BMF for TL 2 is equal to the concentration in TL 2 fish divided by the concentration in TL 1 organisms. Hope instead uses the bioaccumulation factor (BAF) to represent the ratio between concentration in fish of a given TL and ambient exposure concentrations of dissolved MeHg.

Hope (2006) also defines the BAF in a slightly different way as the sum of direct bioconcentration from water to organism, e.g., through gill uptake (represented by a bioconcentration factor [BCF]) and a food term relative to concentrations in lower TLs:

Level 1: $BCF_1 = C_B/C_W$

Level 2: $BAF_2 = BCF_2 + f_2BCF_1$

Level 3: $BAF_3 = BCF_3 + f_3BCF_2 + f_3f_2BCF_1$

Level 4: $BAF_4 = BCF_4 + f_4BCF_3 + f_4f_3BCF_2 + f_4f_3f_2BCF_1$

where C_B is the concentration of chemical in biota (mg/kg), C_W is the exposure concentration in water (mg/L), BCF_k is the bioconcentration factor for the k^{th} trophic level (L/kg), BAF_k is the bioaccumulation factor for the k^{th} trophic level (unitless), and f_K is the food term for the k^{th} trophic level. The food terms are expanded to account for multiple prey types, weighted by dietary fraction.

Following the work of Fordham and Reagan (1990), Hope (2006) notes that the BAFs at TL 2 or higher are not directly additive because this would result in BCFs at lower trophic levels being counted more than once. Instead, Hope (2006) defines BMFs relative to the exposure concentration as follows:

Level 1: $BMF_1 = BCF_1 = C_B/C_W$

Level 2: $BMF_2 = (BCF_2 + \Sigma f_2BCF_1)\cdot f_E$

Level 3: $BMF_3 = (BCF_3 + \Sigma f_3BMF_2)\cdot f_E$

Level 4: $BMF_4 = (BCF_4 + \Sigma f_4BMF_3)\cdot f_E$

Where the food term (f_n) is summed over all food-chain pathways for a given species and f_E is the fraction of equilibrium attained by a prey item at time of consumption or analysis, randomly sampled from the age distribution and MeHg elimination rate distribution for a given species. At TL 3 and TL 4, f_E is typically near 1 for adult fish.

Expanding the iterative definitions of the TL 3 BMF and BAF and assuming, for simplicity of algebra in this example, that a fish in one TL consumes only a single species from the next lower TL, we see:

$BMF_3 = BCF_3\cdot f_E + (f_3BCF_2 + f_3f_2BCF_1)\cdot f_E^2$, and

$BAF_3 = BCF_3 + f_3BCF_2 + f_3f_2BCF_1$.

In addition to the full Monte Carlo BMF calculation evaluating bioaccumulation along multiple food chain pathways, the two representations differ in that the BMF calculation accounts for the fraction of equilibrium (f_E), while the BAF calculation does not. Nonetheless, it is appropriate to compare BMFs (as defined by Hope) from the FWM to BAFs as estimated by USEPA, as both relate concentrations in fish at a given trophic level to dissolved MeHg concentrations in water.

As part of the development of the MeHg criterion, USEPA (2001b, Appendix A) undertook a thorough re-evaluation of data on MeHg BAFs. Three different methods were used. These are, in order of USEPA preference: (1) the direct method, based on the ratio of the chemical concentration in tissue and water; (2) the indirect method, where a BAF is derived by multiplying a BCF by a food chain multiplier, in which the food chain multiplier is the product of BMFs (where the BMF is as defined by USEPA, i.e., the ratio of chemical concentration in one TL to the next lower TL), and (3) a modified direct approach based on the ratio of concentration in tissue and water, but where the water dissolved MeHg concentration was estimated based on chemical translator relationships to other forms of mercury. Tables A-1 through A-9 in USEPA (2001b) summarize the various types of BAF estimates, including separation by lentic versus

lotic systems. The indirect results were discarded due to uncertainties regarding specific food chain pathways in many data sets and lentic and lotic results were combined because there was not a statistically significant difference between the two. Table A-9 in USEPA (2001b) gives the final recommendations for national BAFs, summarized as the median of the distribution but also providing the 95th percentile value. USEPA's discussion of uncertainty in the BAF calculation notes that the lotic BAFs are primarily based on data from canals in the Everglades and a point-source-contaminated stream in Tennessee, while the lentic BAF data are biased toward northern oligotrophic lakes, primarily in the Great Lakes region. In addition, the range of species used was relatively small: Much of the available TL 4 data was limited to walleye, pike, or bass, while much of the TL 3 data were for bluegill and perch. Applicability of the national recommendations to the WRB is uncertain.

USEPA (2010) revisited the issue of MeHg BAFs and "cautions water quality managers that methylmercury bioaccumulation is generally viewed as a site-specific process and that BAFs can vary greatly across ecosystems, leading to significant risk of being either under-protective or over-protective when the national BAF numbers are used." For this reason, USEPA (2010) instead indicated a preference for site-specific BAFs. The FWM model, calibrated to observed distributions, is essentially a data-based BAF (or BCF) calculation method that takes into account characteristics of individual fish species in the WRB.

Despite potential shortcomings, it is useful to compare the BMFs (in the sense used by Hope, 2006) calculated from WRB data for adult fish to the range of BAFs presented in USEPA (2001). As the WRB cumulative BMFs tend to be higher than the median of the distribution presented in Table A-9 of USEPA (2001), we compare the BMFs to the median and 95th percentile of the distribution in Table 3-5. Except for bluegill, the WRB BMFs are between the median and 95th percentile of the national BAFs, as is also shown graphically in Figure 3-7.

Table 3-5. Comparison of [Cumulative] BMFs Calculated for the Willamette River Basin to USEPA's (2001) Draft National BAFs (L/kg)

Trophic Level	Species	WRB Cumulative BMF (Median)	Draft National BAF, Median	Draft National BAF, 95$^{\%le}$.
TL 3	Bluegill (BLU)	7.76E+06	6.80E+05	6.23E+06
	Carp (CAR)	6.77E+06		
	Cutthroat Trout (CTT)	2.23E+06		
	Rainbow Trout (RBT)	4.30E+06		
	Largescale Sucker (LSS)	5.97E+06		
TL 4	Largemouth Bass (LMB)	1.15E+07	2.67E+06	2.84E+07
	Smallmouth Bass (SMB)	7.21E+06		
	Northern Pikeminnow (NPM)	1.83E+07		

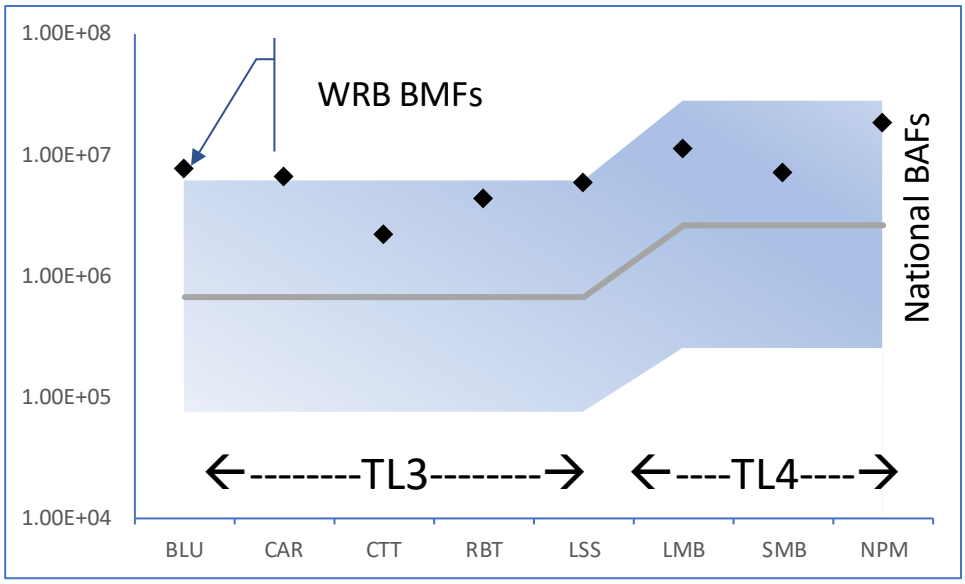

Figure 3-7. Comparison of Willamette BMFs and National BAFs (L/kg)

It is not surprising that carp have a high BMF, as they tend to feed in the sediment and thus may be exposed to greater concentrations of MeHg than are present in the water column. The calculated BMF for bluegill appears to be larger than expected. This could be due to the relatively small size of the historic sample and lack of updated data. From 2002 on there have been 81 bluegill samples collected and analyzed, but all were juveniles collected during July and August 2011 and all from the mainstem of the Willamette River. The FWM assigns a direct BCF for MeHg to bluegill that is higher than any other species, which may account for the high estimated BMF. The sensitivity analysis reported in Table 6 of Hope (2006) suggests that that the BCF is the major contributor to variance in predicted concentrations in bluegill, and that this uncertainty in turn contributes around 11 and 12 percent of the variance in predicted tissue concentrations in largemouth bass and northern pikeminnow. The BMFs for higher trophic level fish, recalculated using the approach of Hope (2006) and updated with newer data, are consistent with the range of national BAFs presented in USEPA (2001).

4.0 MERCURY TRANSLATOR MODEL

In the 2006 TMDL (Hope, 2006), the Mercury Translator Model was used to convert from THg (the form of mercury most commonly measured) to dMeHg (the form that dominates bioaccumulation in the food web). The translator is an empirically determined ratio or statistical model, not a process-based model. Fish THg concentrations are influenced by numerious environmental variables and as a result the spatial variablity in figh THg concentrations is not directly correlated with sediment THg concentrations and only weakly correlated with sediment MeHg concentrations (Eagles-Smith et al., 2016b; Alpers et al., 2016). However, it has proven difficult to predict mercury methylation in the environment. Methylation is a bacteria-mediated process that occurs under low oxygen conditions as a byproduct of the reduction of SO_4 or other terminal electron acceptors for oxidation of organic carbon compounds. Rates of methylation are a complex function of the interaction of redox conditions, microbial populations, temperature, and the carbon and sulfur cycles. Empirical relationships of MeHg to THg based on monitoring from specific waterbodies can be a more reliable approach than detailed simulation. Therefore an empirical analysis approach is retained for the present work, but updated with new data.

4.1 CHALLENGES FOR THE MERCURY TRANSLATOR

There are two important challenges for implementing the mercury translator: data censoring and non-contemporaneity. Data censoring refers to the fact that a large proportion of the MeHg data is not precisely quantified and reported only as below the method detection limit. Non-contemporaneity refers to the concern that the THg present in the water column at a given time is not necessarily a good measure of the THg supply that gave rise to the contemporaneous observations of dMeHg.

4.1.1 THE TRANSLATOR AND CENSORED DATA

In accordance with the QAPP, the translator analysis uses data from 2002 to present; however, data from small streams in the immediate vicinity of the Black Butte Mine tailings were omitted from the translator analysis because they contain some extremely high THg concentrations that are atypical of the rest of the basin, often in conjunction with proportionately very low MeHg concentrations. Initial exploratory analysis suggested that the issue of censored data is paramount in completing this analysis. There are 382 observations for dissolved dMeHg and total MeHg (tMeHg), and 582 observations of THg in water (2002 to present). Because there are multiple observations for some days and locations, paired MeHg and THg observations resolve to 297 unique day-sampling site pairs with which to analyze the translator relationships.

Within these pairs there are a substantial number of censored (below detection limit) data (flagged as “U” or “<”, depending on the source). There are also a substantial number of estimated results (flagged as “J, “Est”, or “E”, depending on the source). The estimated data are results that lie between the method detection limit (MDL) and the practical quantitation limit (PQL). The MDL is the minimum level at which one can be 99 percent sure that the analyte of interest is present, while the PQL is the minimum concentration of an analyte (substance) that can be measured with a high degree of confidence that the analyte is present at or above that concentration – in other words, a level at which the concentration signal can clearly be distinguished from the noise. USEPA suggests “It is recommended that all values between the PQL and MDL be reported. They are real, the concentration is fuzzy, but their values can give indications of trends and should be reported” (USEPA, Region 3, 2006).

The frequency of non-detects and estimated values in the paired data set is summarized in Table 4-1. Note that more than one half of the dMeHg data and more than a third of the tMeHg data fall into these categories.

Table 4-1. Frequency of Non-detects and Estimated Values in WRB Paired Mercury Translator Data

Analyte	Non-detects	Estimated Values
dMeHg	41.9%	11.5%
tMeHg	19.4%	16.85%
THg	12.7%	2.1%

We are primarily interested in the ratio of dMeHg to THg (or, equivalently, the slope of the linear regression between the two). Fortunately, the denominator of the ratio (THg) has relatively few non-detects and estimated values, but the dMeHg samples have nearly 42 percent non-detects. It is essential to properly address the influence of censoring in the analysis.

Censored data can be analyzed using either parametric approaches (in which a distributional form for the data is assumed) or non-parametric approaches (with no distributional assumption). For environmental data, it is common to assume that a lognormal distribution is applicable. This is done primarily because the lognormal distribution is non-negative and exhibits a skew, usually with a long right tail, similar to most environmental data; however, it is rarely the case that environmental data closely match the lognormal or any other single distributional form. Therefore, it is preferable to use either non-parametric approaches, where available, or "robust" approaches that use distributional assumptions only for the censored portion of the data. Details of application of methods for dealing with censored data depend also on whether paired data are used and so are postponed until Section 4.1.3.

4.1.2 NON-CONTEMPORANEITY

Available observations of dMeHg and THg are primarily from the water column. Methylation of mercury, however, occurs primarily under hypoxic conditions, - mostly in saturated soils in wetlands or riparian areas or in the sediment or in stratified bottom waters of reservoirs. The overall approach for this TMDL makes the assumption that THg in the water column (averaged over an appropriate period) is an indicator of the soluble inorganic mercury supply that is available for methylation. However, it does not necessarily follow that individual pairs of simultaneously observed dMeHg and THg will reflect the relationship between mercury supply and the creation of MeHg. Instead, it is more likely that the relationship will reflect the ratio between the central tendency of THg supply and methylation rate over time. Specifically, local measurements of dMeHg and THg are likely to be related to one another in part through equilibrium with local surface sediment conditions.

There are two general ways to approach the ratio calculation. The first, as was done for the 2006 TMDL (Hope, 2006), is to work directly with paired sample data to estimate the slope of the relationship between dMeHg and contemporaneous THg concentrations in water. An alternative choice is to calculate the average or median dMeHg and THg concentrations for a location (possibly subset by season) and then obtain the ratio between the averages or medians. We refer to this as an aggregate approach. The aggregate approach is attractive from a conceptual perspective if it is theorized that methylation occurs primarily in the sediment, in which case the relationship between dMeHg and THg in the water column is indirect and the methylation potential is more closely related to the average supply of THg (as inferred from the water column measurements) than to a single paired measurement matched in time.

The ultimate goal of the analysis is to translate a target dMeHg concentration (derived from the Food Web Model [FWM]) to a THg concentration target. The FWM is steady state and the target from the FWM is thus a temporal average target. From this perspective, the aggregate approach is a simpler and more direct means of getting to the desired answer.

4.1.3 Addressing Censoring in Paired and Aggregated Data

The paired and aggregate approaches to the water column data require different approaches to address censoring. For the first case (slope of relationship between paired data), a parametric distribution assumption is not required to address censoring; instead a non-parametric estimate of slope can be made using the Akritas-Theil-Sen estimator described by Helsel (2005) and available in the "NADA" R package. For the second case, non-detects must be addressed in the calculation of local means, medians, and variances. Helsel (2005) originally recommended using a Kaplan-Meier (KM) approach to estimating statistics when there is less than 50 percent censoring and either Maximum Likelihood Estimation (MLE) or Regression on Order Statistics (ROS) when there is 50-80 percent censoring. However, Helsel later recognized that KM analysis is biased when there is a single censoring level located at or near the lowest detected concentration, as is the case here. More recent recommendations from the USEPA National Nonpoint Source Monitoring Program (Bolks et al., 2014) are to use robust ROS methods for sample sizes less than 50 with up to 80 percent censoring and for sample sizes greater than 50 with up to 50 percent censoring, and to use MLE for sample sizes greater than 50 and 50-80 percent censoring. Both are available in the NADA package. The MLE approach generally assumes a lognormal distribution for environmental data. The robust ROS approach uses the quantified data directly, but assumes a lognormal distribution for the censored data.

When a large fraction of the data is censored, the median is a much more stable estimate of the central tendency of the distribution than the mean or geometric mean. Therefore, it is preferable to use the median as a summary statistic. The median (which is an unbiased estimator of the geometric mean of a lognormally distributed variable) is also an appropriate measure of the typical exposure over time that contributes to food chain bioaccumulation.

4.2 Exploratory Data Analysis

Initial investigations were made to explore the data prior to selecting a final method for the translator. These included examining the influence of spatial variability, paired versus aggregated approaches, weighted versus unweighted regressions, influence of inclusion of data from the Coast Fork HUC8, and seasonal versus annual approaches.

4.2.1 Spatial Variability

THg concentrations show spatial variability across the WRB. To explore spatial variability, we grouped data by HUC8. Results by HUC8 (with censored data imputed using robust ROS) are shown in a box and whisker plot in Figure 4-1.

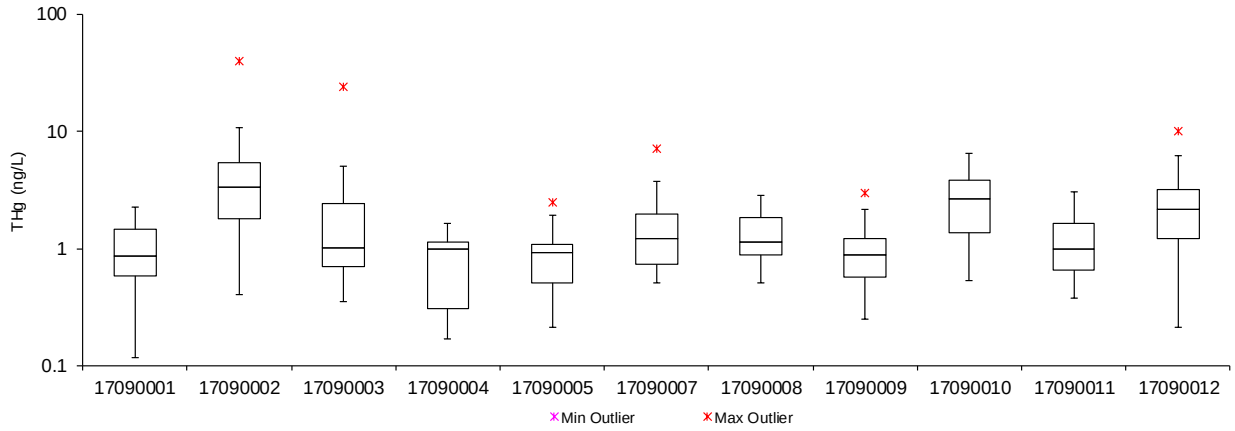

Figure 4-1. Distribution of THg Observations by HUC

Note: The box shows the interquartile range (25th to 75th percentile), and the centerline is the median (50th percentile). The "whiskers" extend 1.5 times the interquartile range from the median, and the maximum and minimum outliers (if any) beyond the whiskers are also plotted. THg observations collected between 2012 and 2019 in the Tualatin and Lower Willamette HUCs are not included as these data were provided after the public comment period for Oregon DEQ's TMDL submittal.

For most HUC8s, the median THg concentration is close to 1 ng/L, with higher medians in HUC 17090002 (Coast Fork), 17090010 (Tualatin), and 17090012 (Lower Willamette).

Although there appear to be some spatial trends in THg, the ratios of tMeHg to THg are relatively constant across HUC8s (Figure 4-2), especially for those HUC8s that have large sample sizes. Sample counts are printed on each bar in Figure 4-2. It is not the case that there are no statistically significant differences between samples for individual HUC8s. A non-parametric Kruskal-Wallis test for comparing populations (Gilbert, 1987) yields a test statistic of Kw = 61, which is greater than the chi-square quantile for df = 8 and 5 percent probability level, indicating rejection of the null hypothesis that the ratios are drawn from the same distribution for all HUC8s. A parametric ANOVA test (implying a normal distribution assumption) yields the same conclusion. However, the few contrasts between HUC8s that appear to indicate statistically significant differences (e.g., 17090001 vs. 17090010) have small sample sizes (n=17 and 9, respectively) and the HUC8s with larger sample sizes yield relatively consistent ratios. From a practical perspective, reliably calculating different translators by HUC8 would not be feasible due to small sample size in many of the HUCs. The inclusion or exclusion of eight paired and uncensored reservoir samples from Cottage Grove in HUC 17090002 (with ratios from 0.01 to 0.08) does not change the interquartile range. (Paired MeHg and THg samples are not available from other reservoirs in the WRB.) The currently available data thus do not support a need for separate spatial analysis of ratios on a HUC by HUC basis.

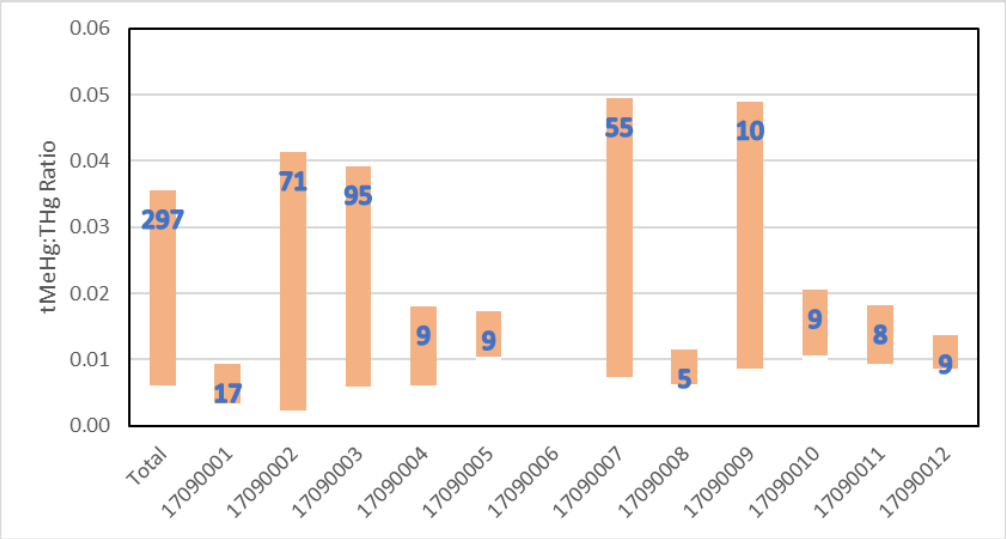

Figure 4-2. Interquartile Range of tMeHg to THg Ratios by HUC8

Note: Labels on bars show sample count.

4.2.2 Paired versus Aggregated Approach

We conducted estimation of the Mercury Translator Model using both the paired data (Akritas-Theil-Sen slope) and aggregated data (robust ROS estimation of medians by HUC8, followed by linear regressed weighted by sample size) approaches. A scatterplot of the paired dMeHg and THg observations shows only a weak linear relationship (Figure 4-3) The linear relationship has an adjusted R^2 value of 0.054, and a slope coefficient of 0.0037 with probability value of <0.001. Thus, the linear relationship explains less than 6 percent of the observed variability, although the slope is significantly different from zero at a 95 percent confidence level. The evident weakness of a direct relationship between THg and dissolved MeHg suggests that there are other important variables that are also influencing this relationship.

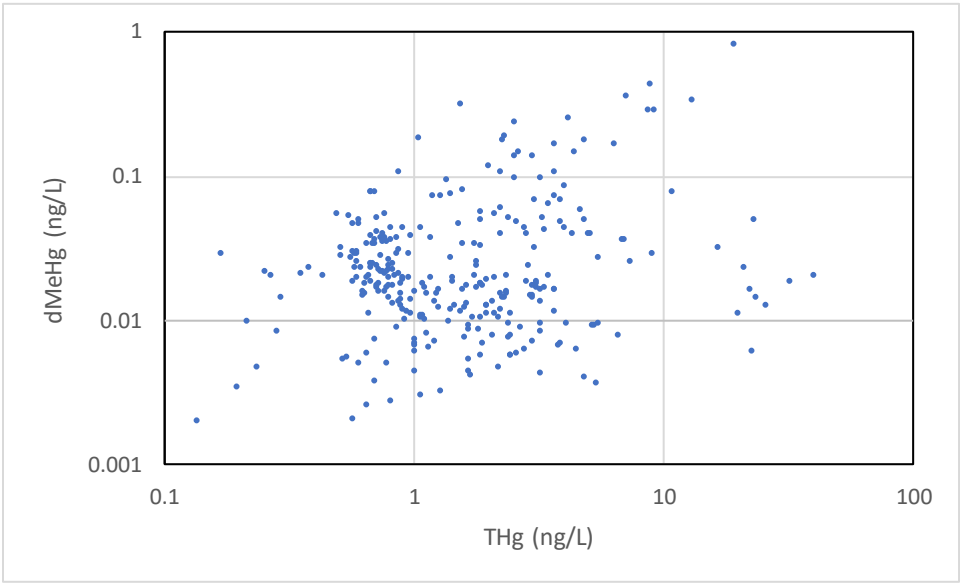

Figure 4-3. Scatterplot of paired dMeHg and THg Observations

As discussed in Section 4.1.2, there are theoretical reasons to suspect that the paired data would not yield a strong predictive relationship and that an aggregate approach may be preferable. The conceptual model in Section 4.1.2 hypothesizes that average dMeHg exposure concentration is correlated with long-term THg load (which can be normalized as flow-weighted concentration), not with contemporaneous ambient THg concentrations. MeHg produced during summer periods of high biological activity is believed to be derived from THg loads accrued during the preceding year. However, THg load is not directly measured and cannot be reliably estimated from limited samples of concentration data. To achieve adequately large datasets to assess translation from dMeHg to THg it is necessary to aggregate samples in space and time. Available data are not sufficient to support the development of separate ratios by HUC8 but HUC8 boundaries provide a useful basis for assembling aggregate samples to define a basin-wide Translator (Section 4.2.1). Because average concentrations are highly leveraged by anomalous outliers, median dMeHg and THg concentrations from aggregated sample datasets were used to develop the basin-wide Translator.

A sample relationship (using the medians by HUC8 as they are more robust against outliers and not accounting for seasonal variability) is shown in Figure 4-4. This suggests that the aggregate approach can yield an approximately linear relationship and may be useful to account for different relationships in areas with higher mercury concentrations. A final translator estimate based on aggregate medians should likely use a weighted regression to account for uneven sample sizes among the HUC8s. A zero-intercept weighted least squares regression on the medians yields a slope of 0.0160 with standard error (SE) of 0.0006 and a probability value of < 0.0001. The corrected squared correlation coefficient (R^2) is 0.99, indicating strong explanatory power. Use of a zero-intercept model is justified based on the finding that an intercept term was not significantly different from zero and the theoretical assumption that no dMeHg should be present when there is no THg. The standard formula for R^2 (1 – [error sum of squares] / [total sum of squares]) can sometimes produce negative results when calculated for a zero-intercept model. To account for this, the default in R software is to adjust the formula for the total sum of squares from $\Sigma(y-\bar{y})^2$ to $\Sigma(y-0)^2$

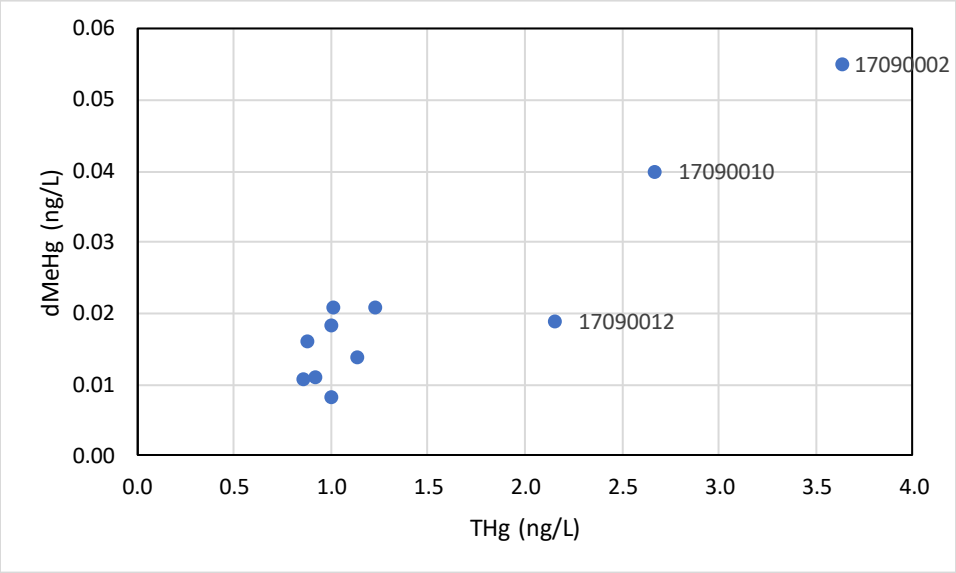

Figure 4-4. Example of Spatial Aggregate Relationship between dMeHg and THg (Medians by HUC8)

4.2.3 Seasonal Variability

The 2006 TMDL noted that the ratio of dMeHg to THg appeared to be higher in the warm summer months when biological activity is greater. This is due both to an increase, on average, in dMeHg in summer and a decrease of THg concentrations (Table 4-2). Analysis of the ratio between average dMeHg and THg by month data (Figure 4-5) suggested that a different, higher translator ratio might be appropriate in June through October than in November through May.

Table 4-2. Two-Sample *t* Tests on Summer vs. Winter dMeHg and THg Concentrations

Season	dMeHg (ng/L)	THg (ng/L)
June - October	0.041	2.78
November - May	0.021	4.27
p value of significant difference	0.0019	0.0033

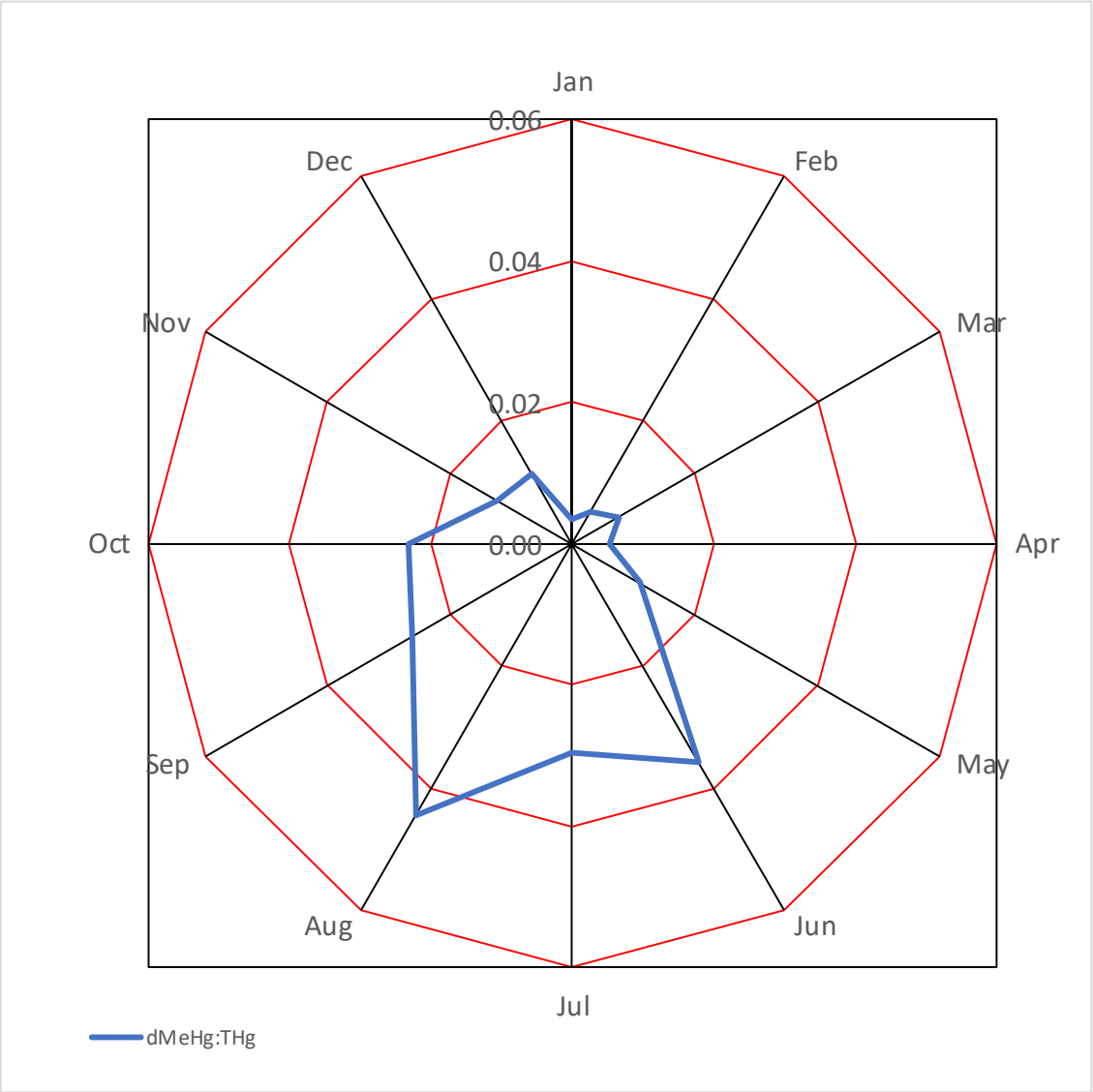

Figure 4-5. Ratio of Average dMeHg to THg by Month

While there do appear to be seasonal differences in the relationship between dMeHg and THg, mercury bioaccumulation is a result of long term, not instantaneous exposure. Riva-Murray et al. (2013) suggest it is most appropriate to use whole-year average values of dMeHg exposure concentrations to describe the relationship between mercury in fish tissue and mercury in the water column.

We undertook several analyses to compare seasonal versus annual models. The results (along with results from various other exploratory scenarios described below) are summarized in Table 4-3. It is further evident from Figure 4-6 that the confidence intervals on the slope estimates are much wider in summer and have less consistency between methods than the whole-year analyses. This suggests that it is preferable to use the annual rather than seasonal analysis. Use of annual results also avoids the issue that dMeHg present in the summer may be derived from THg that was transported during winter high flow periods. Comparison between seasonal and whole-year regressions is shown graphically below in the context of inclusion of Coast Fork Willamette data in the analysis (Figure 4-7 through Figure 4-10), as discussed in the following sections.

Table 4-3. Statistics for Hg Translator Scenarios

Scenario	Season	Slope	Slope SE	Slope P-value	Lower 95%CL	Upper 95%CL	R^2
WLS, All Data	Year	0.0160	0.0006	<0.0001	0.0147	0.0174	0.99
	Summer	0.0347	0.0021	<0.0001	0.0300	0.0393	0.96
	Winter	0.0070	0.0006	<0.0001	0.0057	0.0083	0.93
OLS, All Data	Year	0.0145	0.0010	<0.0001	0.0123	0.0167	0.96
	Summer	0.0260	0.0038	<0.0001	0.0175	0.0346	0.82
	Winter	0.0086	0.0010	<0.0001	0.0063	0.0109	0.87
WLS, No Coast Fork	Year	0.0164	0.0013	<0.0001	0.0136	0.0193	0.95
	Summer	0.0305	0.0038	<0.0001	0.0220	0.0391	0.88
	Winter	0.0075	0.0011	0.0001	0.0050	0.0101	0.83
OLS, No Coast Fork	Year	0.0145	0.0012	<0.0001	0.0118	0.0172	0.94
	Summer	0.0219	0.0038	0.0003	0.0134	0.0305	0.79
	Winter	0.0101	0.0013	<0.0001	0.0071	0.0131	0.86

Note: WLS = weighted least squares; OLS = ordinary least squares, as described in Section 4.2.4. SE = standard error, P-value = probability value, CL = confidence limit.

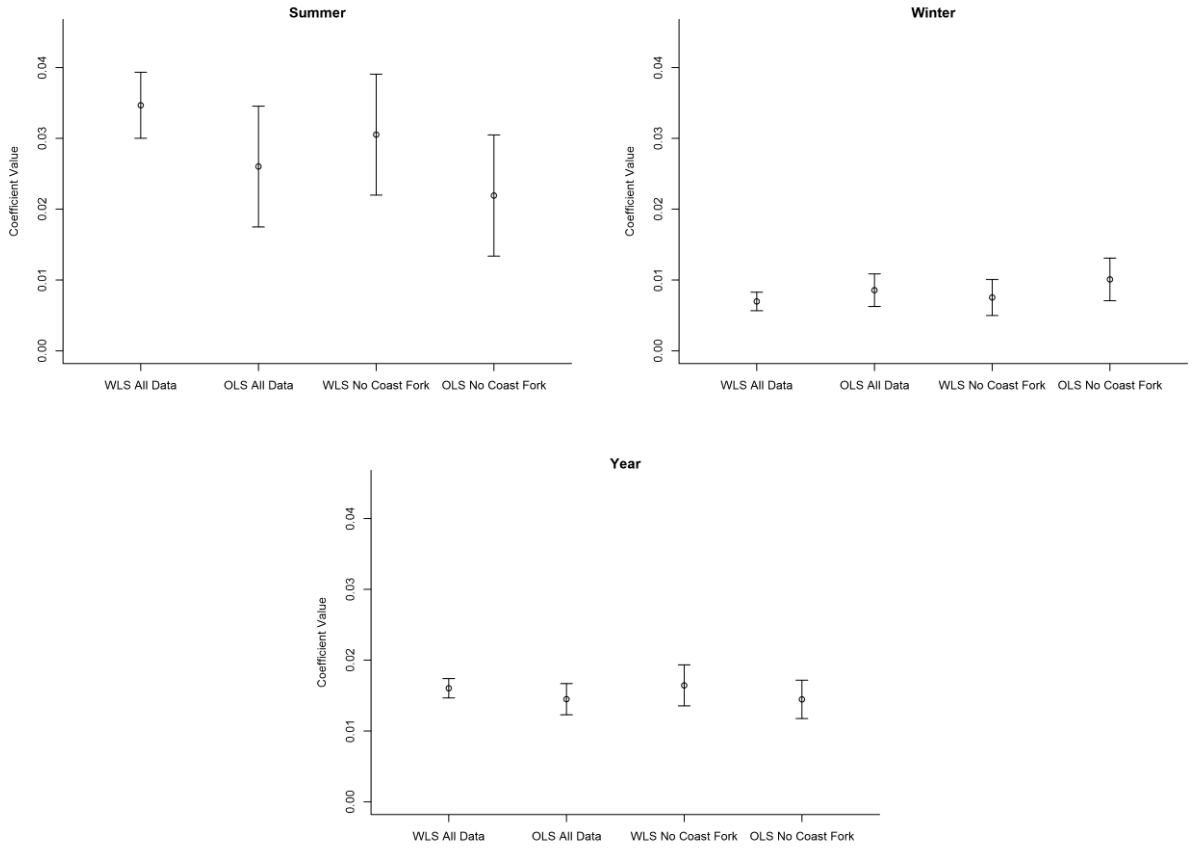

Figure 4-6. 95% Confidence Intervals on the Estimated Slopes for Seasonal and Annual Hg Translator Scenarios

4.2.4 Weighted versus Unweighted Regression Analyses

Even when aggregated to the HUC8 scale, sample sizes remain small for many aggregates. The conceptual model relates observations of average dMeHg concentrations to a measure of THg load. We assume that flow-normalized load (equivalent to flow-weighted average THg concentration) can be represented through use of median THg concentration as a surrogate measure. However, results from small sample sizes have a high risk of being unrepresentative of the central tendency of THg loading in a given pattern. To help compensate for this issue we evaluated use of a weighted regression approach to develop an overall estimate of the Translator relationship. This approach does bias the results towards basins where more data have been collected; however, an approach that attempts to reflect any geographical differences is not feasible with the sample data available for this document.

To account for the wide range of sample sizes among the HUC8 aggregates we use weighted least squares (WLS) regression with zero intercept in which the counts of dMeHg samples (by HUC8) are used as weights. To test the possibility of bias being introduced by the weighting, we also ran the analyses using ordinary least squares (OLS), in which each HUC8 median is given equal weight. Results are presented graphically in Figure 4-7 and again in Figure 4-8 with the Coast Fork Willamette results

removed. Statistics for all scenarios (OLS and WLS, with and without the Coast Fork data) are shown above in Table 4-3.

All models were significant (P-value <0.0005), with relatively large R^2 values ranging from 0.79 to 0.99. Fitted slope coefficients differ between WLS and OLS fits. This is because the data were not distributed equally across the river basin. Data points on the WLS plots are color-coded (darker equals more samples) to indicate sampling frequency for the HUC. It is evident that the OLS slopes are influenced by a few HUC's with only limited samples. There are seven HUC8s with between one and ten samples (and one HUC8 with no samples), while three HUC8s have more than 50 samples. Despite differences in estimates, the confidence intervals on the slopes overlap for the WLS and OLS estimates, especially for the annual slopes. Therefore, we retained the WLS approach.

Figure 4-7 and Figure 4-8 contain a shaded range. The top of this range represents the typical Practical Quantitation Limit (PQL) for dMeHg of 0.05 ng/L. The PQL is the minimum concentration of an analyte that can be measured with a high degree of confidence that the analyte is present at or above the reported concentration. The PQL, determined by the laboratory, is higher than the method detection limit (MDL), which is the minimum concentration at which one can be 99 percent sure that the analyte is present. Data between the MDL and the PQL are reported, but flagged as estimated values. These values are used in the median calculations; even though they are uncertain on an individual basis, collectively they contribute information on the distribution. Many of the site medians fall within this "gray" range, while several are below the MDL and are thus projected estimates from the ROS method. While emphasizing the uncertainty of the procedure, this does not constitute a major problem to application of the Translator because the slope is largely determined by the higher-concentration points.

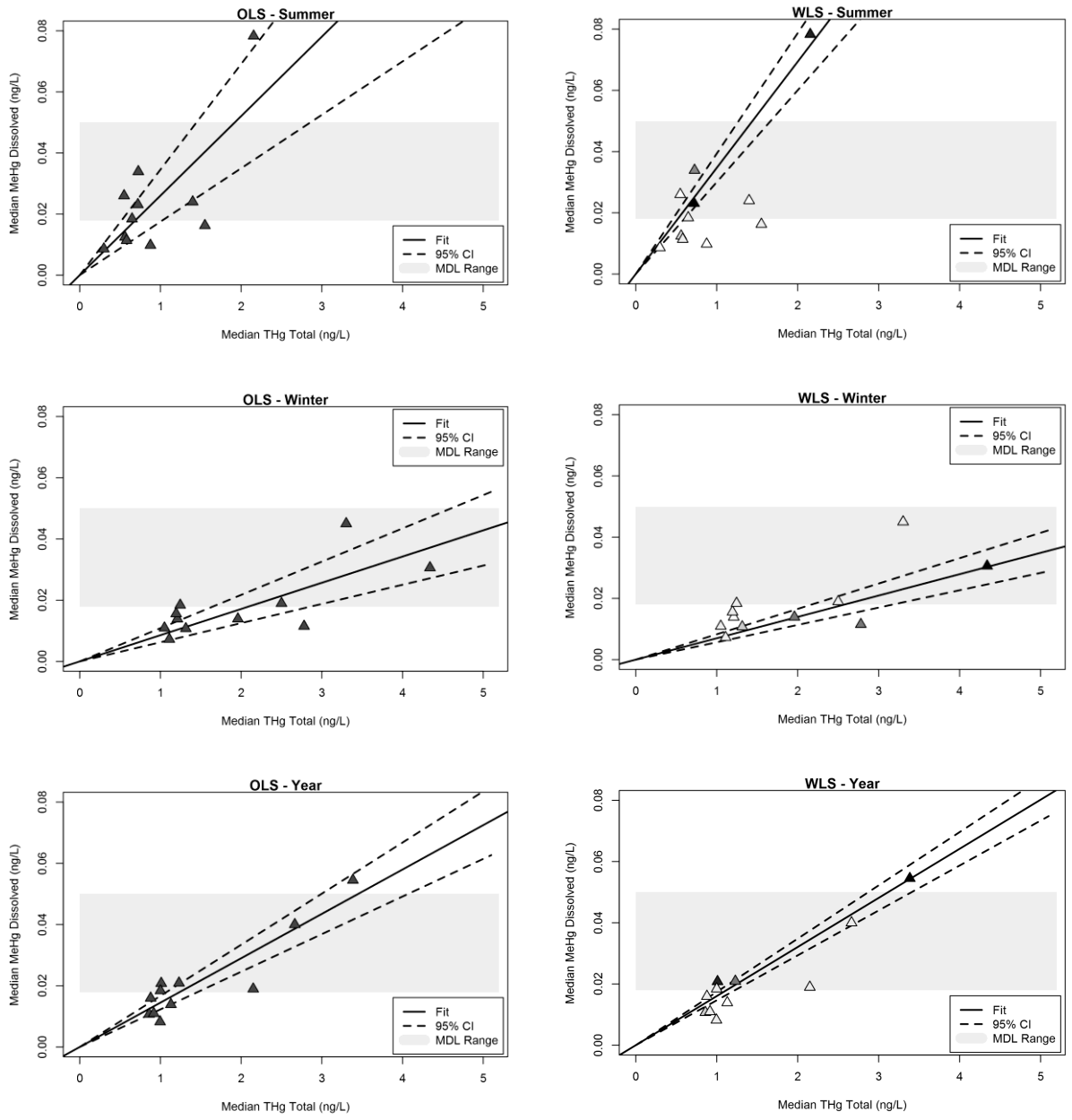

Figure 4-7. Scatterplots and Fitted Lines, using All Data. *Left*: Ordinary Least Squares (OLS). *Right*: Weighted Least Squares (WLS).

Note: Data points are median values for each HUC8. WLS data points are color-coded, with darker colors indicating a larger sample count for that HUC (see Figure 4-2 for sample sizes).

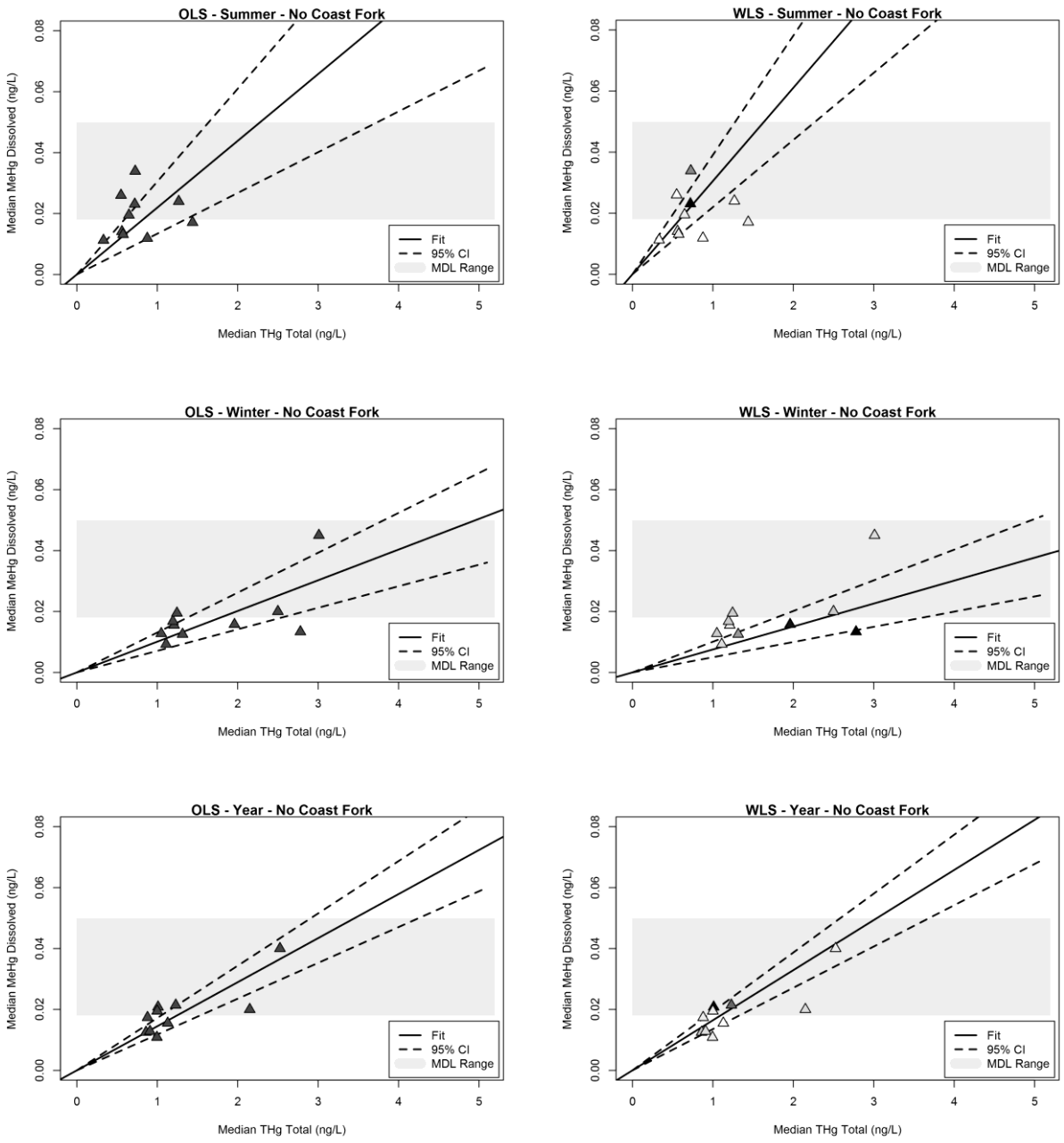

Figure 4-8. Scatterplots and Fitted Lines, with Coast Fork (HUC 17090002) Removed. *Left*: Ordinary Least Squares (OLS). *Right*: Weighted Least Squares (WLS).

Note: Data points are median values for each HUC8. WLS data points are color-coded, with darker colors indicating a larger sample count for that HUC (see Figure 4-2 for sample sizes).

4.2.5 Effect of Inclusion of Coast Fork Willamette Data

Internal reviewers noted that the apparent strength of the aggregate regression – especially the seasonal regression for summer conditions – was influenced by the high-concentration results for the Coast Fork Willamette (HUC 17090002). Figure 4-9 and Figure 4-10 replot the scenarios to provide side-by-side comparison of analyses with and without inclusion of the data from the Coast Fork Willamette HUC8, which has by far the highest THg and dMeHg concentrations. These results are also shown above in Table 4-3. The estimated slopes are nearly identical between the "all data" and "no Coast Fork" scenarios, differing only in the fourth decimal place. Therefore, it does not appear that inclusion of the Coast Fork data biases the estimates and it is not recommended to analyze this part of the watershed separately.

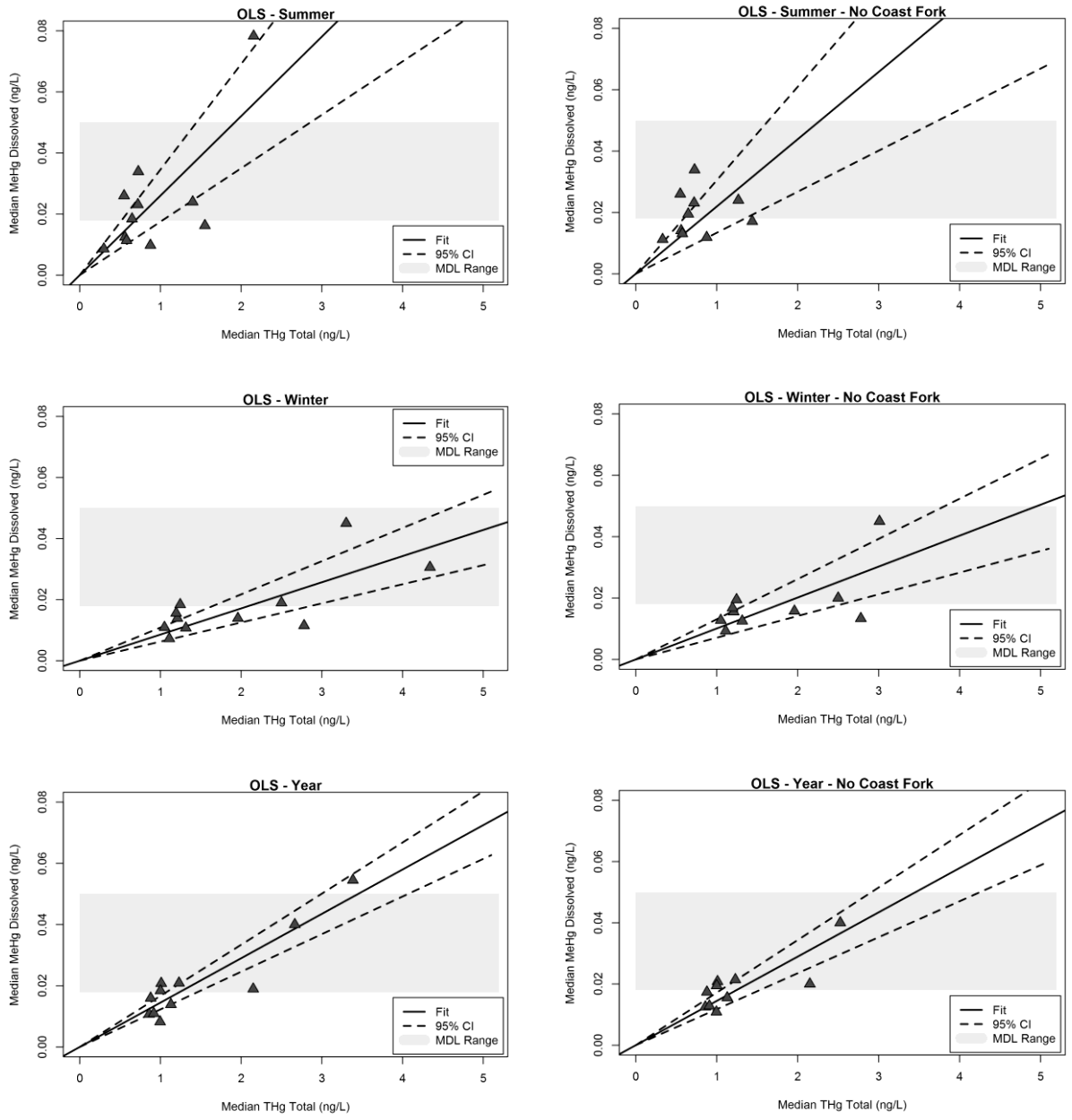

Figure 4-9. Scatterplots and Ordinary Least Squares (OLS) Fitted Lines, Comparison with and without Inclusion of Coast Fork (HUC 17090002)

Note: Data points are median values for each HUC8

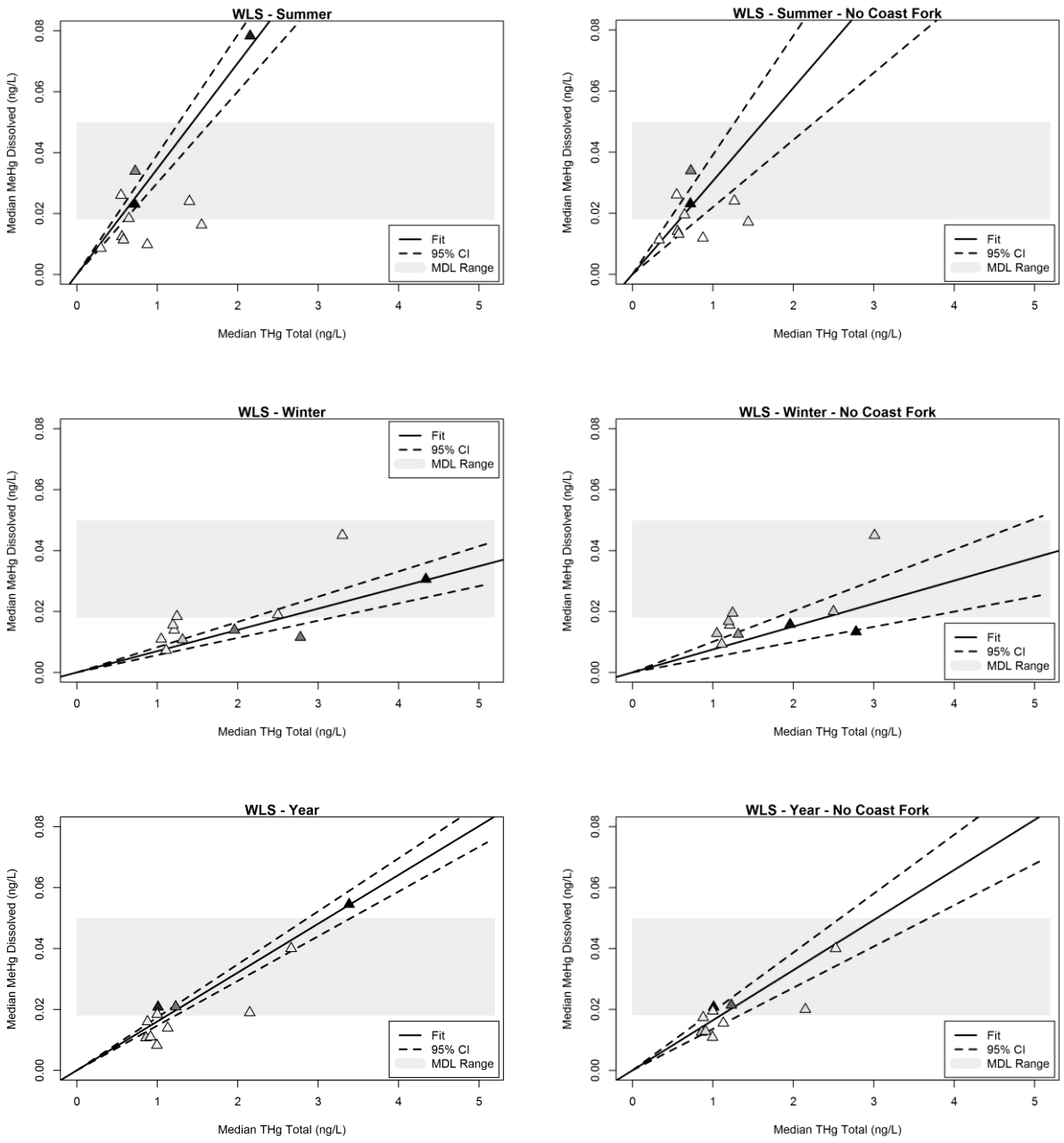

Figure 4-10. Scatterplots and Weighted Least Squares (WLS) Fitted Lines, Comparison with and without Inclusion of Coast Fork (HUC 17090002)

Note: Data points are median values for each HUC8. WLS data points are color-coded, with darker colors indicating a larger sample count for that HUC (see Figure 4-2 for sample sizes).

4.2.6 Final Mercury Translator Approach

Based on the analyses presented in the preceding sections, the final Mercury Translator Model is structured as follows:

- The translator is constructed using aggregated data consisting of medians by HUC8.
- Central tendencies in the data are characterized by the median, which is an appropriate measure of typical chronic exposure concentrations over time, rather than the mean. Use of the median also reduces the influence of outliers and data censoring on the results.
- The analysis is performed on a whole-year basis.
- The analysis uses weighted least squares in a zero-intercept model with weighting by the number of available dMeHg samples per HUC8.
- Exploratory analyses indicate that it is neither necessary nor feasible to develop different translators for different parts of the watershed; an analysis across all stations is sufficient, including observations from the Coast Fork Willamette.

The final translator model fit is shown in Figure 4-11. The slope estimate for this model is 0.0160 (dMeHg:THg), with standard error of 0.0006. The Mercury Translator is included in the Monte Carlo simulations for the FWM as a Normal distribution with these parameters.

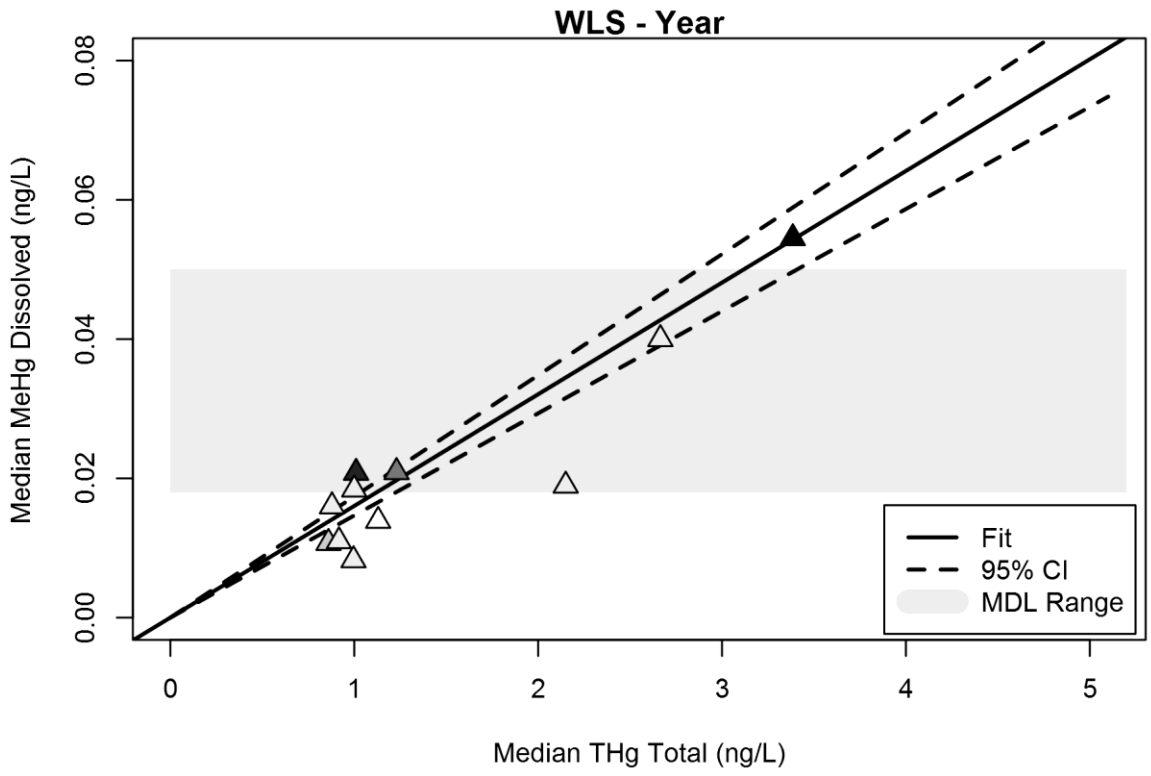

Figure 4-11. Final Mercury Translator Model: Aggregated, Year-round, Zero-Intercept Model by HUC8 Weighted by Sample Size

Note: Data points are median values for each HUC8. WLS data points are color-coded, with darker colors indicating a larger sample count for that HUC (see Figure 4-2 for sample sizes).

4.3 TRANSLATING MEHG TARGETS TO THG TARGETS

Surface water mercury target levels are calculated by combining the updated FWM (Section 0) with the Mercury Translator Model to estimate potential water column THg targets associated with meeting the fish tissue MeHg criterion concentration (Table 4-4). As in Hope (2006), the target concentration is estimated from the BMF for each Monte Carlo run as:

$$TL_n = \left[\frac{TC}{BMF_{ME,n} \cdot \Omega}\right] \cdot CF$$

where:

TL_n is the total mercury target level for the n^{th} fish species (ng/L),
TC is the revised fish tissue criterion for MeHg in fish (0.040 mg/kg),
$BMF_{ME,n}$ is the biomagnification factor for the n^{th} fish species (L/kg – see Table 3-3),
Ω represents the Mercury Translator, and
CF is a conversion factor ($1 \cdot 10^6$ ng/mg).

It is important to realize that this calculation is part of the Monte Carlo simulation, in which 10,000 iterations are done across the distributions of both $BMF_{ME,n}$ and Ω. (That is, it is not a direct calculation of the median TL_n using the median BMF.) The analysis produces a distribution of TL_n values associated with individual samples and it is most relevant to look at the central tendency, in this case summarized by the median. Confidence intervals on the median are the relevant measures of uncertainty regarding targets. As the estimates are derived via a Monte Carlo simulation from many underlying inputs, the median TL_n does not have a parametric distribution and confidence intervals are based on bootstrap resampling of the Monte Carlo output.

Bootstrapping is a generic method of quantifying uncertainty for a statistic of interest (Efron, 1987; Davison and Kinkley, 1997). In nonparametric bootstrapping, the observed dataset (size=n) is resampled with replacement multiple times, creating multiple bootstrapped datasets each of size n. The statistic of interest (e.g., the median) is calculated for each of these bootstrapped datasets. Uncertainty is then quantified using the distribution of bootstrapped median values.

We used the R package "boot" to calculate the confidence intervals (Canty and Ripley, 2017) based on 1,000 bootstrap runs. In most applications, bootstrap datasets are the same size as the original dataset. For each fish species, there are 10,000 Monte Carlo runs; however, 10,000 is not the appropriate sample size for bootstrapping and would result in overly small confidence bounds. Instead, we use a random subset of size equal to the number of relevant environmental samples, specifically the count of 382 water column MeHg measurements on which exposure concentrations in the FWM are based. The bootstrap procedure was repeated 30 times and the confidence interval lower and upper bounds averaged, respectively, to minimize the effect of the pseudo-random seed. This procedure was repeated for each fish species. Resulting 95% confidence limits are also shown in Table 4-4.

Table 4-4. Species-specific Surface Water THg Target Levels (ng/L) to Meet a Fish Tissue Concentration of 0.040 mg/kg MeHg

Fish Species	Mean	Median	Lower 95% Confidence Limit on Median	Upper 95% Confidence Limit on Median
BLU	0.552	0.321	0.269	0.381
CAR	0.488	0.368	0.333	0.408
CTT	2.355	1.110	0.975	1.308
LMB	0.556	0.215	0.188	0.260
LSS	0.564	0.417	0.378	0.467
NPM	0.229	0.136	0.116	0.154
RBT	1.371	0.578	0.501	0.690
SMB	0.652	0.345	0.305	0.398

Notes: Target concentrations are calculated using a one-dimensional Monte Carlo analysis with the biomagnification factor and Ω specified as distributions.

As in Hope (2006), the most restrictive targets are obtained using the results for NPM. We use the *median* surface water THg target value for NPM for this purpose.

5.0 Mass Balance Model

5.1 Mass Balance Model Approach

The purpose of the Mass Balance Model is to provide estimates of the magnitude of mass fluxes of THg that control THg transport into and out of the WRB, distribute mercury within the water column and sediment of the Willamette River and its tributaries, and lead to bioaccumulation of mercury in fish. Specifically, the Mass Balance Model is used to (1) estimate the overall THg load in the WRB, and (2) estimate the fractions of the total load attributable to different source categories, including land use types and permitted point sources. This serves as a basis for understanding the relative contributions of different sources of THg and supports developing load allocations for nonpoint sources and wasteload allocations for permitted point sources.

The Mass Balance Model is supported by a previously developed watershed model of the WRB, described in Section 5.2. Section 5.3 tabulates the sources of THg load to the waterbodies of the WRB in the following categories: (1) atmospheric deposition, (2) soil matrix sources (including erosion), (3) groundwater loading, (4) mining sources, (5) publicly owned treatment works (POTW) sources and minor domestic wastewater treatment plants (WWTPs), (6) permitted industrial sources, and (7) urban stormwater, including permitted stormwater discharges. Processes within the stream network that affect THg delivery are discussed in Section 5.4. Finally, Section 5.5 combines the results of the previous sections to present the final THg mass balance for the WRB.

5.2 HSPF Watershed Model

The Mass Balance Model constructed for the 2006 TMDL (Hope, 2005) was based on a number of approximations and assumptions – especially in regard to delivery ratios for THg loads derived from atmospheric deposition and soil erosion. In large part, this was due to the lack of a pre-existing calibrated watershed model of the WRB, which required assumption of delivery ratios without mechanistic representation and calibration.

For the TMDL revision, we made use of an existing Hydrological Simulation Program – FORTRAN (HSPF; Bicknell et al., 2005) watershed model previously calibrated for flow and sediment in the WRB that was developed for USEPA by Tetra Tech and AQUA TERRA in 2010 (Butcher et al., 2013). The 2006 Mass Balance Model described the movement of dissolved and particulate THg as a function of the flow of water and movement of sediment, respectively. The mass balance analysis based on the watershed model uses a similar, but more rigorous, approach. Detailed representation of flow and sediment yield throughout the watershed derived from the HSPF model provides a more explicit basis for estimating delivery ratios from upland sources to streams. Specifically, the watershed model provides process-based estimates of flow volumes, surface and subsurface flow pathways, and the erosion and transport of particulate material from different land uses throughout the WRB. Both surface and subsurface flows contribute dissolved THg to streams. Overland flow carries dissolved THg across the landscape to streams. Subsurface flows that resurface and feed streams also carry dissolved THg. Overland and subsurface flow volumes simulated by the HSPF model were paired with mercury data to assess the mass transport of dissolved THg in the basin. The mass transport of particulate THg depends on soil erosion, and soil erosion rates simulated by the HSPF were paired with soil THg potency data

(weight of THg per weight of eroded soil) to establish particulate THg loads. The process-based simulation eliminates the need for empirical upland delivery ratios.

The HSPF model also provides estimates of the movement of water and sediment through the stream network. The sources of mercury included in the Mass Balance Model are similar to those used in ODEQ (2006) but are updated based on refined source information.

HSPF is a public domain and well-established model that has a long history of use in support of TMDL analyses. Model development was undertaken in accordance with an approved USEPA QAPP (Tetra Tech, 2008). Full details on the development and calibration of the HSPF model for the WRB are available in Butcher et al. (2013). The HSPF watershed model application incorporates the major reservoirs and point sources in the WRB and is implemented at a moderately coarse spatial scale (75 watersheds at approximately the HUC10 scale, see Figure 5-1) that results in short run times and is adequate for the annual load analyses required for the THg mass balance. The existing HSPF model was extended to add model subbasins and reaches in the lowermost segment of the Willamette River within HUC 07090012 for the Multnomah Channel[1] and Columbia Slough[2].

The existing HSPF model was implemented at an hourly time step for 1976 – 2005 and calibrated for flow and sediment. It used land cover information from the 2001 National Land Cover Database (NLCD) from the Multi-Resolution Land Characteristics Consortium (https://www.mrlc.gov/index.php).

For the WRB Mercury TMDL, land use was updated to the 2011 NLCD coverage (Section 5.2.1). The hourly time step output from the HSPF model is used to provide long-term and seasonal average results to describe the relative contribution of different sources of THg load. Because the Mass Balance Model focuses on long-term average conditions, we did not perform the considerable work necessary to extend the HSPF model to simulate more recent years explicitly, although more recent THg monitoring is used in the estimation of the long-term averages of concentrations at monitored locations. Extending the HSPF model in time up to the current year would require processing and updating meteorological data for 40 weather stations as well as updating flood control reservoir yearly operations and major permitted discharges. Use of a different time period for the HSPF model application (but with updated land use and point source discharges) to support the Mass Balance Model is acceptable because the primary purpose of the HSPF model in this context is to provide estimates of long-term average flow pathways, soil erosion rates, and associated delivery ratios by land use. Current estimates of flows and loads from permitted dischargers are incorporated into the source analysis as described in Sections 5.3.5 and 5.3.6.

It is important to note that the HSPF watershed model is not itself a mercury fate and transport model; rather it is applied to characterize THg transport mechanisms across the landscape for the Mass Balance Model. Information about flow volumes, surface and subsurface flow pathways, and erosion and particulate constituent transport is combined with data from other sources (e.g., gridded atmospheric deposition fluxes) to evaluate landscape-based THg loads.

[1] The lowest reaches of the Willamette mainstem as well as the Multnomah Channel are tidally influenced. HSPF does not simulate tidal mixing; however, the focus of the modeling is on long-term average concentrations and loads averaged over multiple tidal cycles.

[2] Columbia Slough is included within HUC 07090012 and is therefore within the scope of this TMDL; however, the Columbia Slough is upstream of the mouth of the Willamette and not closely tied to conditions within the Willamette itself. Therefore, only local sources draining directly to the Columbia Slough are calculated for this listed reach.

A conceptual framework diagram of the Mass Balance Model is shown in Figure 5-2. Information from the HSPF model is used to characterize flow pathways, associated flow rates, sediment erosion, and the transport of eroded sediment to streams. The upland land use in the model is represented by Hydrologic Response Units (HRUs), which are unique combinations of land use, soil infiltration characteristics (summarized by Hydrologic Soil Group or HSG), and weather zones that serve as the foundation of the upland simulation in HSPF (Figure 5-3). Upland hydrologic and water quality processes are simulated on a unit-area basis for each HRU, and then are routed to model reaches based on the area of the HRU within the model subbasin (these are of finer resolution compared to HUC8s in the basin). Non-point source loads were computed at the HRU level, and this approach allows for landscape-based THg loads to be tracked and attributed to different land use categories for the THg Mass Balance Model.

The HSPF model estimates soil erosion and the portion of rainfall that is converted to ground water or surface flow. Flow partitioning is used to estimate the fraction of atmospheric deposition that is washed directly into streams with surface runoff (Section 5.3.1). Watershed model simulation of sediment transport across the land surface accounts for delivery of soil matrix sources (Section 5.3.2). Finally, the watershed model also supports the analysis of THg transport and losses within the stream network (Section 5.4).

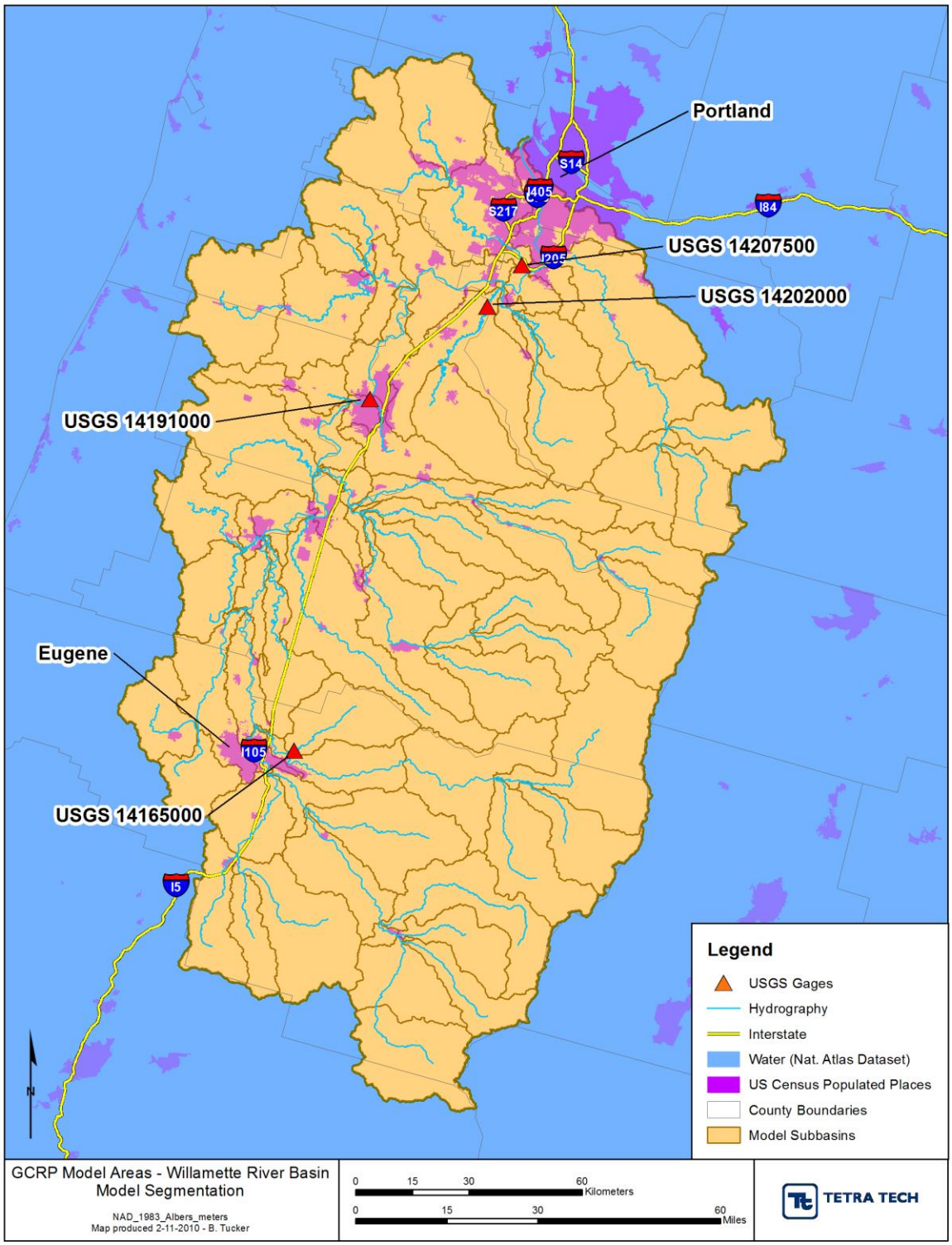

Figure 5-1. Existing HSPF Model Domain for the Willamette River Basin

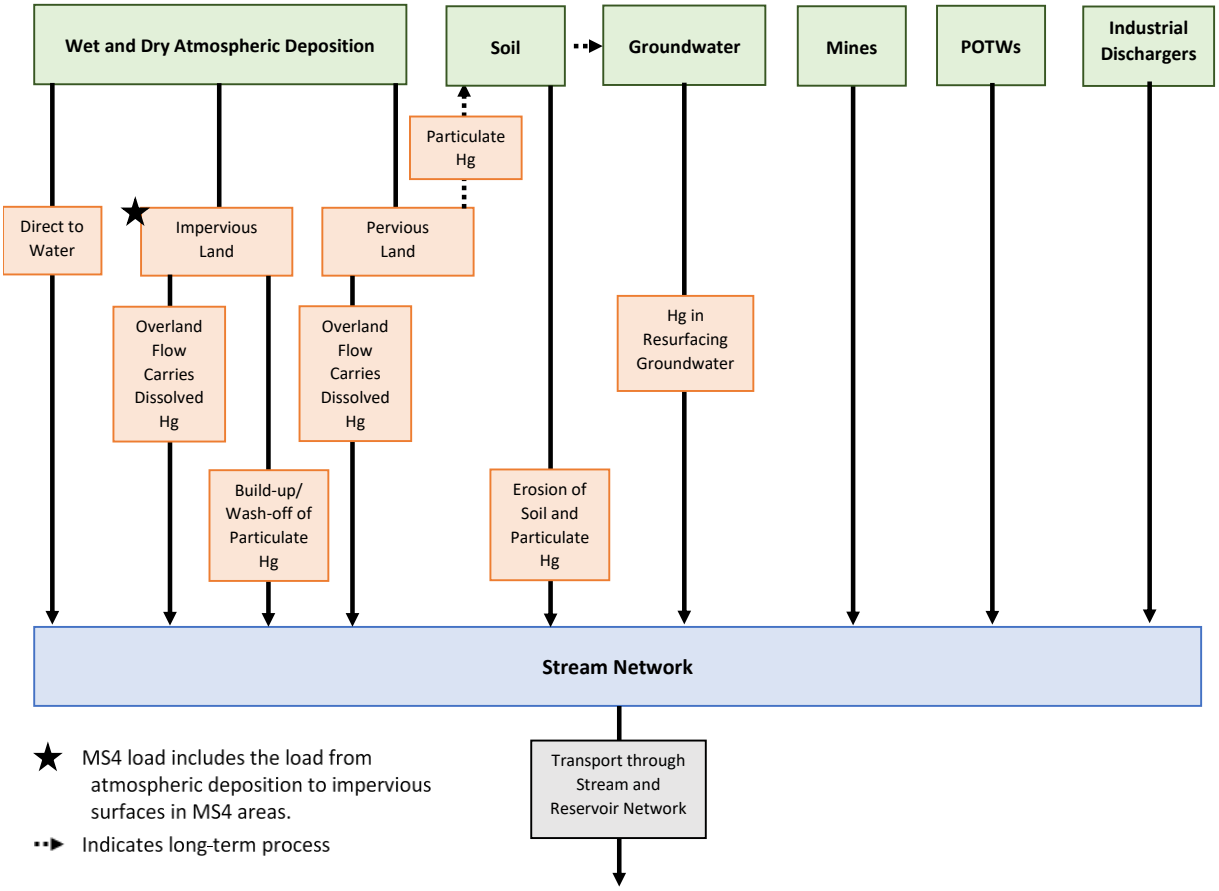

Figure 5-2. Conceptual Framework for the THg Mass Balance Model

Note: The HSPF watershed model provides estimates of overland and subsurface flow rates, sediment yield, the build-up and wash-off of solids on impervious surfaces, and transport of water and sediment through the stream and reservoir network.

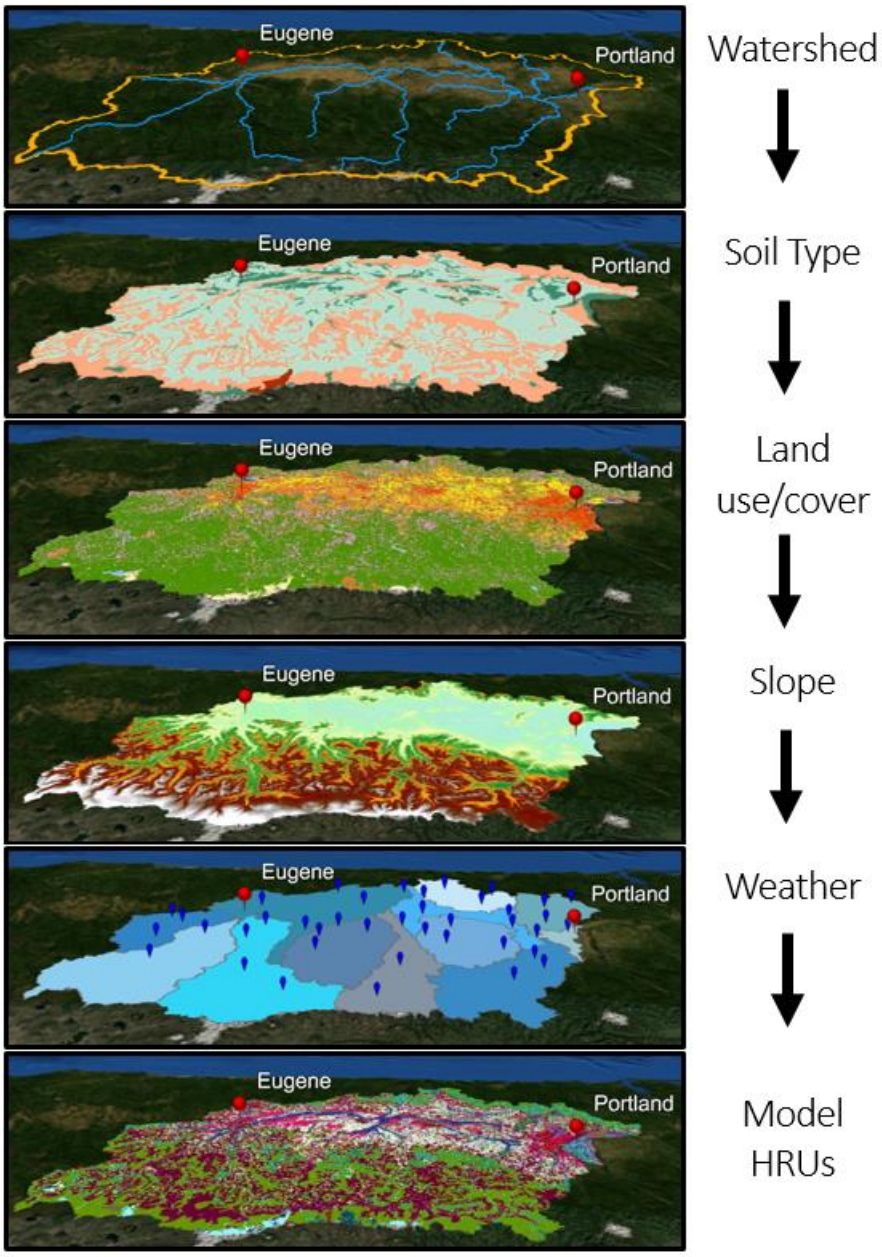

Figure 5-3. Schematic of Model Hydrologic Response Unit (HRU) Development

5.2.1 Updated Land Use in the Willamette River Basin

The existing HSPF model of the WRB was built using the 2001 NLCD. For application in the Mass Balance Model and the TMDL it is desirable to use more current land use. For this purpose, we used the most recent available NLCD coverage for 2011 (Homer et al., 2015; see Figure 5-4). Impervious area is also estimated from the 2011 NLCD (Xian et al., 2011). The 2011 NLCD grids were cross-tabulated with Hydrologic Soil Group for each HSPF subbasin to derive the corresponding 2011 land cover HRUs for use in the Mass Balance Model. Further tabulation was done to separate out those areas subject to Municipal Separate Storm Sewer (MS4) permits.

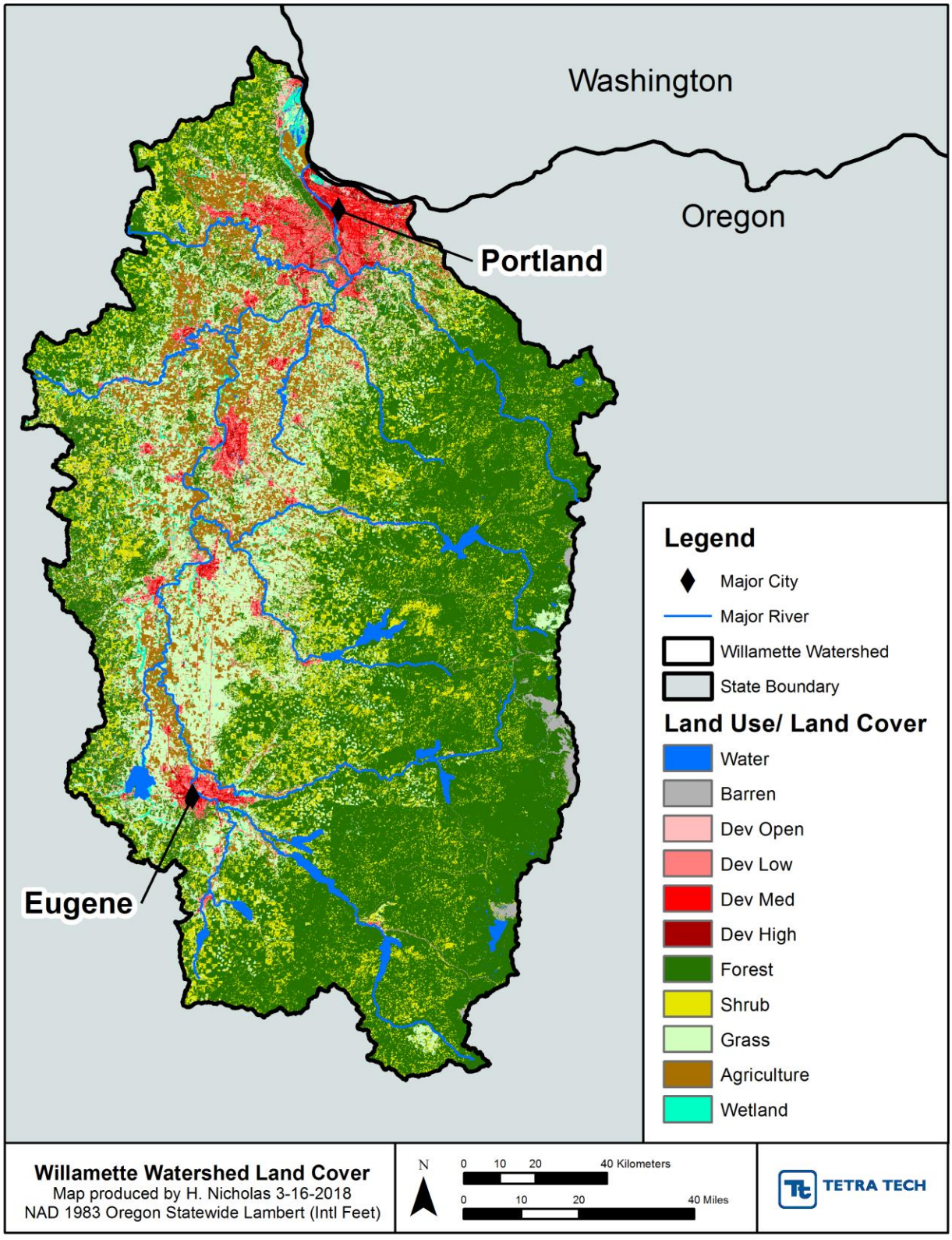

Figure 5-4. 2011 NLCD Land Cover in the Willamette River Basin

Land cover areas and aggregated land use categories for presentation of the Mass Balance Model results are listed in Table 5-1. Forestry is the most dominant land use, occupying 53 percent of the land area of the WRB.

Forest cover occupies 53% of the land area in the WRB. Undisturbed forest is generally a large mercury sink, accumulating THg in soils and biomass with THg inputs (primarily from atmospheric deposition) greater than outputs. Forest harvest or other human or natural activities that result in removal of forest cover can result in less storage of THg with more THg volatilization back to the atmosphere and more THg export in surface runoff, although results are variable for different sites (see summary in Eckley et al., 2018 and Hsu-Kim et al., 2018). Removal of the forest canopy results in less interception of rainfall and less evapotranspiration of soil moisture, increasing surface runoff. This increased runoff can carry more of the dissolved THg present in rainfall to streams. Removal of the forest canopy also increases the rate of soil detachment by rainfall, which increased surface runoff can enhance the transport of particulate THg associated with detached soil and through gully erosion, unless mitigated by erosion control activities.

NLCD does not identify forest harvest as a separate land use; however, it appears that recently harvested forest appears primarily as shrubland (13 percent of area). We intersected the NLCD shrubland area with the USFS LANDFIRE (https://www.landfire.gov/) expected vegetation type (EVT) and found that a preponderance of NLCD shrubland in the WRB (93.7%) has an expected vegetation type in one of the many forest categories, indicating that disturbed forest areas are generally classified as shrubland. (This likely includes areas where tree cover has been lost to landslides, fire, or blowdowns as well has harvested forest.)

Newly constructed and unpaved forest roads that are not properly maintained can be a significant source of sediment erosion, which may mobilize geologic and atmospheric-derived THg. Linear features such as roads are not well resolved on the 30 m NLCD grid, but an approximation of forest road area is also expected to be represented in the shrubland (or barren) land cover group, depending on the net vegetation density within a Landsat pixel.

In sum, the watershed model resolution based on NLCD is not sufficient to resolve the details of effects of forest management practices and other forest disturbance sources on erosion and THg loading; however, this loading should be primarily associated with the shrubland category. Therefore, shrubland is presented as a separate class in the Mass Balance Model results and is expected to include THg loads attributable to forest management for the purpose of allocations and broad-scale implementation planning.

All the developed land classes are aggregated in the Mass Balance Model results, while various classes with small areas are lumped with grassland as an “Other” category for reporting purposes.

Table 5-1. 2011 NLCD Land Cover Summary for the Willamette River Basin

Land Cover	Pervious (mi^2)	Impervious (mi^2)	Total Area (mi^2)	Percent of Total Area	Category for Presentation of Mass Balance Model Results
Agriculture (row crop)	912	0	912	8%	Agriculture
Barren	102	0	102	1%	Other
Developed-High Density	9	72	81	0%	Developed
Developed-Medium Density	78	125	204	1%	Developed
Developed-Low Density	225	108	333	2%	Developed
Developed-Open	276	29	305	2%	Developed
Forest	5,920	0	5,920	53%	Forest
Grassland (including hay and pasture)	1,902	0	1,902	17%	Other
Shrubland	1,412	0	1,412	13%	Shrub
Water	103	0	103	1%	Other
Wetland	192	0	192	2%	Other
Total	11,131	334	11,466	100%	

Simulation with the HSPF model requires an estimate of the connected or Effective Impervious Area (EIA) rather than the total impervious area. EIA is defined as the area of impervious surfaces that is directly connected to the stream network and should exclude impervious surfaces that drain onto pervious lands or are routed alternatively (e.g., to an infiltration basin or underground injection well). Detailed information on EIA within the WRB was not available; however, the NLCD impervious area data products are known to underestimate total impervious area in areas with significant tree canopy cover as well as in less densely developed areas. Therefore, the HSPF modeling assumed that the NLCD impervious area fractions tabulated from the NLCD (as an average across each developed land class) provide a reasonable estimate of EIA because a substantial amount of the disconnected part of total impervious area and no better estimate is available (Butcher et al., 2013, Appendix H). The EIA fractions by NLCD Land Class are shown in Table 5-2.

Table 5-2. Percent of Effective Impervious Area for NLCD 2011 Developed Land Use Classes

NLCD 2011 Developed Land Class	Effective Impervious Area
Developed, open	9.56%
Developed, low density	32.3%
Developed, medium density	61.5%
Developed, high density	88.9%

Some additional explanation is needed regarding the agricultural land cover class as determined from the NLCD. Agricultural land can be defined in various ways. A major difference is between a functional definition based on land cover and management and a property tax or regulatory definition that identifies areas classed as “agricultural land (Exclusive Farm Use)” or taxed in the “farmed deferral” category. The latter definitions would be expected to yield larger acreage because land subject to farm zoning and taxation rules includes portions of other land uses, such as forest, houses, pasture, and so on.

The interpretation of the NLCD uses a functional definition of agriculture, which should more precisely be referred to as cultivated crop lands. These lands are NLCD Land Cover Class 82, based on the spectral reflectance signature and defined as “Areas used for the production of annual crops, such as corn, soybeans, vegetables, tobacco, and cotton, and also perennial woody crops such as orchard and vineyards. Crop vegetation accounts for greater than 20 percent of total vegetation. This class also includes all land being actively tilled.” Class 82 is a subclass of the general planted/cultivated classification, in which “herbaceous vegetation accounts for 75-100 percent of the cover.”

Note that the Class 82 definition does not include pasture and hay (NLCD Class 81) and may omit fallowed cropland that has not recently been tilled. It is also worth remembering that the NLCD is based on satellite data at a 30m x 30m resolution and there are undoubtedly classification errors for individual satellite pixels, although the method is subject to ground-truthing and the errors tend to average out at larger scales.

This functional definition of cultivated cropland is appropriate for the Mass Balance Model because it generally aligns with important characteristics relevant to mercury loading, including seasonally sparse vegetative cover (primarily annual herbaceous cover) and soil mixing/disturbance by tillage, both of which affect both the runoff potential and the concentration of mercury in surface soil in response to atmospheric deposition. The pasture/hay classification in NLCD is managed “typically on a perennial cycle” and tillage, if used, would occur only once every several years, resulting in different runoff and mercury concentration characteristics.

To check whether the NLCD 2011 estimates are reasonable we compared results to those provided in the USDA Cropland Data Layer (CDL), which attempts to identify specific crop types from satellite imagery, and the USFS LANDFIRE Existing Vegetation (EVT) data set, which focuses on forest types, but also identifies agricultural land. The current LANDFIRE coverage is a composite, but is primarily based on 2014 imagery. We examined two different years from the CDL. Results are summarized in Figure 5-5.

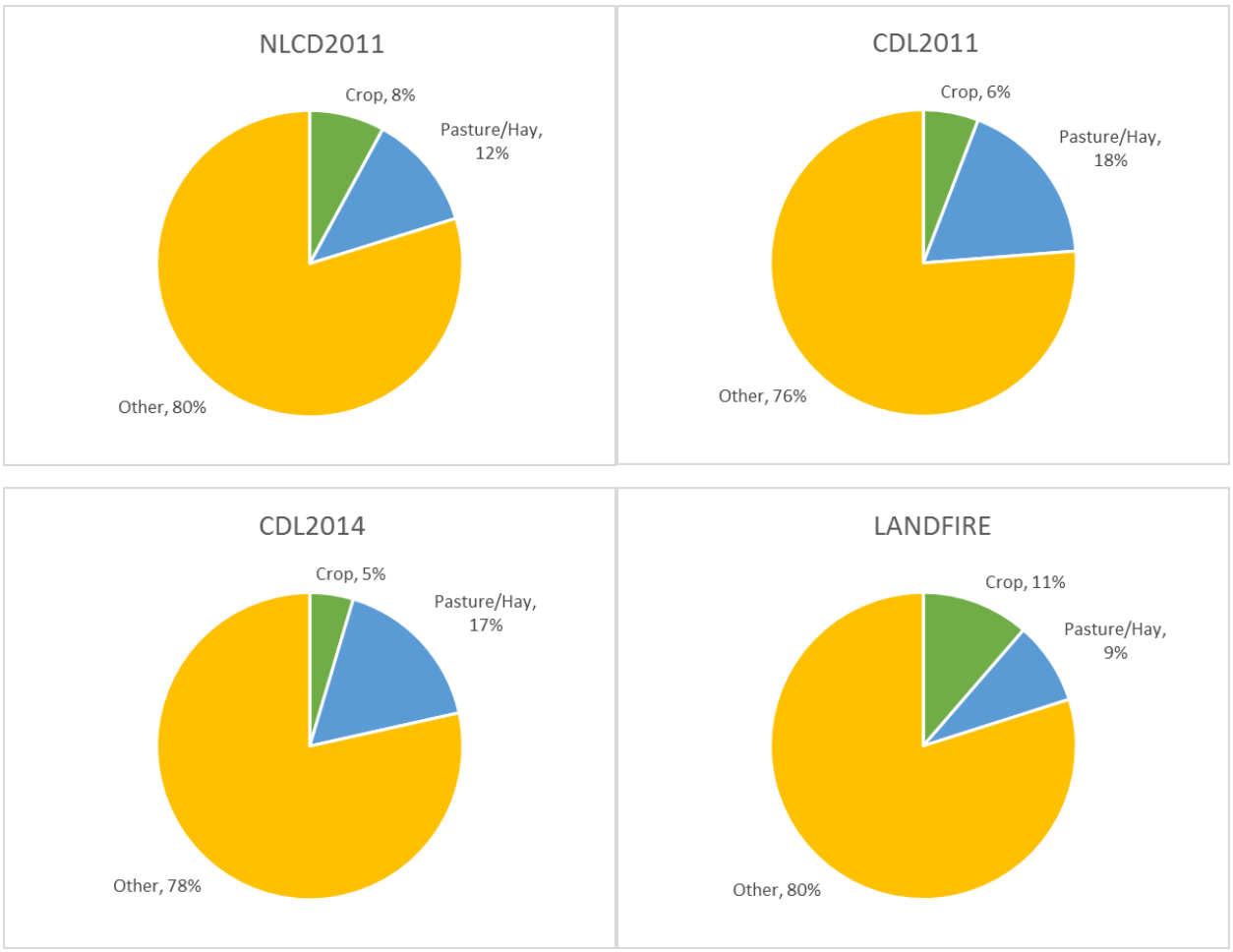

Figure 5-5. Estimates of Agricultural Land Area in the WRB

The NLCD 2011 coverage shows a somewhat greater percentage of tilled cropland (but less pasture/hay) than the CDL. LANDFIRE shows a slightly larger fraction of cropland, but is not intended to focus on agricultural land uses. Over all four coverages, the sum of crop and pasture/hay is in the range of 20-24 percent of the total land area in the WRB. The boundary between tilled cropland and pasture/hay is likely blurred by periodic tillage and replanting of alfalfa, as well as the inherent uncertainty present in satellite-based data products.

The WRB model lumps pasture/hay and native or semi-native grassland into a single category for modeling purposes. The NLCD does distinguish these two classes (Class 81, Pasture/Hay, and Class 71, Grassland/Herbaceous), but the distinction based on satellite imagery is not a clean one, as the description of Class 71 says “These areas are not subject to intensive management such as tilling, but can be utilized for grazing.” Class 71 accounts for about a quarter of the sum of the two grassland classes, or about 4 percent of the total area of the WRB. Because the model was calibrated using the combined grassland classes, and because these two NLCD classes cannot be used to reliably distinguish between managed grassland within farms and unmanaged native grassland, we did not split the two grassland classes within the Mass Balance Model.

In sum, examination of alternative coverages shows that use of the 2011 NLCD for cropland area is reasonable.

5.2.2 Representation of Impoundments

Impoundments can play an important role in mercury cycling because they slow the flow of water and can encourage the deposition of sediment and sediment associated mercury. Impoundments can also produce low oxygen conditions that encourage bacterial conversion of Hg[II] to MeHg. The net effects of impoundments on THg transport in the WRB is discussed in Section 5.4.3.

The existing HSPF model included the major U.S. Army Corps of Engineers flood control reservoirs present in the WRB. There are 13 Corps dams and 11 major reservoirs in the study area (Figure 5-6). Two of the dams (Big Cliff and Dexter) are re-regulation dams that allow the Corps to adjust the downstream flow more smoothly than the releases from the upstream reservoir, so these are not represented separately.

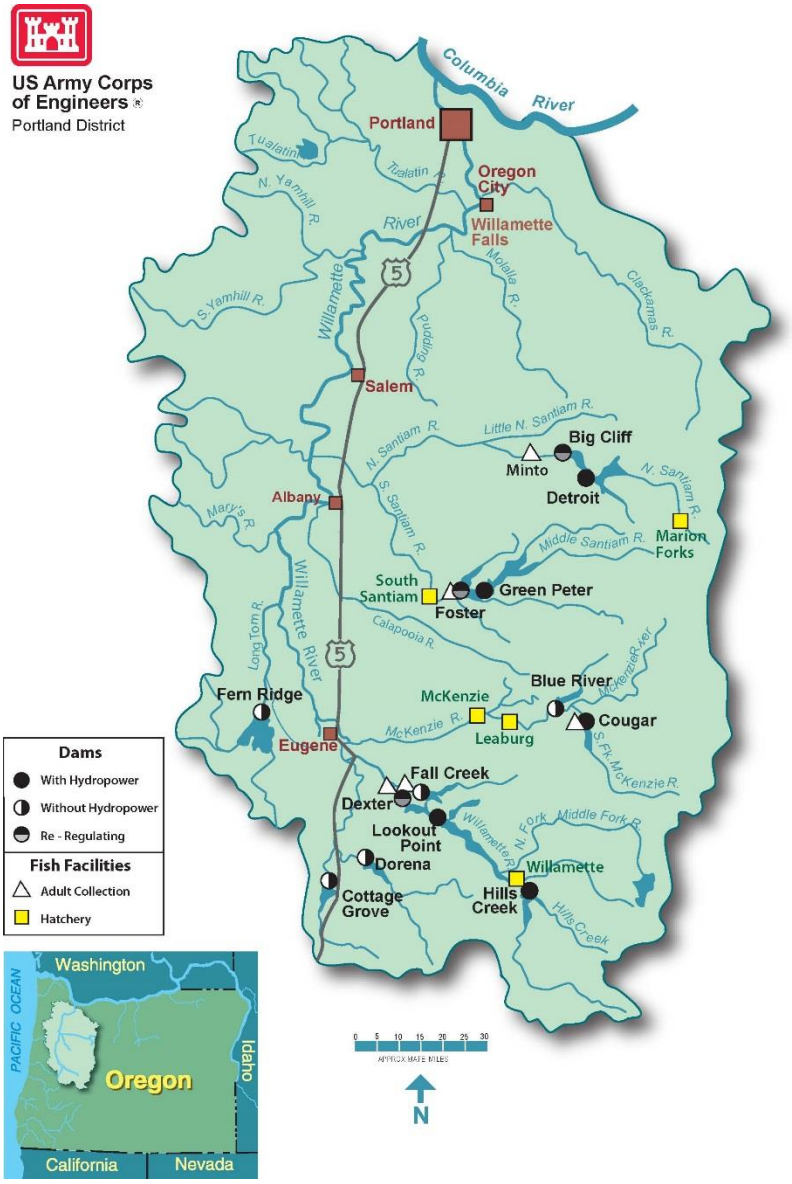

Figure 5-6. U.S. Army Corps of Engineers Dams and Reservoirs in the Willamette River Basin

Portland General Electric (PGE) also operates a series of hydropower dams on the Clackamas River, which were not included in the original version of the HSPF model of the WRB. Because this system can have a substantial impact on travel times and sedimentation an approximate representation of the effect of the PGE dams was added to the model.

A detailed description of the Clackamas River Hydroelectric Project, along with results of various modeling studies, is provided in the relicensing Draft Environmental Impact Statement (FERC, 2006). The full project includes upstream storage at Timothy Lake on Oak Grove Fork, and, on the lower Clackamas, the sequence of North Fork Reservoir, Faraday Diversion Dam, Faraday Lake, and Estacada Lake (River Mill Development). The four downstream dams are operated to minimize water level fluctuations in North Fork Reservoir and Estacada Lake. The largest storage pool is that of the North Fork Reservoir, which has a gross storage capacity of 18,630 AF. However, the reservoir is operated in peaking mode using 1 to 2 feet of storage, so that the usable hydropower capacity is only 700 AF. Faraday Diversion Dam (on the Clackamas mainstem) and Faraday Lake (located off the Clackamas mainstem) are much smaller, with gross storages of 1,200 and 430 AF respectively, of which somewhat less than half is used by PGE with drawdowns around 5 feet. Finally, Estacada Lake is operated to minimize flow fluctuations. The Lake has 2,300 AF gross storage, of which PGE uses 200 AF with a maximum 2 ft drawdown. Minimum flow releases are specified by season to mimic natural flow in the lower Clackamas.

The major sediment trap in this system is the North Fork Reservoir (Figure 5-7), which "essentially eliminates upstream sediment supply" (FERC, 2006, p. 208). McBain and Trush (2002) estimated that approximately 269,000 tons/yr of sediment are trapped behind North Fork Dam. Gravel replenishment is used to protect spawning areas downstream of Estacada Lake to compensate for the upstream trapping of sediment.

Figure 5-7. PGE's North Fork Dam and Reservoir on the Clackamas River

The Clackamas Project is a complex and highly managed system and it was not feasible to simulate it in full detail. As used in this project, the HSPF model provides upland water and sediment loading rates,

along with instream travel times and empirical estimates of THg losses, represented as an exponential decay applied to travel time. As the bulk of the water storage and sediment trapping capacity on the lower Clackamas is provided North Fork Reservoir and the downstream dams operate primarily in run-of-river mode, it is sufficient for our purposes of estimating travel time to only add North Fork Reservoir to the model setup.

To accomplish representation of North Fork Dam, existing subbasin and model reach 63 was split into two new subbasin, 263 and 363. Subbasin 263 is above North Fork Dam, and subbasin 363 is downstream of North Fork Dam. The reach length for reach 263 is then 4.15 miles with a direct drainage area of 24,164.8 acres, and for 363, the length is 29.35 miles with a direct drainage area of 176,680.3. The hydraulics of the two reaches are described with Functional Tables (FTables) in HSPF. The dead storage volume of North Fork Dam (17,930 AF with an average depth of 52 ft) is added to the FTable for reach 263 prior to any outflow occurring. Channel dimensions for the original reach 63 were created using BASINS defaults that calculate width as a function of cumulative upstream drainage area raised to the 0.6 power and depth as a function of cumulative upstream drainage area raised to the 0.4 power (personal communication from Paul Duda, AQUA TERRA Consultants, to Scott Job, Tetra Tech, March 20, 2007). Therefore, the dimensions for the new reach 263 were adjusted by the ratio of the new to old cumulative drainage area raised to the appropriate power.

These revisions result in substantially lower velocities and longer travel times across what was originally reach 63. This enables the model to make an approximate adjustment for net THg loss processes that occur within the hydropower project. See Section 5.4.3 for a discussion of processing affecting THg transport through reservoirs.

The final set of reservoirs represented in the model is shown in Table 5-3.

Table 5-3. Reservoirs Represented in the Willamette River Basin HSPF Model

Dam Name	River	HUC8
Blue River	Blue River-McKenzie	17090004
Cottage Grove	Coast Fork-Willamette	17090002
Cougar	South Fork-McKenzie	17090004
Detroit	North Santiam River	17090005
Dorena	Row River	17090002
Fall Creek	Fall Creek	17090001
Fern Ridge	Long Tom River	17090003
Foster	South Santiam River	17090006
Green Peter	Middle Santiam River	17090006
Hills Creek	Middle Fork-Willamette	17090001
Lookout Point	Middle Fork-Willamette	17090001
North Fork	Clackamas	17090011

5.3 Source Characterization

5.3.1 Atmospheric Deposition and Surface Runoff

Elemental Hg exists in a gaseous form and is readily transported long distances in the atmosphere. Because of its high volatility, deposition rates of elemental Hg to the land surface are low. Significant deposition occurs when elemental Hg is converted to ionic forms by chemical reactions in the atmosphere and also through the uptake of elemental mercury by plant leaves. In areas without local geologic or industrial sources of Hg, atmospheric deposition is the primary source of Hg to waterbodies (e.g., Watras et al., 1994).

Atmospheric deposition of Hg occurs in both wet and dry forms, corresponding to fluxes dissolved in rainfall and fluxes associated with dust and foliar uptake. Wet deposition concentrations are straightforward to measure, but dry deposition is more difficult to characterize. For the 2006 TMDL, Hope (2005) used the estimates of THg deposition (both wet and dry) from monitoring and simulation models that were then available, then applied an empirical delivery ratio to account for the fraction of deposited load delivered to streams. The delivery ratio was set at 5 percent for forested land and 20 percent for other lands, based on a summary of values used in other Hg studies (Hope, 2005). The uncertain delivery ratio assumptions strongly affect the resulting estimate of load.

More detailed and recent mercury summaries of Hg deposition covering the watershed have now been prepared for the Western North America Mercury Synthesis project (Domagalski et al., 2016) and were made available for use in this TMDL revision.

The deposition grids developed by Domagalski et al. (2016) provide annual wet and dry THg deposition estimates for the period 2000 to 2013. The wet THg deposition grids were developed from monitoring data collected by the Mercury Deposition Network (MDN; http://nadp.sws.uiuc.edu/mdn). The point estimates of THg concentration were converted to loads and interpolated based on gridded precipitation data from PRISM (Parameter-elevation Relationships on Independent Slopes Model; http://prism.oregonstate.edu). The gridded data for wet deposition of THg included annual deposition rates (µg/m^2) for 2000 – 2008 (~ 800 m resolution) and for 2010 – 2013 (~2,300 m resolution). A wet deposition grid was also provided for 2009 however the extent of the 2009 data did not cover the Willamette River Basin. The average annual flux of wet atmospheric deposition of THg to land in the Willamette River Basin was 9.62 µg/m^2, which corresponds to an average THg concentration in precipitation of 6.05 ng-THg/L. Domagalski's wet deposition grids showed no systematic spatial patterns in THg wet deposition concentration across the watershed (although loads vary as a function of precipitation), so this average concentration is applied to local precipitation across the whole model domain.

Wet and dry deposition to waterbodies constitutes a direct contribution to the THg load in the river network (listed as the atmospheric deposition load in the Mass Balance Model results tables in Section 5.5. This direct load was established based on the surface area of streams, rivers, and reservoirs represented in the model. THg from wet atmospheric deposition on pervious surfaces is either transported directly to the river network via overland flow or contributes to the soil Hg concentration if associated with precipitation that infiltrates (listed as the surface runoff and sediment erosion loads in the Mass Balance Model results tables in Section 5.5). For pervious surfaces the load associated with precipitation that infiltrates into the soil matrix is assumed to contribute to the soil Hg concentration balance that is addressed with other soil matrix sources (Section 5.3.2) and is not included in the direct

atmospheric deposition load. THg in precipitation that becomes overland flow is categorized as the surface runoff load and it not included in the direct atmospheric deposition load. The HSPF model distinguishes surface and subsurface flow pathways for each land use, soil type, and weather zone combination, and model output was summarized to estimate the fraction of annual precipitation that is converted to overland flow. The unit area wet deposition load to the stream network for each model HRU is calculated as follows:

$$L_{HRU} = f_{HRU} P_{HRU} W \alpha$$

where L_{HRU} is the unit area wet deposition load for a HRU (kg/acre/year), f_{HRU} is the fraction of precipitation that becomes overland flow for a HRU (unitless), P_{HRU} is the annual average precipitation volume to a HRU (L/acre/year), W is the wet deposition THg concentration for the basin (ng/L), and α is a unit conversion factor.

On impervious surfaces, all runoff occurs as overland flow and most precipitation becomes direct runoff and thus contributes THg to the stream network, except where impervious surface runoff is captured and infiltrated (see Section 5.3.7). Water lost to evaporation from the plant canopy and the land surface is not part of the surface runoff and therefore not included in the tabulation of surface runoff THg loads. This provides an approximate accounting for re-emission of mercury to the atmosphere from surface storage. The estimated surface runoff THg load delivered to the stream network ranges from 0.02 to 2.61 kg-THg/yr for individual HUC10 subbasins in the WRB, with a total load across the entire WRB of 38.7 kg-THg/yr. The wet atmospheric deposition load direct to water bodies is 0.22 kg-THg/yr. Surface runoff in MS4 regulated areas and urban DMAs is classified under the MS4 and urban DMA load categories in the Mass Balance Model to support TMDL allocations. Therefore, this total excludes THg from surface runoff in MS4 regulated areas and urban DMA areas. The surface runoff load for MS4 regulated areas and urban DMAs is 3.9 kg-THg/yr (Section 5.3.7).

Accounting for dry atmospheric deposition of THg is more challenging, in part because it occurs during non-runoff conditions, and in part because the major flux pathway in heavily vegetated areas is through leaf uptake and subsequent deposition of litter to the forest floor. It is also extremely difficult to directly measure net dry deposition because there are complex bi-directional fluxes and much of the deposited THg is re-emitted to the atmosphere. Eckley et al. (2016) used flux chamber data to examine soil-air THg fluxes in the Western North America region and demonstrated that most of the variability in soil-air THg fluxes could be explained by variations in soil-THg concentrations, solar radiation, and soil moisture. Due to the lack of direct monitoring data, THg dry deposition was estimated by Domagalski et al. (2016) from the Community Multiscale Air Quality (CMAQ; https://www.cmascenter.org/cmaq/) model run for 2009 conditions at a 40-km spatial resolution. The annual dry deposition rate across the watershed in 2009 was 4.24 µg/m^2, and this rate is assumed to be representative of other years as well. As with wet deposition, there is no evidence for significant spatial gradients across the WRB.

Dry atmospheric deposition to pervious surfaces is assumed to contribute to the THg in surface soils and is transported to streams by erosion processes, as described in Section 5.3.2, and is not explicitly represented as a separate source in the Mass Balance Model (it is included in the sediment erosion loads). Dry deposition direct to water is tabulated as a direct atmospheric deposition contribution.

The contribution of dry deposition to impervious surfaces is treated differently as there is not a soil matrix present. Significant re-emissions also occur from urban surfaces exposed to sunlight (Eckley et al., 2016). For impervious surfaces, THg from dry deposition is represented as a buildup-washoff process in the HSPF model, characterized by constant input and removal rates that approach an equilibrium concentration over time since last washoff event. This equilibrium concentration (which implies a removal

rate believed to be due largely to photoreduction) appears to be in the neighborhood of 150 ng/m^2 based on data summarized by Eckley and Branfireun (2008). The surface runoff load from dry deposition to impervious surfaces is estimated to be 0.08 kg-THg/yr and direct dry atmospheric deposition to waterbodies in the WRB is estimated to be 1.27 kg-THg/yr. As discussed above, the surface runoff load from MS4 regulated areas and urban DMAs is classified separately in the Mass Balance Model. The combined portions of the MS4 and urban DMA surface runoff loads from dry deposition of mercury to impervious surfaces is 0.13 kg-THg/yr (Section 5.3.7).

Total THg loads to the stream network from surface runoff and from wet and dry atmospheric deposition direct to water surfaces are shown for subbasins in the Willamette River Basin HSPF model in Figure 5-8. The overall THg load attributed to wet and dry atmospheric deposition direct to water surfaces is 1.49 kg-THg/yr. The overall THg load attributed surface runoff is 38.8 kg/yr (42.9 kg/yr with atmospheric deposition to MS4 regulated areas and urban DMAs) – slightly lower than the earlier estimate of 53.7 kg/yr reported by Hope (2005).

The average annual total estimated net atmospheric deposition flux of THg onto the entire WRB (including fractions that are retained in the soil) amounts to 413 kg/yr (910 lb/yr), of which 69 percent is wet deposition.

In an application of a simplified global mercury transport model, Seigneur et al. (2004) found that anthropogenic sources of mercury from North America comprised about 30 percent of the total deposition over the conterminous U.S., with larger contributions in the east. Natural sources (including emissions from oceans) account for 33 percent, while anthropogenic emissions from other continents account for the rest. In the vicinity of the WRB, North American anthropogenic sources contribute 2 – 5 µg/m^2/yr total deposition (10 – 20 percent), according to the model. Total deposition was predicted to be 15 – 20 µg/m^2/yr, which is somewhat greater than the rate of 13.86 µg/m^2/yr used in this study. A complete source attribution is provided by Seigneur et al. for several locations, but all but one location was in the eastern or central U.S., and none were on the Pacific coast.

As part of the modeling analyses for the Clean Air Mercury Rule, USEPA (2005) conducted a run with a "zero-out" of all mercury emissions from U.S. power plants. Results of this scenario indicate that the resulting decrease in total mercury deposition in the Willamette watershed for 2001 following cessation of all U.S. power plant emissions would be less than 2 µg/m^2/yr. The findings of Seigneur et al. (2004) and USEPA (2005) suggests that a relatively small percentage of atmospheric mercury deposition in the WRB originates from U.S.-based anthropogenic sources.

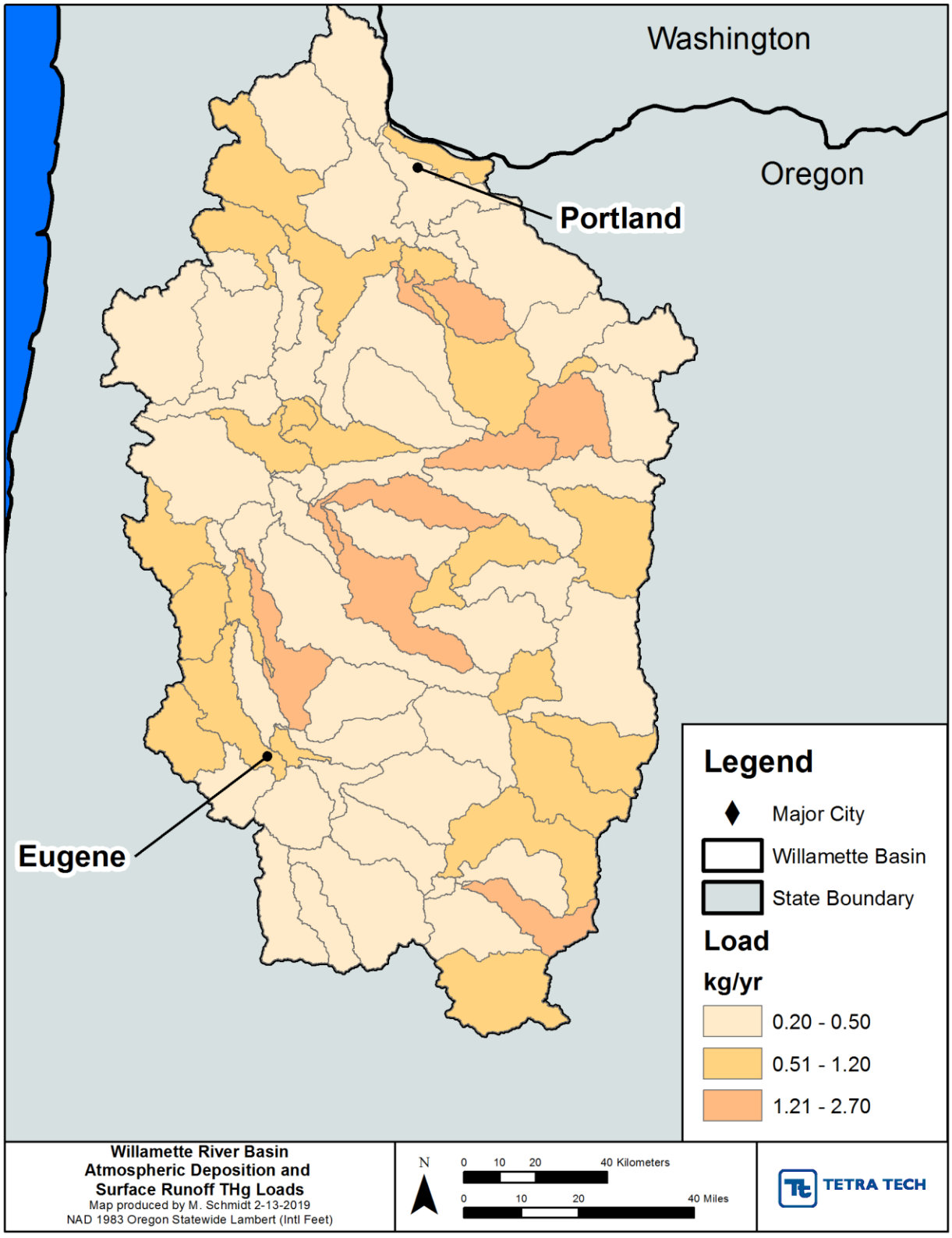

Figure 5-8. Total Surface Runoff and Wet and Dry THg Atmospheric Deposition Loads Delivered to the Stream Network in the Willamette River Basin

Detailed air quality modeling has not been undertaken to estimate the fraction of the total atmospheric deposition load that arises from sources within the WRB; however, it is inferred to be small because total emissions of THg to the atmosphere within the WRB are well less than the total deposition load to the WRB. Atmospheric deposition of THg from both local and long-range sources is included within the net dry and wet THg and surface runoff loading rates described above.

The fraction of air emissions of mercury that is deposited locally depends on the form of mercury. Hg[II] has a lifetime in the atmosphere against deposition of 3.7 days, whereas elemental mercury (Hg[0]) has a lifetime of 6 months, making it part of the global pool (Corbitt et al., 2011). Further, while Hg[II] is likely to deposit within a local area, some of this Hg[II] is photo-reduced to Hg[0] and re-emitted to the atmosphere, so the contribution to the net load to water and to soil concentrations will be less.

Information on anthropogenic air emissions of THg in the WRB was provided by the ODEQ Air Quality Division (provided via emails from Paula Calvert, ODEQ Watershed Management Section, July 25, 2018, and December 3, 2018). Estimated THg air emissions from 11 larger stationary sources within the WRB for 2002, including steel mills and wood products producers, summed to 55.97 kg/yr (123.4 lb/yr). Smaller sources were not included in the 2002 tabulation. Estimated THg air emissions from 221 large and small sources within the WRB in 2016 dropped to 31.8 kg/yr (71.2 lb/yr) despite including additional minor stationary emissions sources. This drop is at least in part due to better controls on emissions. In other instances, plants have closed or cut back operations. The majority of stationary source loads are associated with a few larger facilities. The four facilities that emitted at least 1 kg/yr THg in either 2002 or 2016 accounted for 76 percent of the emissions within the WRB in 2002 and 86 percent in 2016 (Table 5-4). For comparison, the ODEQ Air Quality Division estimates that about 69 kg/yr were emitted by stationary sources in all parts of the state (including areas outside the WRB) in 2016.

Table 5-4. Stationary Source Air Emissions of THg within the WRB

Source	2002 (kg/yr)	2016 (kg/yr)
Cascade Steel Rolling Mills	16.71	22.89
Covanta Marion, Inc.	14.43	2.98
EVRAZ Rivergate (formerly Oregon Steel)	10.87	0.18
Cascade Pacific Pulp, LLC (formerly Pope & Talbot)	0.51	1.30
Sum of Other Sources	13.45	4.48
Total	55.97	31.83

Notes: Sources emitting at least 1 kg/yr in either 2002 or 2016 are listed individually. The 2002 tabulation includes only the 11 largest sources and omits minor sources, while the 2016 tabulation includes all identified stationary sources.

The ODEQ Air Quality Division also provided estimates of additional nonpoint THg releases for the 2014 National Emissions Inventory (NEI, https://www.epa.gov/air-emissions-inventories/national-emissions-inventory-nei), which is the most recent complete estimate for Oregon, for the ten counties that intersect the WRB (Benton, Clackamas, Columbia, Lane, Linn, Marion, Multnomah, Polk, Washington, and Yamhill). Because portions of some of these counties lie outside the WRB, the estimates are greater than the emissions occurring within the WRB. These include nonpoint or area sources (including fuel oil and wood burning, dental amalgamation, fluorescent lamp breakage, and landfill and recycling

emissions), on-road mobile sources (THg from fuel combustion), and nonroad mobile sources (such as agricultural and construction equipment, rail, boats, etc.). The total estimated air emissions from these sources (for 2014) was 59.6 kg/yr (131.4 lb/yr), as summarized in Table 5-5.

Table 5-5. Nonpoint THg Emissions to Air for Counties Intersecting the WRB, 2014

Source	Emissions (kg/yr)	Emissions (lb/yr)
Nonpoint (area)	55.3	121.9
On-road	2.2	5.0
Nonroad	2.1	4.6
Total	59.6	131.4

Note: "Nonpoint" refers to emissions from dispersed area sources, "On-road" refers to emissions from fuel combustion by road vehicles, "Nonroad" refers to emissions from mobile equipment not on roads, such as agricultural and construction equipment, rail, boats, etc.

5.3.2 Soil Matrix Sources

There are two types of THg loading pathways associated with the soil matrix: (1) erosion and transport of particulate-associated mercury, and (2) loading of dissolved mercury via subsurface (groundwater) pathways (dissolved mercury is also associated with overland flow as discussed in the previous section). The groundwater component is discussed separately (Section 5.3.3). THg loads associated with the erosion of mine tailings and seepage are also addressed separately (Section 5.3.4). This section discusses the Hg loads associated with the erosion of upland soil and solids from land uses throughout the watershed.

On pervious land, precipitation energy or mechanical disturbance (e.g., from tillage, roads, or forest harvest) detaches sediment from the soil matrix. Areas with reduced vegetative cover (such as plowed fields, roads, or forest converted to shrubland) will have greater rates of sediment detachment. Overland flow carries eroded soil across the land surface. Along the way, some of the sediment is deposited back on the land surface, while the remaining fraction is transported to streams. The net capacity for transport of sediment to streams is estimated as a function of the depth of overland flow, which in turn depends on precipitation, soil infiltration capacity (indexed by HSG), slope, and cover. If the concentration of mercury bound to sediment (referred to as a potency factor when expressed as mass per mass) is known, it can be combined with sediment transport rates to estimate erosion-related mercury loads delivered to the stream network. Management actions that increase cover, decrease overland flow, or otherwise trap sediment can all reduce the delivered loads.

For the 2006 TMDL, Hope (2005) estimated sediment-associated THg loads by combining estimates of soil detachment obtained with the Universal Soil Loss Equation, a sediment delivery ratio based on an empirical relationship to drainage area, and a single constant soil THg concentration. Sediment loads were not calibrated, and the use of a drainage area-based delivery ratio potentially introduces large uncertainty. In contrast, the WRB HSPF model is calibrated to observed total suspended sediment concentrations and loads and provides estimates of soil erosion for each HRU; reflecting the influence of land use, soils, slopes, and local meteorological characteristics. The HSPF model simulates detachment of solids from the soil matrix, reincorporation due to compaction, and overland transport of particulate matter to waterbodies (where carrying capacity is a function of overland flow depth) and instream

transport downstream. This provides a more sophisticated basis for estimating mercury loads associated with soil erosion than was previously available – and no separate empirical estimates of delivery ratio are needed.

THg soil potency factors are expected to vary by geology, soil properties, and land use due to the varying THg retention and re-emission rates associated with different land use/cover types (Eckley et al., 2016). USGS (Smith et al., 2013) developed a gridded map of soil mercury concentrations throughout the conterminous US which we obtained for use in this project. The mapping is based on relatively sparse soil samples, with inverse distance weighting between measured points. Only 16 observations lie within the WRB, with 33 in or near the watershed. We use the results reported for the top 5 cm of soil as most relevant to erosion and washoff. Reported potencies in or near the WRB range from 10 to 20 µg-THg/kg-soil.

Obrist et al. (2016) provides a detailed summary of available literature and data on soil mercury in Western North America and shows that soil concentrations differ significantly among land cover types, with the highest concentrations (but lowest erosion rates) in forest soils and the lowest concentrations (but highest erosion rates) in barren soils. The mapping of Smith et al. (2013) identifies land cover for observation points, but interpolates across all measurements. This mixing of land use types limits the usefulness of the mapping, and potentially obscures spatial patterns.

The majority of samples reported by Smith et al. in or near the WRB are for forest cover, and these have sufficient sample density to reveal a spatial pattern with higher concentrations to the north and east of the watershed, where rainfall rates tend to be higher. We peformed a kriging interpolation of the forest points in ArcGIS (ESRI ArcMap version 10.3, Spatial Analyst Tools) and used the resulting average soil potency by HUC8 to reflect this spatial pattern. The average forest THg potency across the WRB of 83 µg/kg is substantially higher than the average for forest across the whole western US of 35.6 µg/kg reported by Obrist et al. (2016), consistent with the mapping of Smith et al. (2013) that shows concentrations in near-coastal Oregon elevated relative to much of the rest of the West. As discussed in Section 5.2.1, LANDFIRE coverages indicate that the natural land use for most shrubland in the basin is forest. Therefore, forest potency factors were applied to shrubland as well.

Other than forest, the data set of Smith et al. (2013) contains only three observations points for cultivated land, three for herbaceous upland, and one for residential land. These are not sufficient to detect spatial patterns, so we use the average for cultivated land and herbaceous uplands. Potency for herbaceous uplands is less than cultivated land, which is in turn less than forest, consistent with the results reported by Obrist et al. (2016). Potency for all other land cover types is set to a value that reflects an equal mix of shrubland and cultivated land and applying the average ratio between shrubland and cultivated land in Obrist et al.'s Table 2C to estimate the shrubland component. Resulting potency factor estimates are shown in Table 5-6.

Using land use/land cover as described in Section 5.2.1, monthly average unit-area sediment export rates from HSPF, and the soil THg potency outlined above, upland soil matrix THg loads were tabulated on an average monthly basis (Figure 5-9). The total average annual at-source THg load from sediment washoff is 56.5 kg/yr and 40.7 kg/yr is delivered to the stream network; these total loads exclude sediment erosion from developed land in MS4 regulated areas and urban DMAs, which is accounted for separately in those respective categories. The estimated THg load entering the stream network from upland pervious areas is smaller than the load estimated by Hope (2005) of 59.8 kg/yr (after excluding urban land). Note, however, that Hope did not account for a separate load associated with groundwater discharge from pervious land.

Table 5-6. Soil THg Concentration Assumptions for WRB

Land Cover	HUC8	THg Potency (µg/kg)
Forest and Shrub	17090001	49.7
Forest and Shrub	17090002	48.2
Forest and Shrub	17090003	85.4
Forest and Shrub	17090004	60.7
Forest and Shrub	17090005	80
Forest and Shrub	17090006	79.7
Forest and Shrub	17090007	96.8
Forest and Shrub	17090008	105.1
Forest and Shrub	17090009	90.2
Forest and Shrub	17090010	115.9
Forest and Shrub	17090011	77.3
Forest and Shrub	17090012	111
Cultivated Land	All	36.7
Herbaceous Upland	All	23.3
Other	All	30.1

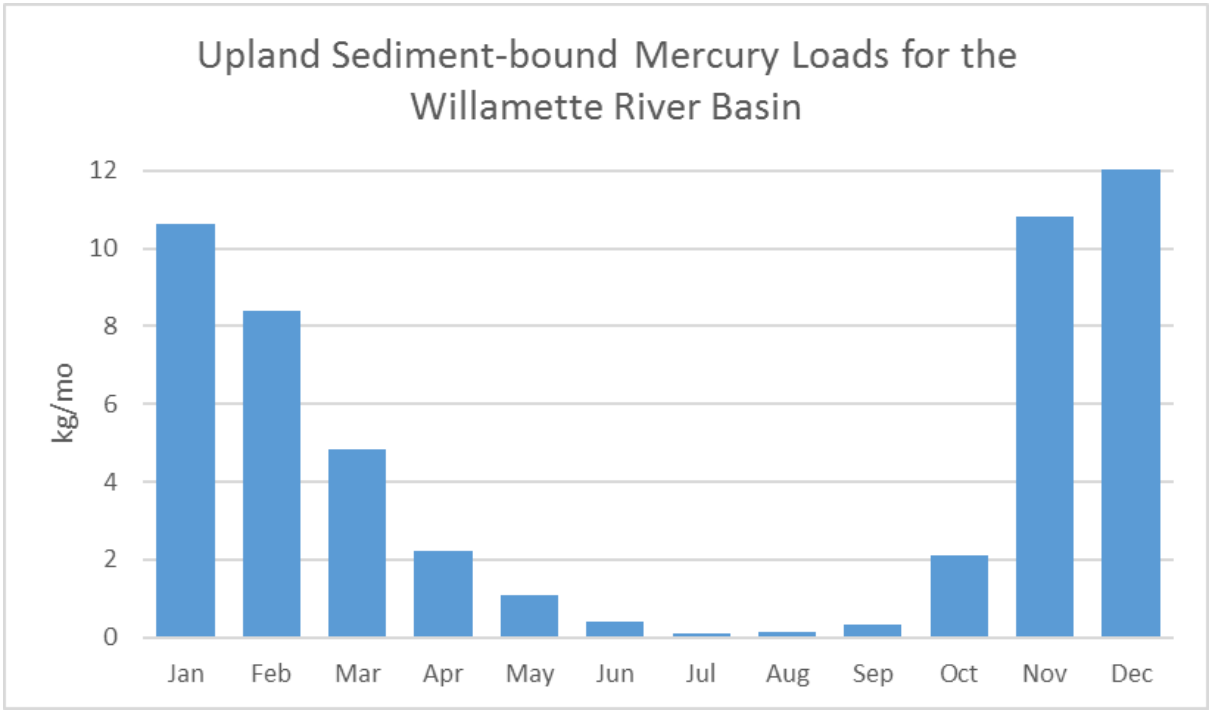

Figure 5-9. Monthly Average THg Loads from Erosion of the Soil Matrix in the WRB

5.3.3 GROUNDWATER LOADING

Dissolved mercury is present in groundwater, derived from leaching from surface soils and native geology. As groundwater seeps into streams it can carry dissolved mercury with it into the aquatic environment. Mercury loading from groundwater can be estimated if groundwater flow and the associated THg concentration are known. HSPF estimates unit area groundwater discharge by land use/weather station combination at an hourly time step; these are scaled to the subbasin level using land use/land cover areas. Groundwater THg concentration is more difficult to estimate. No studies were found to accurately characterize mercury in groundwater in the Willamette, or in the Pacific Northwest. Sampling of wells in the vicinity of Black Butte Mine in the Coast Fork Willamette HUC8 was undertaken in 1998, but all samples for THg were reported as non-detect at a detection limit of 200 ng/L (Oregon Health Authority, 2013). Additional well sampling with low detection limits for THg was done in 2013 in conjunction with the Remedial Investigation of Operable Unit 1 at the Black Butte Mine Superfund site (CDMSmith, 2018). Well MW-13 was sampled as a reference location for background groundwater quality upstream of the mining area in the shallow alluvium of Garoutte Creek. Of three samples for dissolved THg at this well, two were below a detection limit of 0.5 ng/L, while a third had dissolved THg quantified at 1.19 ng/L. Finally, Hinkle et al. (2013), in the course of examining mercury dynamics in hyporheic flow in an island in the Coast Fork Willamette near London, OR, sampled groundwater from a deep (37 m) supply well and reported a filterable THg concentration of 0.25 ng/L; however, two samples from discharging springs in the same area had filterable THg concentrations of 5.19 and 1.25 ng/L.

Few other studies appear to be available to characterize typical mercury concentrations in groundwater, although there are some that can be used to infer likely concentration ranges. Krabbenhoft and Babiarz (1992) conducted a study of ground water mercury loading to a Wisconsin lake, and found that ambient groundwater concentrations ranged from 2 – 4 ng/L. Barringer et al. (1997) report on unpublished research from the New Jersey coastal plain, where researchers found background mercury concentrations of “a few ng/L” in groundwater. Grigal et al. (2000) found a groundwater concentration of 0.9 ng/L in a forested watershed in Minnesota.

Grigal (2002) provides a review of mercury in terrestrial watersheds. In a section discussing groundwater, the author focuses on the interaction of mercury and dissolved organic matter (DOM). Hg transport is facilitated by DOM, and low transport rates are found in soils with low DOM. In most cases, mercury concentrations in pore water were higher near the surface than at depths below 50 cm, often ranging more than an order of magnitude between the sampled depths. Ambient groundwater concentrations in the studies reviewed by Grigal (mostly from northern Europe) ranged from 1 to 7 ng/L; however, this may over-represent the contribution in discharging groundwater. Studies from colder regions may also be biased high relative to the WRB due to the prevalence of peat bogs, which contribute to elevated DOM concentrations and associated elevated THg transport. In the Trask River Watershed Study (Eckley et al., 2018) baseflow THg concentrations in a forested watershed in coastal Oregon were consistently low and generally less than 1 ng/L, suggesting groundwater THg concentrations must also be low, although some losses during transit may have occurred.

While groundwater THg concentrations are expected to be low, the total volume of groundwater discharge is high, making this a significant potential source. We lack direct evidence for concentrations of THg in groundwater seepage in the WRB, but found that assigning a concentration of 1 ng/L, at the low end of the range reported in the literature, appeared to provide reasonable results in mass balance calculations (see Section 5.4).

Using land use/land cover areas, monthly unit-area interflow, and groundwater flow from HSPF, and a groundwater mercury concentration of 1 ng/L, mercury loads from groundwater discharge were tabulated on an average monthly basis (Figure 5-10). Note that mercury loads from shallow interflow in MS4 regulated areas and urban DMAs are included with those categories in the final tabulations and not the groundwater category. The total groundwater load is 22.2 kg-THg/yr.

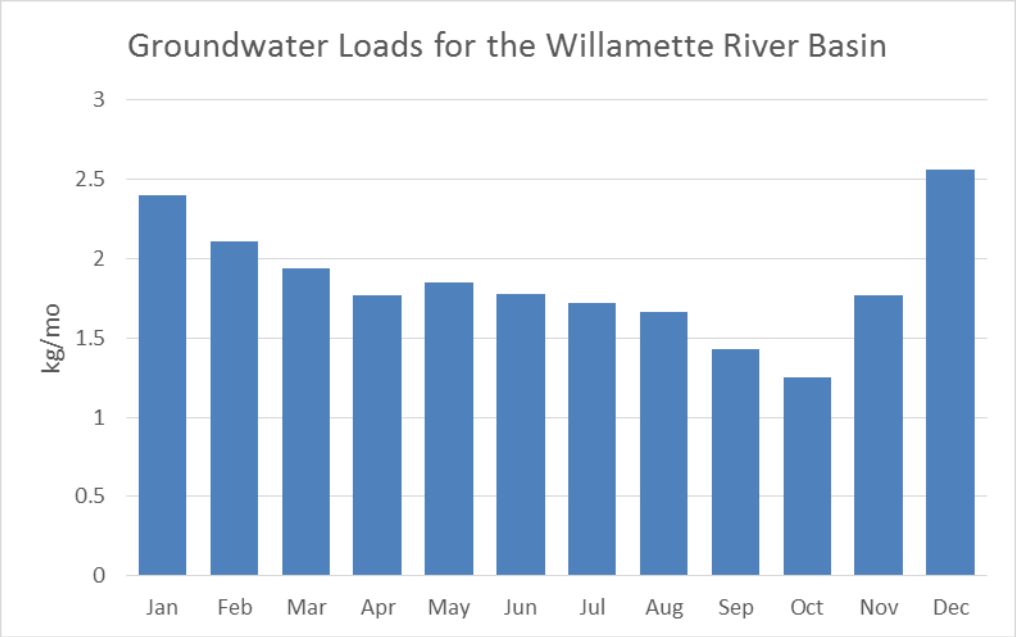

Figure 5-10. Monthly Average THg Loads Derived from Groundwater in the WRB

5.3.4 Mining Sources

The WRB contains former mercury mines as well as gold mines that employed mercury amalgamation to extract ore. These mine sites left a legacy of surface and downstream mercury contamination, primarily in the form of mine tailings and residue from ball mill furnace operations to extract mercury-amalgamated gold. The bulk of the known mercury-related mining features in the WRB are in the Coast Fork Willamette watershed (17090002). Others are found in the Clackamas (17090011) and South Santiam (17090006) HUC8s (Table 5-7).

The most significant mercury source associated with mining is the Black Butte Mine site, a former mercury mine in the Coast Fork Willamette watershed that is on the National Priorities ("Superfund") list (ODEQ Environmental Cleanup Site Information [ECSI] website # 1657). This site is situated about 10 miles south of Cottage Grove, Oregon, in southern Lane County and is immediately upstream of Cottage Grove Reservoir. While Cottage Grove resevoir receives some THg loads from atmospheric deposition and natural geologic background, mining-related pollution has been identified as the primary THg source (USEPA, 2018; Eckley et al., 2015; Park and Curtis, 1997). The Black Butte Mine was opened in the late 1890s and it was intermittently operated through the 1960s, extracting over a million pounds of elemental Hg from the site (Brooks, 1971; USEPA, 2012). Extensive amounts of exposed mine tailings were dumped into adjacent streams and left as waste piles. The site has been studied in some detail, with extensive sampling (USEPA, 2018; USEPA 2012). High concentrations of mercury in soils around the old and new furnace areas, likely due to spilling during processing along with deposition of furnace exhaust, and around the main tailings pile, release mercury in both particulate and dissolved forms to downstream

creeks. Heavily contaminated areas were capped and steep slopes were stabilized in 2007 (USEPA, 2008). Additional remediation work around the Black Butte Mine site was completed in 2018.

The second most significant mining area for mercury loading is the Bohemia Mining District that is situated along Upper Row River upstream of Dorena Reservoir in the Coast Fork Willamette watershed (Ambers and Hygelund, 2001). Gold was discovered in this region in the mid-1850s but most of the mining activity in the Bohemia Mining District did not start until several decades later (MacDonald, 1908). Mercury amalgamation was used to extract gold from ore mined in the Bohemia Mining District. A small amount of mercury mining also occurred in this region. Based on limited sampling above Dorena Reservoir (n=4), concentrations of THg entering the reservoir average around 1.8 ng/L, which is elevated relative to samples from elsewhere in the WRB (95th percentile THg of 0.24 ng/L). Hygelund et al. (2001) identified mining sources as the primary cause of elevated mercury in fish tissue in Dorena Reservoir. Henny et al. (2005) demonstrated that THg concentrations in benthic macroinvertebrates were more than double those found in the Middle Fork Willamette, a nearby watershed with no known gold or mercury mining sites.

A number of other former gold, silver, and mercury mines are also present in the WRB outside of the Coast Fork Willamette subwatershed. Table 5-7 is taken from Hope (2006) with additional notes from the ECSI website (http://www.oregon.gov/deq/Hazards-and-Cleanup/env-cleanup/Pages/ecsi.aspx) where available. Among these, three notable mines in the Oak Grove Fork area of the Clackamas watershed - Aimes-Bancroft, Kiggins, and Nisbet Mines - extracted mercury from cinnabar deposits in the 1930s and 40s, generating about 300 flasks total in this period (Brooks, 1963). ODEQ considers these abandoned mines to be a low priority because there are insufficient data to indicate they are significant sources of THg. Other abandoned mines outside the Coast Fork Willamette watershed did not score high enough to be included in the ECSI database. However, new data or observations showing that an abandoned mine may be a significant contributor of THg would initiate a response by ODEQ to conduct assessments and possible follow-up actions.

For the well-studied Black Butte Mine, site-specific loads associated with mine tailings and contaminated furnace areas were derived from monitoring data. The Black Butte Mine area drains to two small creeks - Dennis Creek and Furnace Creek - both of which exhibit elevated concentrations of THg in water and bed sediment. Mean concentration of THg measured between 2013 and 2016 for Dennis Creek (n = 27) and Furnace Creek (n = 19) were paired with daily flow estimates from the HSPF model to derive an annual average load for the Black Butte Mine of 1.34 kg/yr. A similar approach was used to estimate the THg load from the historic Bohemia Mining District. Brice Creek receives runoff from this historic mining site, and based on monitoring records (n = 4) and simulated flow, the annual average load of THg from the Bohemia Mining District was estimated as 0.12 kg/yr.

Note that THg loads from both Black Butte Mine and the Bohemia Mining District are subsequently altered by processes within the downstream Cottage Grove and Dorena Reservoirs. Loads leaving these reservoirs and flowing to the Coast Fork Willamette are calculated separately as described in Section 5.4.3.

Table 5-7. Mining Activities in the WRB that are Potential Sources of Mercury

Name	County	Subbasin	Comments
Aimes-Bancroft	Clackamas	Clackamas River	Old structures are present. Adit is caved.
Kiggins Mine (ECSI Site 3812)	Clackamas	Clackamas River	Discharge (1 gpm, pH 8.3) to Oak Grove fork of Clackamas River; flow. Mercuric oxides present in waste rock. Mill structure and other buildings present. Open adits. History of the mine is provided in O'Leary (2004). This is a CERCLA site and a removal action of contaminated sediment was completed in 2008.
Nisbet Mine (ECSI Site 3811)	Clackamas	Clackamas River	Oak Grove fork of Clackamas River is eroding tailings. Old structures are still present on site. Adit is still open. History of the mine is provided in O'Leary (2004).
North Fork Claims	Clackamas	Clackamas River	
Cheeney Creek	Clackamas	Clackamas River	Clear discharge (@ 5gpm, pH 8.1) to Cheeney Creek and Salmon River. Has eroded rock waste pile. Adit is open. Shaft appears caved.
Graham Property	Lane	Coast Fork, Willamette River	
Knott Claim	Lane	Coast Fork, Willamette River	
Treasure	Lane	Coast Fork, Willamette River	4000' of workings. Mill on-site.
Union	Lane	Coast Fork, Willamette River	1200' of workings. Mill on-site.
Bald Butte Prospect	Lane	Coast Fork, Willamette River	
Black Butte Mine (ECSI Site 1657)	Lane	Coast Fork, Willamette River	Was a mercury mine with three mills during its operating years from 1890-1909, 19161943, and 1956. Mine had two main tailing piles. The lower tailing pile was 30 feet away from Dennis Creek, which flows westerly to Garoutte Creek, which flows northerly to the Coast Fork of the Willamette River. Elevated mercury levels have been found in the sediment and in downstream Cottage Grove Reservoir. Remedial actions have been pursued and are described in the text for this section.
Champion & Evening Star Mine (ECSI Sites 2657 and 3659)	Lane	Coast Fork, Willamette River	Discovered in 1892 near the Champion Saddle on the divide of Champion and City Creeks. Mine had gold, silver, copper, lead, and zinc. Ore was processed in 3 mills. Mine has more than 15,000 feet of drifts and crosscuts, and about 3,000 feet of raises on 9 levels. Major years of production were from 1932 through 1939. Discolored discharge to Champion Creek (10 gpm, pH 5.5). Champion Creek flows to Brice Creek which dumps into the Row River. No structures. ECSI says that remedial action is recommended for tailings on USFS property, while site investigation is recommended for the portion on private land. Extensive information on the USFS property is in the ECSI file at http://www.deq.state.or.us/Webdocs/Forms/Output/FPController.ashx?SourceIdType=11&SourceId=2657&Screen=Load.

Name	County	Subbasin	Comments
Columbia Vein (ECSI Site 3169)	Lane	Coast Fork, Willamette River	Champion Creek watershed. Drainage (5 gpm, pH 7.2) not to surface water. According to ECSI, "the Site Assessment Program recommends no further action, for the following reasons: 1) there is no historical or visual evidence that ore was milled at the site, 2) there was no evidence of acid mine drainage or other impacts to surface water related to the site; and 3) there was no evidence of mill tailings on the site."
Excelsior Vein	Lane	Coast Fork, Willamette River	Champion Creek watershed. Part of Champion Mine.
Leroy Mine (ECSI Site 3167)	Lane	Coast Fork, Willamette River	Champion Creek watershed. Most of the development work was done between 1900 and 1910. There are numerous cuts and tunnels having a total length of 1,100 feet. A large volume of material was developed which contained a low percentage of base metals. According to ECSI, "the Site Assessment Program recommends a preliminary assessment."
Mayflower Mine	Lane	Coast Fork, Willamette River	
Lower Musick	Lane	Coast Fork, Willamette River	Adit and dump. No structures. Discharge (10 gpm, pH~7.5) directly to Sharps Creek (tributary to Brice Creek).
Noonday Mine (ECSI Site 3974)	Lane	Coast Fork, Willamette River	Major producer of gold, silver, copper, and lead. Mill on-site. This mine was discovered in 1891 and produced gold, silver, copper, lead, and zinc. According to literature, there was approximately 4,000 feet of workings, three mill sites, and 7,000 tons of ore mined. According to ECSI, "ODEQ has completed a non-sampling investigation of the Noonday Mine. Based on information developed during ODEQ's evaluation, the Noonday Mine is considered a medium priority for a Preliminary Assessment."
Peekaboo Mine	Lane	Coast Fork, Willamette River	Mill on-site. Not found in ECSI.
Pitcher Prospect	Lane	Coast Fork, Willamette River	
Star Mine	Lane	Coast Fork, Willamette River	1300' of workings. Brice Creek watershed.
Sultana Mine	Lane	Coast Fork, Willamette River	2000' of workings. Mill on-site. Champion Creek watershed.
Sweepstakes	Lane	Coast Fork, Willamette River	1000' of workings. Champion Creek watershed.

Name	County	Subbasin	Comments
Vesuvius (ECSI Site 3166)	Lane	Coast Fork, Willamette River	6000' of workings. Mill on-site. Brice Creek watershed. The Vesuvius vein was discovered in 1895, and the adit driven to explore the vein was known as the German Tunnel. A five-stamp mill was moved in from the old Knott Mill and operated at the German Tunnel until 1902. During the same time period, the Stocks-Harlow vein was being mined and this location also had a five-stamp mill. In 1902, both of these properties were organized into one mining company, and a new camp was built about a mile down the mountain below the German Tunnel. Near the camp site, a new adit called the Wild Hog was driven into the hillside, and a five-stamp mill was moved to this new location. In all, the entire mine's production was considered]. There is acid drainage from the mine and ECSI recommends an expanded preliminary assessment to evaluate metals in soil, sediment, and surface water.
Woodard Prospects	Lane	Coast Fork, Willamette River	
Sullivan (Bald Butte)	Lane	Coast Fork, Willamette River	
Amalgamated Mine	Marion	North Santiam River	
Black Eagle Mine (ECSI site 4455)	Marion	North Santiam River	Per ECSI, the Black Eagle Mining & Milling Co. owned the mine in 1916. A small concentrator mill was used on-site. There were no signs of waste rock or tailings piles, despite the site having a small concentrator mill in 1916." The adit was blasted shut in 2001 and the site is listed as "No further state action required."
Morning Star Mine (a.k.a. Blue Jay Mine) and Ruth Mine (ECSI site 4503)	Marion	North Santiam River	Morning Star is 8.5 miles northeast of the town of Elkhorn, Oregon. The Site is situated on steep side slopes. The Site consists of an open adit with water discharge, a collapsed structure, and waste rock piles. Nearby Ruth Mine consists of two adits at the 4th and one adit at the 5th Level. Small waste rock dumps occur at the 4th Level. These mines drain to Battle Axe Creek, Ruth Creek, and Blue Jay Creek and are within the Willamette National Forest and the USFS undertook investigations and cleanup under the Federal CERCLA program. Mercury is present in waste rock but has not been identified as a contaminant of concern in water or sediment. Extensive documentation is available at https://www.fs.usda.gov/detail/willamette/landmanagement/resourcemanagement/?cid=stelprdb5050007.
Bonanza Mine	Marion	North Santiam River	
Crown Mine	Marion	North Santiam River	
Silver King Mine	Marion	North Santiam River	
Silver Star Mine	Marion	North Santiam River	
Breitenbush Mineral Springs	Marion	Breitenbush River, North Santiam River	

Name	County	Subbasin	Comments
Bob & Betty	Linn	Quartzville Creek, Middle Santiam River	1650' of workings.
Poorman	Linn	Quartzville Creek, Middle Santiam River	Mill on-site.
Albany Mine	Linn	Quartzville Creek, Middle Santiam River	Gold mine first prospected in 1888. Ore was processed in 3 mills. There were approximately 1,090' of workings.
Lawler	Linn	Quartzville Creek, Middle Santiam River	Discovered in 1861 on White Bull Mountain and Dry Gulch. Mine had gold, silver, lead, copper, and zinc. There were 2,000' of workings by 1903, with four principal adit levels and numerous open cuts.

5.3.5 POTW Sources

Publicly owned treatment works (POTWs) primarily process and treat domestic sewage. Discharge monitoring records from 23 major POTWs that discharge to the WRB were provided by ODEQ to characterize POTW loads for the Mass Balance Model (Table 5-8 and Figure 5-11). The major POTWs provided flow and mercury concentration data that were used to compute representative mercury loads, as discussed below. The City of Portland's Columbia Boulevard POTW is the largest POTW in the Oregon that collects sanitary discharges from most of Portland and treats up to 450 MGD in the rainy season; all the mercury collected in the sanitary system is passed through biosolids and landfilled or discharged in effluent to the Columbia River. Therefore, it is not included in the WRB Mass Balance Model. The Gresham POTW is also physically located within the WRB, but discharges effluent to the Columbia River and is therefore not included in the WRB Mass Balance Model.

Daily effluent records, where available, were used to estimate an average annual discharge for each POTW. Daily effluent records for each POTW were subjected to QA review. There were several instances where a reported daily flow volume was several orders of magnitude higher than typical flows reported by the entity, potentially due to units or data entry error. To avoid an overestimation of mercury loads from POTWs, these extreme outliers were adjusted to the average of flows reported on the surrounding days. Monthly average flow was used for POTWs that did not report or had very limited daily monitoring information, as this was the best currently available information. Actual effluent records were unavailable for some POTWs. Therefore, flow information submitted to DEQ in 2017 as part of the variance applications for the four Clean Water Services wastewater treatment plants was used to establish representative annual average flows for the four POTWs.

Some permit holders are authorized to discharge to multiple outfalls. Data for each outfall underwent a separate QA review and outfalls were combined to compute an overall discharge flow for the permittee. Duplicate flow records identified by permit number, date, and pipe (if applicable) were infrequent but also addressed; duplicate records were averaged to produce a single daily representative flow.

Annual flow was computed for every year a POTW reported discharge information. We derived a representative average annual flow using only years with complete (or nearly complete) flow records (defined as at least 11 months out of the year), as this accounts for seasonal variations in effluent volume. Nearly complete annual records (e.g., daily records available for 11 of 12 months) were filled

using monthly average values, and these years were included in the calculation of average annual flow for a POTW (Table 5-9). A continuous time series of flow records was not available for POTW #101518 [City of Dallas], thus the daily average of the flow record (n=18) was taken and then multiplied by 365.25 to obtain an annual value. Available mercury samples from effluent were used to estimate an average mercury concentration for each POTW. There were several steps used to account for concentrations reported as below the method detection limit. First, if all non-detects were at levels greater than the highest detected value reported by a POTW (due to a change in detection limit over time), these non-detects were eliminated from the analysis. For POTWs that reported both censored (non-detect) and detected mercury concentrations, the Kaplan-Meier method of addressing non-detects (Helsel, 2005) was applied in R to calculate a representative mean concentration. Some POTW datasets have THg results with multiple detection limits. The Kaplan-Meier method was used because it is preferred over ROS (Regression on Order Statistics) for datasets that have multiple detection limits (Bolks et al., 2014; see also more detailed discussion in Section 4.1.3). If all mercury data reported by a POTW were non-detect or if no data were available, an average concentration was estimated using mercury monitioring records from facilities of similar type and size, identified based on NPDES domestic major class. Average annual mercury concentrations for the POTWs are provided in Table 5-9, as are POTW loads estimated for the mass balance model. The total major POTW THg load for the WRB is 1.07 kg/yr.

Loads were also estimated for minor domestic WWTPs that discharge to waters in the WRB. ODEQ provided average dry (May 1 – October 31) and wet (November 1 – April 30) weather design flows that were used to calculate average annual effluent flows for the minor facilities. Design flows were replaced with actual discharge records where available. No THg monitoring data were available for the minor domestic WWTPs. Therefore, the median THg concentration from the major POTWs (2.60 ng/L) was applied as a representative concentration to approximate the minor loads. The combined THg load for the minor domestic WWTPs is 0.095 kg/yr.

Table 5-8. Major Domestic (POTW) Discharges in the Willamette River Basin

Name	Permit #	City	County	HUC8
Albany-Millersburg Water Reclamation Facility	102024	Albany	Linn	17090003 (Upper Willamette)
Canby, City of	101063	Canby	Clackamas	17090007 (Middle Willamette)
Clackamas County Service District #1	100983	Milwaukie	Clackamas	17090012 (Lower Willamette)
Clean Water Services (Durham Facility)	101141	Tigard	Washington	17090010 (Tualatin)
Clean Water Services (Forest Grove Facility)	101142	Forest Grove	Washington	17090010 (Tualatin)
Clean Water Services (Hillsboro Facility)	101143	Hillsboro	Washington	17090010 (Tualatin)
Clean Water Services (Rock Creek Facility)	101144	Hillsboro	Washington	17090010 (Tualatin)
Corvallis, City of	101714	Corvallis	Benton	17090003 (Upper Willamette)
Cottage Grove, City of	101300	Cottage Grove	Lane	17090002 (Coast Fork Willamette)
Dallas, City of	101518	Dallas	Polk	17090007 (Middle Willamette)
Lebanon, City of	101771	Lebanon	Linn	17090006 (South Santiam)
McMinnville, City of	101062	McMinnville	Yamhill	17090008 (Yamhill)
Metropolitan Wastewater Management Commission	102486	Eugene	Lane	17090003 (Upper Willamette)
Newberg, City of	100988	Newberg	Yamhill	17090007 (Middle Willamette)
Oak Lodge Water Services District	100986	Milwaukie	Clackamas	17090012 (Lower Willamette)
Portland, City of (Tryon Crk)	101614	Lake Oswego	Clackamas	17090012 (Lower Willamette)
Salem, City of	101145	Keizer	Marion	17090007 (Middle Willamette)
Silverton, City of	101720	Silverton	Marion	17090009 (Molalla / Pudding)
Stayton, City of	101601	Stayton	Marion	17090005 (North Santiam)
Sweet Home, City of	101657	Sweet Home	Linn	17090006 (South Santiam)
Tri-City Service District	101168	Oregon City	Clackamas	17090011 (Clackamas)
Wilsonville, City of	101888	Wilsonville	Clackamas	17090007 (Middle Willamette)
Woodburn, City of	101558	Woodburn	Marion	17090009 (Molalla / Pudding)

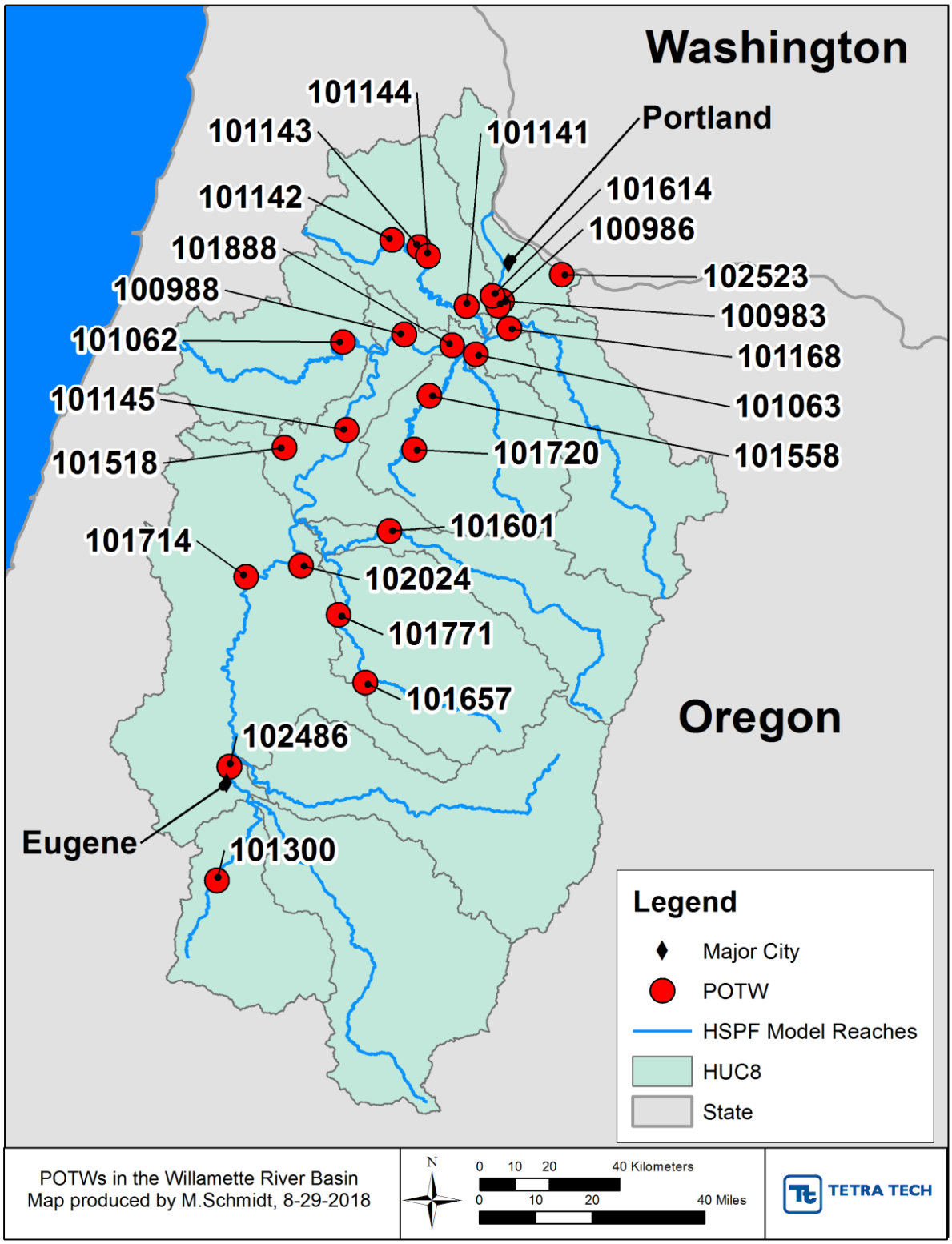

Figure 5-11. POTW Discharges in the Willamette River Basin

Table 5-9. Annual Average Effluent Flow, THg Concentration, and Estimated THg Load for POTWs in the Willamette River Basin

Permit #	Name	HUC 8	Average Flow (MG/yr)	Average THg (ng/L)	Load (kg-THg/yr)
100983	Clackamas County Service District #1	17090012	2,885	6.2	0.068
100986	Oak Lodge Water Services District	17090012	1,268	11.7 [A]	0.056
100988	Newberg, City of	17090007	1,163	4.1	0.018
101062	McMinnville, City of	17090008	1,822	1.7 [C]	0.012
101063	Canby, City of	17090007	366	2.7	0.004
101141	Clean Water Services (Durham Facility)	17090010	12,382 [D]	1.7	0.080
101142	Clean Water Services (Forest Grove Facility)	17090010	2,593 [D]	2.6	0.026
101143	Clean Water Services (Hillsboro Facility)	17090010	1,424 [D]	3.2	0.017
101144	Clean Water Services (Rock Creek Facility)	17090010	20,965 [D]	1.7	0.135
101145	Salem, City of	17090007	690	25.2	0.0664
101168	Tri-City Service District	17090011	3,467	5.9	0.077
101300	Cottage Grove, City of	17090002	829	1.01	0.003
101614	Portland, City of (Tryon Creek)	17090012	2,149 [C]	14.1	0.115
101518	Dallas, City of	17090007	535 [B]	1.4	0.003
101558	Woodburn, City of	17090009	830	2	0.006
101601	Stayton, City of	17090005	601	11.7 [A]	0.027
101657	Sweet Home, City of	17090006	657	11.7 [A]	0.029
101714	Corvallis, City of	17090003	4,131	6.8	0.106
101720	Silverton, City of	17090009	609	11.7 [A]	0.027
101771	Lebanon, City of	17090006	121	11.7 [A]	0.005
101888	Wilsonville, City of	17090007	776	30	0.088
102024	Albany-Millersburg WRF	17090003	3,058	1.7	0.02
102486	Metropolitan Wastewater Mgt Commission	17090003	12,744	1.7	0.083
Total					**1.07**

Notes: A: THg data were not available, estimated from facilities of similar type and size defined as having the same NPDES domestic major class, e.g., class C.
B: Full time series of flow data not available (< 20 flow records)
C: Monthly average values used (limited or no daily data available)
D: Flow from variance applications submitted to DEQ in 2017. Flow and mercury concentration records collected between 2004 to 2017 were used to establish average flows and THg concentrations.

5.3.6 Industrial Discharges

Mercury loads associated with industrial process wastewater are characterized in the Mass Balance Model. (Discharges of non-contact cooling water are assumed to not increase THg mass in the receiving waterbody.) Loads from major pulp and paper mill sources were represented in the 2006 TMDL, although

smaller industrial sources were omitted. Major industrial discharges from these facilities constituted 1.5 percent of the overall THg load in the WRB in the 2006 TMDL. Of the eight pulp and paper mills listed in the 2006 TMDL, three have closed and most of the others have changed ownership (and names). The Mass Balance model incorporates the mills that were active during the 2007-2014 period when most of the MeHg in water and recent fish tissue data were collected, even though some have since ceased operation. A full summary of current ownership and operational status of the pulp and paper mills will be provided in the TMDL implementation plan. The changes in industrial discharges since 2006 are accounted for in the updated Mass Balance Model, and new monitoring data are incorporated from industrial facilities holding active wastewater permits.

To estimate industrial effluent loads of THg, direct monitoring data provided by the facilities via ODEQ were applied as first priority (available for Cascade Pacific Pulp, Hollingsworth & Vose, West Linn Paper, International Paper, and Georgia Pacific). When direct monitoring data were used, the average annual THg load for an industrial discharger was computed as:

$$L_i = F_i \cdot C_t \cdot \alpha$$

where L_i is the average annual load for industrial discharger *i* in kg/yr; F_i is the average annual flow for industrial discharger *i* in L/yr; C_t is the representative effluent THg concentration in ng/L; and α is a conversion factor.

For pulp and paper mills where THg monitoring records were not available, loads to water reported in the USEPA Toxics Release Inventory (TRI) were applied (WestRock Northwest). The TRI contains estimates of the annual THg load released to water and, thus, were applied directly instead of using the equation shown above.

In addition to the pulp and paper mills discussed above, there are also a wide variety of other permitted industrial discharges that have the potential to release small amounts of THg. These industrial permits are addressed in the TMDL, but, as THg monitoring has generally not been required for these permits, there is a paucity of data. ODEQ provided the limited amount of industrial discharge data available for this purpose (from Discharge Monitoring Reports (DMRs) and permit application and renewal documents). The remainder of this section discusses the approach for accounting for THg loads from industrial dischargers classified under Standard Industrial Classification (SIC) categories (other than the pulp and paper mills) that have the potential to release small amounts of THg.

Monthly or quarterly flow records from 2017 DMRs provided by ODEQ were used to estimate an average annual effluent flow for each facility. In the absence of 2017 DMR flow records, design flow information from the permit applications, also provided by ODEQ, was used. Facilities that lacked both DMR flow records and design flow information are excluded from the analysis because discharge volumes from these facilities are thought to be negligible. Many of these permits are for industrial stormwater. Stormwater THg loads derived from atmospheric deposition and soil erosion are modeled separately in the Mass Balance Model and implicitly include industrial stormwater THg loads with other urban stormwater sources (see Section 5.3.7). Permits for several facilities without DMR flow data have been terminated.

Effluent THg monitoring data are not available for most industrial dischargers in the WRB. Therefore, representative THg concentrations are used for the load assessment of permits without THg monitoring. There are limited THg concentration data available from timber product and primary metal industries in the WRB. Data from these facilities are averaged to estimate representative concentrations for SIC categories (Table 5-10). These averages were applied to facilities of similar type in the basin.

Table 5-10. Representative THg Concentrations for Industrial Dischargers

SIC Code	Categorical Description	Average THg Concentration (ng/L)	Relevant THg Concentration Data from Dischargers in the Willamette River Basin
24xx	Timber products	5.5	Stimson Lumber (n = 1, 9.8 ng/L), Engineered Lumber (n = 1, 0.5 ng/L), Hollingsworth & Vose Fiber Co. (n = 6, 11 ng/L) and McFarland Cascade Holdings (n = 1, 0.5 ng/L)
26xx	Paper products	9.1	Cascade Pacific Pulp (n = 7, 8.2 ng/L), Halsey Mill (n = 1, 10 ng/L)
33xx	Primary metal industries	10	Allvac Albany Plant (n = 1, 10 ng/L)

Note: Effluent from timber product facilities includes log pond discharges and process wastewater. Several observations listed as non-detects at a high method detection limit (300 ng/L) were omitted from the analysis. The remaining data shown above contain no censored values.

Statewide and regional USEPA-approved mercury TMDLs provide information for estimating an appropriate THg concentration for other types of industrial dischargers, and these are summarized in Table 5-11. The Minnesota Statewide Mercury TMDL (MPCA, 2007) applied a uniform representative concentration of 5 ng/L to estimate industrial discharger loads. Likewise, a single representative concentration of 7.7 ng/L was assumed for the northeast U.S. regional mercury TMDL (NEIWPCC, 2007). The assumed mean concentration for other (not municipal or petroleum refineries) National Pollutant Discharge Elimination System (NPDES)-permitted facilities in the California Statewide Mercury Control Program for Reservoirs was 7.2 ng/L (Austin and Smitherman, 2017).

A representative concentration of 7.0 ng/L is applied for industrial discharger types with reasonable potential to be sources of THg but without supporting monitoring data. This concentration is used because it is comparable to available monitoring data (Table 5-10), and to the reference sources discussed (Table 5-11).

Table 5-11. Reference THg Concentrations for Industrial Dischargers

Source	THg Concentration (ng/L)	Additional Information
Minnesota Statewide Mercury TMDL (MPCA, 2007)	5.0	Assessed based on combined POTW and industrial discharger monitoring data; applied uniformly for TMDL load assessment
Northeast Regional Mercury TMDL (NEIWPCC, 2007)	7.7	Assessed based on combined POTW and industrial discharger monitoring data; applied uniformly for TMDL load assessment
HDR (2013) Treatment Technology Review and Assessment	10 – 50	Typical concentration in industrial secondary effluent based on Puget Sound study
California Statewide Mercury Control Program for Reservoirs (Austin and Smitherman, 2017)	1st Quartile: 1.3 Median: 3.1 Mean: 7.2 99th Percentile: 63	Values for other NPDES-permitted facilities (excludes municipal WWTPs, municipal combined stormwater sewer systems, and petroleum refineries)

Several permit types are not believed to be significant sources of THg (e.g., fish hatcheries, food/beverage production facilities, non-contact cooling water) because production processes at these facilities do not involve mercury, and these are excluded. Permits identified by ODEQ as being terminated are not represented in the Mass Balance Model either. Table 5-12 outlines the approach used to assess loads for industrial discharger types believed to contribute THg in the basin, and notes those that are not expected to be sources of THg. Estimated annual average THg loads from industrial effluent are presented by facility in Table 5-13. The estimated THg load from all industrial discharges in the WRB is 0.46 kg/yr.

Table 5-12. Methods for Estimating Industrial Discharger THg Loads

SIC	Categorical Description	Method
921	Operating fish hatchery	Not expected to be a THg source, excluded from analysis*.
20xx	Food and kindred products	Not expected to be a THg source, excluded from analysis.
24xx	Timber products	Estimated THg concentration of 5.5 ng/L (Table 1) combined with available flow information.
26xx	Paper products	Estimated THg concentration of 9.1 ng/L (Table 1) combined with available flow information.
28xx	Chemical products	Estimated THg concentration of 7.0 ng/L based on relevant references combined with available flow information.
32xx	Glass, clay, cement, concrete, gypsum products	Estimated THg concentration of 7.0 ng/L based on relevant references combined with available flow information.
33xx	Primary metal industries	Estimated THg concentration of 10 ng/L (Table 1) combined with available flow information.
34xx	Fabricated metal products	Estimated THg concentration of 7.0 ng/L based on relevant references combined with available flow information.
36xx	Electronics and instruments	Estimated THg concentration of 7.0 ng/L based on relevant references combined with available flow information.
45xx	Air transportation	Not expected to be a THg source, excluded from analysis.
46xx	Pipelines, except natural gas	Not expected to be a THg source, excluded from analysis.
49xx	Electric, gas, and sanitary services	Not expected to be a THg source, excluded from analysis.
51xx	Wholesale trade	Not expected to be a THg source, excluded from analysis.
79xx	Amusement and recreation	Not expected to be a THg source, excluded from analysis.
82xx	Educational services	Not expected to be a THg source, excluded from analysis.
87xx	Engineering and management services	Not expected to be a THg source, excluded from analysis.
92xx	Justice, public order, and safety	Not expected to be a THg source, excluded from analysis.

* Fish hatcheries can be low level sources of THg due to contamination of fish feed. However, the potential THg loads associated with operating fish hatcheries were considered negligible for purposes of the TMDL. Loads were included for facilities with a SIC code that is generally not expected to be a significant THg source but which had available THg monitoring data.

Table 5-13. Permitted Industrial Facilities in the Willamette River Basin and Estimated THg Loads (kg/yr)

Legal Name	ODEQ Permit Number	USEPA Permit Number	Notes	Estimated THg Load (kg/yr)
ANKRON MOISAN ASSOC ARCHITECTS INC	101536	OR0040363	Terminated	-
ARCLIN	101544	OR0000892	SIC not expected to be THg source, excluded from analysis	-
ARCLIN U.S.A. LLC	101235	OR0021857	Used DMR flow data and representative concentration for SIC	0.00159
ARKEMA	100752	OR0001597	Flow data not provided, excluded from analysis	No data
ARKEMA	103075	OR0044695	Used DMR flow data and facility monitoring data for THg concentration	0.000510
ASH GROVE CEMENT - RIVERGATE LIME PLANT	102465	OR0001601	Non-contact cooling water determined not to be a source of mercury in permit evaluation	-
BDC/WILLAMETTE LLC	101536	OR0040363	SIC not expected to be THg source, excluded from analysis	-
BLOUNT OREGON CUTTING SYSTEMS DIVISION	101162	OR0032298	Used DMR flow data and facility monitoring data for THg concentration	0.000938
BLUE HERON PAPER COMPANY	102229	OR0000566	Currently being redeveloped for alternative use, excluded from analysis	-
BOEING OF PORTLAND - FABRICATION DIVISION	101761	OR0031828	Flow data not provided, excluded from analysis	-
CANBY WATER TREATMENT PLANT	101896	OR0040649	Flow data not provided, excluded from analysis (note states permit has expired)	-
CASCADE CORP.	101630	OR0034924	Terminated	-
CASCADE PACIFIC PULP, LLC	101114	OR0001074	Used DMR flow data and facility monitoring data for THg concentration	0.145
CASCADE STEEL ROLLING MILLS, INC.	101487	OR0027260	Used DMR flow data and representative concentration for SIC	0.00265
CHEVRON/TEXACO SERVICE STATION NO 211-517	102744	OR0034347	Terminated	-
CLACKAMAS RIVER HATCHERY	102663	OR0034266	Terminated	-
CLEAR CREEK RAINBOW RANCH	101493	OR0030171	Flow data not provided, excluded from analysis	-
COLUMBIA HELICOPTERS, INC.	101906	OR0033391	SIC not expected to be THg source, excluded from analysis	-
COVANTA MARION, INC	101240	OR0031305	Used DMR flow data and facility monitoring data for THg concentration	0.00895

Legal Name	ODEQ Permit Number	USEPA Permit Number	Notes	Estimated THg Load (kg/yr)
EUGENE WATER & ELECTRIC BOARD	101329	OR0000680	SIC not expected to be THg source, excluded from analysis	-
EVRAZ OREGON STEEL	101007	OR0000451	Used DMR flow data and facility monitoring data for THg concentration	1.99×10^{-5}
FLAKEBOARD AMERICA LIMITED	100668	OR0000426	Used DMR flow data and representative concentration for SIC	5.54×10^{-10}
FOSTER POULTRY FARMS, INC.	101590	OR0026450	SIC not expected to be THg source, excluded from analysis	-
FRANK LUMBER CO., INC.	101583	OR0000124	Used DMR flow data and representative concentration for SIC	0.00576
FUJIMI CORPORATION - SW COMMERCE CIRCLE	103033	OR0040339	Used DMR flow data and facility monitoring data for THg concentration	0.000132
GEORGIA-PACIFIC CHEMICALS LLC	102603	OR0032107	Flow data not provided, excluded from analysis (note states that the facility has not discharged in a few years)	-
GEORGIA-PACIFIC CHEMICALS LLC	101474	OR0002101	Used design flow and representative concentration for SIC	0.00193
GEORGIA-PACIFIC CONSUMER OPERATIONS LLC	101488	OR0033405	Used DMR flow data and facility monitoring data for THg concentration	0.00324
GRAPHIC PACKAGING - NORTH PORTLAND	101002	OR0000400	Flow data not provided, excluded from analysis	-
GROUNDWATER PUMPING STATION - MARINE DR	101617	OR0031135	SIC not expected to be THg source, excluded from analysis	-
HOLLINGSWORTH & VOSE FIBER COMPANY	101331	OR0000299	Used DMR flow data and facility monitoring data for THg concentration.	0.00537
HULL-OAKES LUMBER CO.	101466	OR0038032	Used DMR flow data and representative concentration for SIC	0.0331
I.WATER SERVICES	102833	OR0034371	Used DMR flow data and facility monitoring data for THg concentration	4.44×10^{-6}
INTEL - ALOHA CAMPUS	101533	OR0030929	Used DMR flow data and facility monitoring data for THg concentration	4.28×10^{-7}
INTERNATIONAL PAPER COMPANY	101081	OR0000515	Used DMR flow data and facility monitoring data for THg concentration	0.102
J.H. BAXTER & CO., INC.	102432	OR0021911	Used DMR flow data and representative concentration for SIC	0.000788
JASPER WOOD PRODUCTS, LLC	101427	OR0042994	Flow data not provided, excluded from analysis	-
JLR, LLC	101253	OR0001015	SIC not expected to be THg source, excluded from analysis	-
KINDER MORGAN BULK TERMINAL 4	102446	OR0031402	Terminated	-

Legal Name	ODEQ Permit Number	USEPA Permit Number	Notes	Estimated THg Load (kg/yr)
KINGSFORD MANUFACTURING COMPANY	102153	OR0031330	Used DMR flow data and representative concentration for SIC	0.000450
KNIFE RIVER CORPORATION - NW	103022	OR0044652	Flow data not provided, excluded from analysis	-
KOPPERS	101642	OR0000779	Flow data not provided, excluded from analysis	-
LINNTON SAND DISTRIBUTION FACILITY	102452	OR0039896	Terminated	-
LUCKY FARM, INC	102324	OR0035939	Terminated	-
MCFARLAND CASCADE HOLDINGS, INC.	101267	OR0029726	Used DMR flow data and representative concentration for SIC	0.0000173
MCFARLAND CASCADE POLE & LUMBER COMPANY	102392	OR0031003	Used DMR flow data and representative concentration for SIC	0.000438
MURPHY COMPANY	101777	OR0021741	Used DMR flow data and representative concentration for SIC	0.000259
NORPAC FOODS, INC.	100907	OR0021261	SIC not expected to be THg source, excluded from analysis	-
NORPAC FOODS, INC. Stayton	101265	OR0001228	SIC not expected to be THg source, excluded from analysis	-
NW NATURAL GAS SITE REMEDIATION	103061	OR0044687	Used DMR flow data and facility monitoring data for THg concentration	5.07×10^{-7}
ODFW - CLACKAMAS RIVER HATCHERY	102663	OR0034266	SIC not expected to be THg source, excluded from analysis	-
OREGON DEPARTMENT OF CORRECTIONS	101619	OR0043770	SIC not expected to be THg source, excluded from analysis	-
OREGON DEPARTMENT OF FISH & WILDLIFE	101914	OR0027642	SIC not expected to be THg source, excluded from analysis	-
OREGON DEPARTMENT OF FISH & WILDLIFE	101917	OR0027847	SIC not expected to be THg source, excluded from analysis	-
OREGON DEPARTMENT OF FISH & WILDLIFE	101918	OR0029769	SIC not expected to be THg source, excluded from analysis	-
OREGON FRESH FARMS, INC.	102324	OR0035939	Terminated	-
OREGON METALLURGICAL, LLC	102223	OR0001716	Used design flow and representative concentration for SIC	0.00415
OREGON SYSTEM OF HIGHER EDUCATION	102512	OR0032573	SIC not expected to be THg source, excluded from analysis	-
OREGON-CANADIAN FOREST PRODUCTS - NORTH PLAINS	101634	OR0039322	Terminated	-
PERMAPOST	101489	OR0039594	Used DMR flow data and facility monitoring data for THg concentration	0.000266

Legal Name	ODEQ Permit Number	USEPA Permit Number	Notes	Estimated THg Load (kg/yr)
PINNACLE CONDOMINIUM COMPLEX	102880	OR0038156	Terminated	-
PORTLAND INTERNATIONAL AIRPORT	101588	OR0040291	Terminated	-
PORTLAND INTERNATIONAL AIRPORT	101647	OR0040291	SIC not expected to be THg source, excluded from analysis	-
PORTLAND MEADOWS	102710	OR0034291	SIC not expected to be THg source, excluded from analysis	-
ROSBORO COMPANY, LLC	101467	OR0026999	Used DMR flow data and representative concentration for SIC	0.000530
ROYAL PACIFIC INDUSTRIES, INC.	101213	OR0037834	Flow data not provided, excluded from analysis	-
RSG FOREST PRODUCTS - LIBERAL	100929	OR0021300	Used DMR flow data and facility monitoring data for THg concentration	0.000444
SENECA SAWMILL COMPANY	101893	OR0022985	Used design flow (as DMR data gives only flow velocity) and representative concentration for SIC	0.00580
SFPP, L.P.	103042	OR0044661	Used DMR flow data and facility monitoring data for THg concentration	7.80×10^{-6}
SILTRONIC CORPORATION	101128	OR0030589	Used DMR flow data and facility monitoring data for THg concentration	0.00491
SLLI	101180	OR0001741	Used DMR flow data and facility monitoring data for THg concentration	0.000240
STIMSON LUMBER COMPANY - FOREST GROVE	101480	OR0001295	Used DMR flow data and facility monitoring data for THg concentration	0.00193
SUNDIAL MARINE	102890	OR0044601	Flow data not provided, excluded from analysis	-
SUNSTONE CIRCUITS	101015	OR0031127	Used DMR flow data and facility monitoring data for THg concentration	0.000167
TDY INDUSTRIES, LLC	100522	OR0001112	Flow data not provided, excluded from analysis	-
TEKTRONIX BEAVERTON CAMPUS (INDUSTRIAL WWTP)	101534	OR0001589	Flow data not provided, excluded from analysis	-
THE METROPOLITAN CONDOMINIUM COMPLEX	102881	OR0038229	Terminated	-
UNIVAR USA INC	101613	OR0034606	SIC not expected to be THg source, excluded from analysis	-
USFW - EAGLE CREEK NATIONAL FISH HATCHERY	101522	OR0000710	SIC not expected to be THg source, excluded from analysis	-

Legal Name	ODEQ Permit Number	USEPA Permit Number	Notes	Estimated THg Load (kg/yr)
VALLEY LANDFILLS, INC.	101545	OR0043630	SIC not expected to be THg source, excluded from analysis	-
VIGOR INDUSTRIAL	101393	OR0022942	SIC not expected to be THg source, excluded from analysis	-
WEST LINN PAPER COMPANY - EVERGREEN MILL	100976	OR0000787	Used DMR flow data and facility monitoring data for THg concentration	0.00438
WESTROCK NORTHWEST, LLC	101299	OR0000558	Used TRI load to water	0.0936
WEYERHAEUSER NR COMPANY (Purchased by Murphy Company)	101449	OR0000698	Used DMR flow data and representative concentration for SIC	0.0292
WILLAMETTE OAKS BUILDING	101536	OR0040363	Terminated	-
YARDS AT UNION STATION, THE	101700	OR0040533	Terminated	-
TOTAL				0.46

5.3.7 URBAN STORMWATER (MS4S)

Stormwater discharges from designated municipal separate storm sewer systems (MS4s) are subject to NPDES permits and are therefore analyzed separately for the Mass Balance Model. To comprehensively account for THg in urban stormwater, loads from both currently permitted Phase I and Phase II MS4s and urban Designated Management Areas (DMAs) that may be required to have an MS4 permit in the future, were estimated.

City and county MS4 areas were defined spatially. Coverages provided by Phase I and Phase II cities and counties were used directly to determine the boundary of the regulated MS4 area. For Phase I and Phase II MS4 cities that did not provide a spatial coverage, the 2017 city limits coverage was used as a proxy. For Phase I MS4 counties that did not submit a coverage, the regulated MS4 area was established as the area outside of the city MS4s and within the Metro Urban Growth Boundary (Metro UGB). This approach was used because USEPA's 1990 Phase I regulation required medium and large cities, and some counties with populations of 100,000 or more, to obtain NPDES permit coverage for their stormwater discharges. This evaluation was not performed based on urbanized area, as in the Phase II permit, because urbanized areas had not yet been defined by the US Census Bureau. Medium and large cities and counties were automatically designated for permit coverage. In the Portland Metro area, the Metro UGB was used, and included several small MS4s that were located within the Metro UGB. For Phase II MS4 counties that did not submit a coverage, the regulated MS4 area was delineated as the area outside of the city MS4s and within the county's Census-defined urbanized areas. USEPA used U.S. Census Bureau "defined urbanized areas" to identify which small Phase II MS4s were required to obtain NPDES permit coverage. The permit applies to the geographic area served by the regulated small MS4 that is located fully, or partially, within an urbanized area in the State of Oregon as defined by a Decennial Census conducted by the U.S. Census Bureau. If the small MS4 is not located entirely within an urbanized area, only the portion that is within the urbanized area is considered the minimum permit coverage area. Urban areas defined in the 2000 and 2010 Census were aggregated to provide a

comprehensive analysis of Phase II county MS4s. Boundaries for urban DMAs (i.e., jurisdictions not currently required to obtain a MS4 permit) were identified spatially as the area outside of Phase I and Phase II city and county MS4 boundaries but within the Urban Growth Boundary (UGB). Certain areas identified by the jurisdictions were excluded from the MS4 load tabulations, which include areas that drain to a combined sewer network that treats the water prior to discharging it to the receiving stream, areas where stormwater is collected for infiltration or underground injection, and land that drains directly to the Willamette River or Columbia River that does not pass through the MS4 system.

Stormwater discharged from Oregon Department of Transportation (ODOT) property is also regulated under the statewide ODOT MS4 permit. State-owned roads were identified from an ODOT linear right-of-way coverage ("signed_rtes.shp"). ODOT responsible areas were delineated by buffering the state-owned roads by the ODOT defined surface width ("surf_width_type.shp"), which covers right-of-way lanes and shoulders, such that the full buffer width equaled the total surface width. Where the ODOT MS4 area intersects city or county MS4s the regulated area is attributed to the city/county MS4 except in the case of Federal interstate highways.

Phase I and Phase II MS4s are listed in Table 5-14 and Table 5-15. MS4 regulated pervious and impervious lands were estimated as land classified as developed by NLCD 2011 within MS4 boundaries (Table 5-16); the additional urban DMAs are listed in (Table 5-17).

Table 5-14. Phase I MS4s in the Willamette River Basin

Permit Group	Jurisdiction	Type
Eugene	Eugene	City
Salem	Salem	City
Clackamas County	Gladstone	City
Clackamas County	Happy Valley	City
Clackamas County	Johnson City	City
Clackamas County	Lake Oswego	City
Clackamas County	Milwaukie	City
Clackamas County	Oregon City	City
Clackamas County	Rivergrove	City
Clackamas County	West Linn	City
Clackamas County	Wilsonville	City
Clean Water Services	Banks	City
Clean Water Services	Beaverton	City
Clean Water Services	Cornelius	City
Clean Water Services	Durham	City
Clean Water Services	Forest Grove	City
Clean Water Services	Hillsboro	City
Clean Water Services	King City	City
Clean Water Services	North Plains	City
Clean Water Services	Sherwood	City
Clean Water Services	Tigard	City
Clean Water Services	Tualatin	City
Gresham	Fairview	City
Gresham	Gresham	City
Portland	Portland	City
Multnomah County	Multnomah County	County
Clean Water Services	Washington County	County
Clackamas County	Clackamas Co. Dept. of Transportation and Development	Other
Clackamas County	Clackamas Service District #1	Other
Clackamas County	Oak Lodge Sanitary District	Other
Clackamas County	Surface Water Management Agency of Clackamas County	Other
Clackamas County	Water Environment Services	Other
Portland	Port of Portland	Other
ODOT	Oregon Dept. of Transportation	Other

Table 5-15. Phase II MS4s in the Willamette River Basin

Jurisdiction	Type
Albany	City
Corvallis	City
Keizer	City
Millersburg	City
Philomath	City
Springfield	City
Turner	City
Wood Village	City
Benton County	County
Lane County	County
Linn County	County
Marion County	County
Polk County	County

Table 5-16. Estimated Pervious and Impervious Regulated Areas for Phase I and Phase II MS4s

MS4 Permit Type	Permit/Jurisdiction	Pervious Area (ac)	Impervious Area (ac)
Phase I	Eugene	9,668	10,810
Phase I	Fairview	585	652
Phase I	Gladstone	633	640
Phase I	Happy Valley	1,501	1,225
Phase I	Johnson	18	24
Phase I	Lake Oswego	2,507	1,799
Phase I	Milwaukie	1,382	1,483
Phase I	Oregon City	2,164	2,241
Phase I	Rivergrove	34	17
Phase I	West Linn	1,748	1,311
Phase I	Wilsonville	1,510	1,780
Phase I	Portland	5,325	6,830
Phase I	Salem	9,066	9,993
Phase I	Clean Water Services	27,552	29,036
Phase I	Gresham	1,091	1,515
Phase I	Washington County	878	729
Phase I	Multnomah County	1,261	974
Phase I	Clackamas County	6,724	6,388
Phase I	ODOT	0	8,716
Phase II	Albany	3,537	4,127
Phase II	Corvallis	3,013	3,113
Phase II	Philomath	396	349
Phase II	Turner	213	187
Phase II	Wood Village	210	319
Phase II	Keizer	1,904	1,915
Phase II	Millersburg	407	595
Phase II	Springfield	3,479	4,560
Phase II	Polk County	437	289
Phase II	Linn County	832	638
Phase II	Benton County	943	615
Phase II	Marion County	2,744	2,573
Phase II	Lane County	6,302	6,202

Coverages provided by Phase I and Phase II cities and counties were used directly to determine the boundary of the regulated MS4 area. Only land classified as developed by NLCD 2011 was included. Areas draining to combined sewers or underground injection (UIC) systems were excluded where information was available. Loading rates vary across the landscape due to a variety of factors, such as soil type and weather, thus, regulated areas cannot be used directly to accurately attribute the total urban stormwater load to individual jurisdictions.

Table 5-17. Urban DMAs in the Willamette River Basin

Jurisdiction		
Adair Village	Halsey	Sandy
Amity	Harrisburg	Scappoose
Aumsville	Hubbard	Scio
Aurora	Idanha	Scotts Mills
Barlow	Independence	Sheridan
Brownsville	Jefferson	Silverton
Canby	Junction City	Sodaville
Carlton	Lafayette	St. Helens
Coburg	Lebanon	St. Paul
Columbia County	Lowell	Stayton
Cottage Grove	Lyons	Sublimity
Creswell	Maywood Park	Sweet Home
Dallas	McMinnville	Tangent
Dayton	Mill City	Veneta
Detroit	Molalla	Waterloo
Donald	Monmouth	Westfir
Dundee	Monroe	Willamina
Estacada	Mt. Angel	Woodburn
Falls City	Newberg	Yamhill
Gates	Oakridge	Yamhill County
Gervais		

THg loads in urban stormwater are believed to derive primarily from atmospheric deposition to impervious and pervious surfaces that route to the storm sewer network with overland flow, but THg associated with sediment erosion and shallow interflow on pervious lands in regulated areas also contribute to urban stormwater loads and are subject to MS4 permits, while groundwater discharge is not. THg loads from impervious and pervious surfaces outside of the MS4 regulated or urban DMA areas are represented under the surface runoff, sediment, and groundwater categories. Regulated urban stormwater is limited to low, medium, and high density developed land (based on NLCD 2011) within permitted MS4 and urban DMA boundaries to approximate the contribution to regulated storm sewer conveyance systems. THg from other land uses (refer to Table 5-1 for other land use classes) within permitted MS4 and urban DMA

boundaries are attributed to the respective non-MS4 source category (loads from areas identified as draining to combined sewers are excluded from the MS4 and non-MS4 categories).

To support estimation of THg loads from MS4s, the HSPF model was used to estimate sediment yield rates from developed pervious surfaces, interflow rates from developed pervious surfaces, and surface runoff rates from developed impervious and pervious surfaces. The MS4 THg load associated with sediment erosion and transport was estimated by multiplying sediment load times soil THg concentration (Section 5.3.2) and the interflow load was estimated by multiplying the flow times the nominal subsurface THg concentration of 1 ng/L (Section 5.3.3). The THg load from surface runoff was estimated from the wet atmospheric deposition concentration (Section 5.3.1) and the portion of the annual average precipitation that runs off via surface pathways. Part of the THg load associated with surface runoff is from dry atmospheric deposition to impervious surfaces. A unit-area HSPF model (described below) was built to test the representation of THg buildup and washoff, given the dry deposition rate specified in Section 5.3.1. This part of the surface runoff load was derived from the fraction of the total dry deposition that is simulated as washing off rather than being re-emitted to the atmosphere.

Calculations for developed land uses in the Portland area (HSPF model upland HRU number 821) are provided for example. THg loads delivered to waterbodies (excluding the groundwater pathway) from pervious developed land average 11.9 mg/ac/yr, while THg loads from impervious surfaces are about twice as high, at 23.2 mg/ac/yr. Impervious surfaces also generate larger volumes of runoff, and the net result is that runoff concentrations from both pervious and impervious developed land are predicted to be similar, at 6.8 and 6.3 ng/L, respectively. If an MS4 drainage area is assumed to be around 50 percent impervious, the resulting mixed concentration is 6.5 ng/L, and 78 percent of the THg load is predicted to derive from wet atmospheric deposition (Figure 5-12).

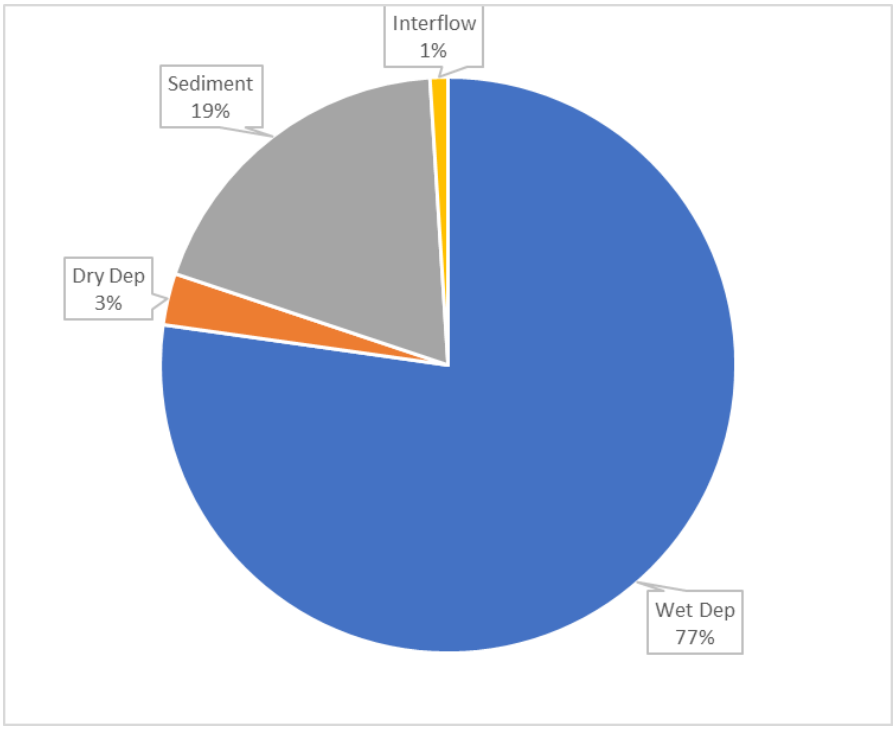

Figure 5-12. Example of THg Source Attribution for THg Load from MS4 Developed Land (50% Impervious) in the Portland Area

Figure 5-12 shows the fractions of THg runoff attributed to various source pathways and not the ultimate source contributions, which are predominantly from atmospheric deposition. The sediment and interflow fractions are largely derived from atmospheric deposition, but the wet and dry fractions are not known. In addition, re-emission to the atmosphere is attributed only to the dry deposition fraction, which may tend to over-estimate the relative importance of wet versus dry deposition.

As a further check on the MS4 load estimation, THg monitoring data supplied by MS4s were compiled and screened. Monitoring from best management practice (BMP) outlets was excluded when identified as such in the databases. Samples labeled as "stormwater" were included, while "surface" samples were excluded. Sample counts by MS4 entity are provided in Table 5-18. While the values ranged across a few orders of magnitude (0.25 ng/L to 120 ng/L), most of the data fell in a narrower range with a first quartile of 2.94 ng/L, a median of 4.62 ng/L, and a third quartile of 8.31 ng/L. The estimated MS4 THg concentration shown above for the Portland area example (6.5 ng/L) falls squarely within the inter-quartile range of the monitoring data.

Table 5-18. THg Monitoring Data from MS4s

Organization	Count
Clackamas County	6
Clean Water Services (Washington County)	148
Eugene	150
Gresham	317
Lake Oswego	4
Milwaukie	2
Oregon City	3
Portland	10
Salem	13
West Linn	2

Most of the MS4 samples appear to represent runoff from a mixture of impervious and pervious surfaces, in some cases including non-urban land uses. However, the land use draining to monitoring sites is not consistently documented and cannot be used to directly constrain or calibrate the loading rates from pervious and impervious surfaces beyond the qualitative check for consistency described above.

As noted above, a modified HSPF model representing unit area impervious land was developed to explore the fate of build-up and wash-off of mercury from atmospheric deposition onto impervious surfaces. We used the unit-area model to examine the shape of the THg response function with the literature-based rates of wet and dry atmospheric deposition. This experiment suggested that the cumulative distribution shape of reported MS4 THg concentrations could be matched in the impervious buildup/washoff model by setting the effective dry deposition accumulation limit to 167 ng/m^2, and reducing the rate of surface runoff that removes 90 percent of THg stored on the surface from an initial value of 0.50 in/hr to 0.08 in/hr (Figure 5-13). The shape parameters for accumulation limit and rate of

surface runoff determined from the model experiment were assumed to be applicable to the simulation of dry deposition washoff from impervious surfaces and were incorporated in the Portland example shown above.

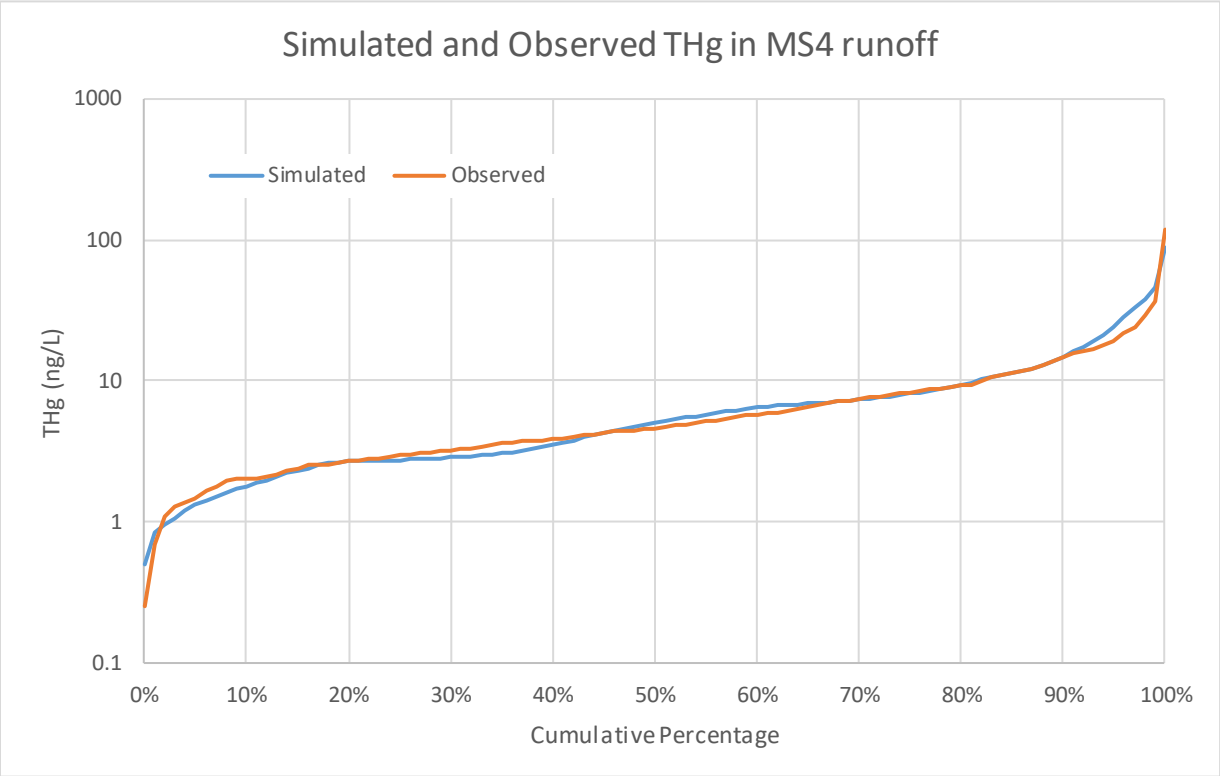

Figure 5-13. Cumulative Distributions of Modeled and Observed THg Concentrations Representing MS4 Discharges

The buildup-washoff process is represented through an exponential accumulation rate n (ng/m^2-day) and a depletion rate constant, β (day^{-1}). The rate of accumulation of THg mass (N, ng) is given by the differential equation $dN/dt = n - \beta N$ and the solution at time t is $N(t) = N(0)\, e^{-\beta t} + (n/\beta)(1 - e^{-\beta t})$. As t gets large, the solution asymptotes toward the accumulation limit of n/β.

Dry atmospheric deposition in the WRB is estimated to occur at a rate of 4.24 µg/m^2/yr = 11.608 ng/m^2/day. For the calibrated accumulation limit of 167 ng/m^2, this implies that β= 0.0695 day^{-1} and that 90% of the accumulation limit would be reached in 33.13 days in the absence of washoff. Total accumulation over 33.13 days is 384.57 ng/m^2, while 90% of the accumulation limit is 150.3 ng/m^2. This implies that 61% of the dry deposition is lost prior to any washoff, primarily by photoreduction and re-emission to the atmosphere, which is generally consistent with research suggesting that 39 – 61 % or "roughly half" of the THg deposited to urban surfaces is delivered in runoff (see summary in Hsu-Kim, 2018).

Portions of the City of Portland and several smaller municipalities in the WRB have combined sewer systems in which stormwater from highly urbanized areas is combined with sanitary sewage; however, only the City of Portland provided boundaries of the combined sewer drainage areas. Stormwater mixed with sanitary sewage from these combined sewer areas is routed to POTWs for treatment and does not discharge directly to streams except during combined sewer overflow (CSO) events. For the City of

Portland, areas in the combined sewer drainage area were excluded from the MS4 and urban non-MS4 load estimates.

The majority of historic CSOs in the WRB were from the City of Portland and discharged to the Willamette River and Columbia Slough. Under an order issued by DEQ, the City of Portland funded and implemented a long-term Combined Sewer Overflow Abatement Project, commencing in 1991 and complieted in 2011. This project resulted in an estimated 94% reduction in CSOs to the Willamette River and a 99% reduction in CSOs to Columbia Slough (Portland Environmental Services, 2017). The remaining occasional Portland CSOs contribute only a minor amount of THg load and are not tabulated separately in this document.

For communities with combined sewer systems other than Portland (e.g., Corvallis), the diversion of THg loads to the POTW in combined sewer areas cannot currently be accounted for as the combined sewer drainage areas were not provided. CSOs are predominantly composed of stormwater and THg loads associated with CSOs are considered to be already represented by estimates of THg load associated with urban stormwater. For these communities, there is thus a small over-estimation of the MS4 THg surface load representing stormwater flows that are actually routed to the POTW. Credit for such captured THg loads could be accounted as part of the progress toward reaching the MS4 reduction target if an analysis of the fraction of urban runoff entering the combined sewer system is developed.

Information was not available to differentiate industrial stormwater loads (subject to a separate general permit) from other sources within MS4 drainages. Therefore, industrial stormwater loads are implicitly included within the urban stormwater loads for MS4s and urban DMAs.

Estimated MS4 loads are shown by HSPF model subbasin in Figure 5-14 Model subbasins with the highest MS4 loads are concentrated around urban centers in the basin, near the cities of Portland and Eugene. The total estimated at-source THg loads for regulated MS4s and urban DMAs in the WRB are 4.13 kg/yr and 0.92 kg/yr, respectively.

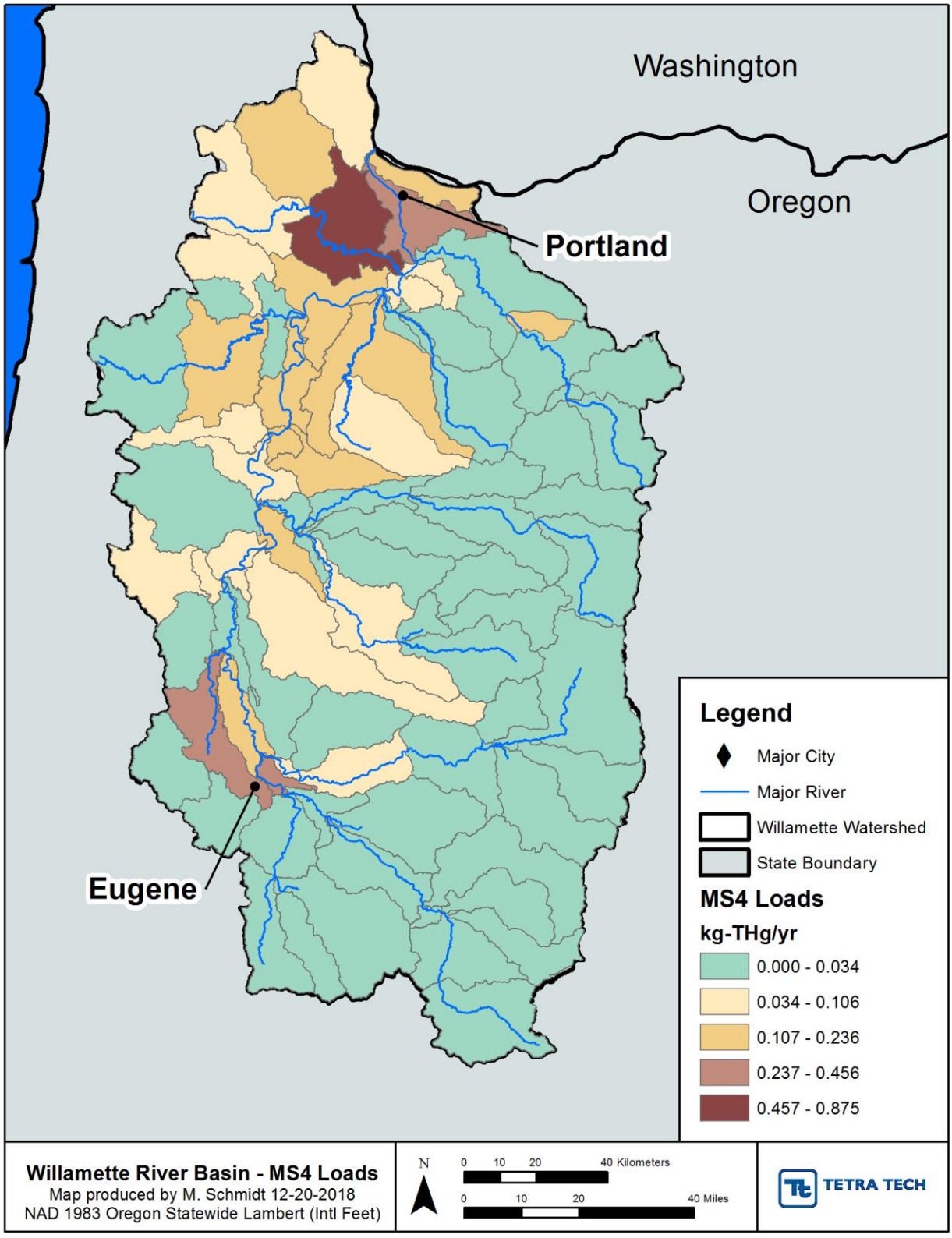

Figure 5-14. MS4 THg Load Estimates (kg/yr) for Subbasins in the Willamette River Basin HSPF Model

5.4 Instream Delivery of THg

5.4.1 Estimates of Riverine Loads

Examining the changes in loads between river stations enables estimation of mercury loss rates during transit as well as helping to confirm THg load estimates. Loads of pollutants in streams and rivers are difficult to estimate because concentration is usually observed only sporadically and measurements of both flow and concentration are required. Because concentration is often strongly correlated to flow it is not sufficient to simply combine average concentration with continuous flow. However, statistical tools have been developed that allow for optimal estimation of pollutant loads in riverine systems. These use continuous flow records paired with point-in-time pollutant monitoring data. Regression is used with the monitoring data and paired flow values to develop the relationship between concentration and load, which can then be used to estimate a complete time series of pollutant concentrations (using the continuous flow with the regression equation). One tool for this purpose is the Load Estimator (LOADEST), developed by USGS (Runkel et al., 2004). We used LOADEST to estimate loads of total mercury in reaches where continuous flow monitoring is available along with THg concentrations.

Loads were calculated only where the number of THg samples was at least 15. Sufficient data to apply LOADEST are available at six locations (Table 5-19 and Figure 5-15), and include four locations on the Willamette mainstem, one on the Coast Fork Willamette (downstream of Cottage Grove Lake) and one on the Clackamas River. Much of the THg sampling in the watershed has not occurred at same location as the USGS flow gages, but extends longitudinally up or downstream along a reach. To derive enough samples for the analyses, samples were aggregated when collocated on the same reach as the flow monitoring gage, and, in some cases, were also incorporated from reaches immediately upstream or downstream of the flow gages.

Table 5-19. LOADEST Analysis Locations and Data Counts

USGS gage	Location	THg Sample Count
14153500	Coast Fork Willamette R below Cottage Grove Dam	91
14166000	Willamette River at Harrisburg	64
14191000	Willamette River at Salem	41
14197900	Willamette River at Newberg	15
14211010	Clackamas River rear Oregon City	15
14211720	Willamette River at Portland	88

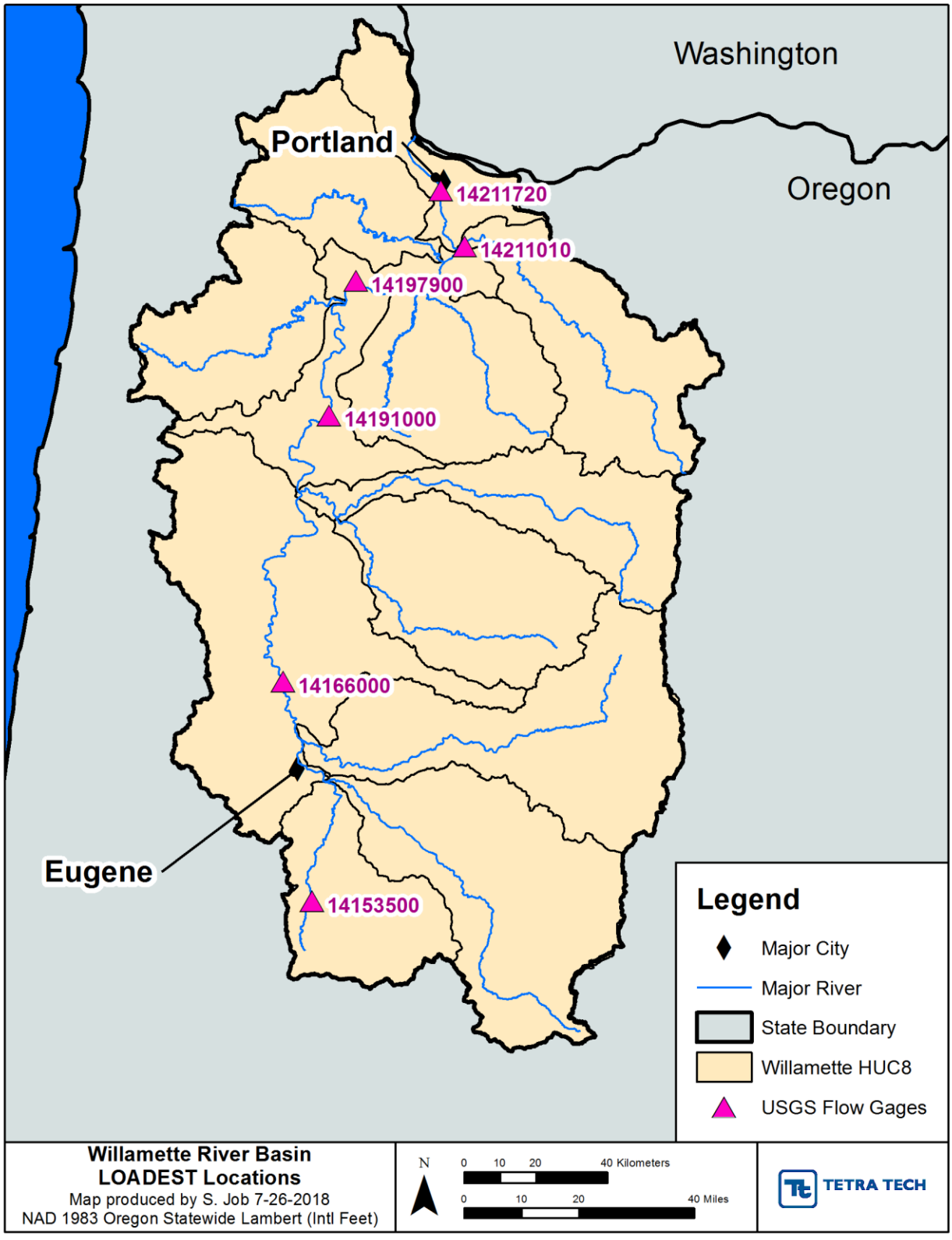

Figure 5-15. Locations of LOADEST Analyses in the WRB

LOADEST provides nine different regression models that do not include seasonal factors. For each location, each of the nine models was executed. The best model was selected based on goodness-of-fit evaluated with error statistics, primarily percent bias. The models selected and the average annual estimated THg loads are shown in Table 5-20.

Table 5-20. LOADEST Results

USGS Gage	Name	Regression Method	Regression Load Bias	Annual Average Load (kg/yr)
14153500	Coast Fork Willamette R below Cottage Grove Dam	3	-8.35%	2.45
14166000	Willamette River at Harrisburg	4	2.19%	26.1
14191000	Willamette River at Salem	3	0.70%	47.8
14197900	Willamette River at Newberg	6	-3.73%	70.2
14211010	Clackamas River near Oregon City	1	-0.24%	5.67
14211720	Willamette River at Portland	3	1.73%	83.7

5.4.2 Losses during Transit

Outside of reservoirs, instream sediment deposition and re-suspension continuously modify the transported flux of mercury through the river system. Dissolved Hg[II] can react with sulfide to form cinnabar (HgS), which has very low solubility under oxidizing conditions and can be buried or exported from streams to riparian areas. There is also gradual loss of THg in the river network through photo-demethylation of MeHg and other processes that convert THg to the elemental form that escapes to the atmosphere.

The magnitude of losses during transit is expected to be small relative to the total THg load in the WRB on an annual basis. The 2006 TMDL (Hope et al., 2005) essentially treated the net effect of these processes as a residual term in the mass balance and reported a net loss rate of 1.3 percent without any independent confirmation. Ambrose et al. (2003) suggest that THg loss rates in rivers should be represented as an exponential decay as a functionof travel time (t, days) and a decay rate (k, day^{-1}) such that loss of an initial load L_0 is given as $L_0 \cdot \exp(-k \cdot t)$. Ambrose et al. further suggest that k should be within the range of 0.005 to 0.2 day^{-1}.

For the major reservoirs located downstream of historic mining operations (Cottage Grove Reservoir and Dorena Lake), monitoring data were paired with flow records to approximate THg loads at the reservoir outlets (Section 5.4.3), thus implicitly account for gains or losses in THg during flow through the reservoirs. Mercury losses within the stream network were approximated with the exponential decay model based on travel time. Travel time to a point of interest (e.g., mouth of the Willamette River or HUC8 outlet) was computed for each HSPF model reach using average reach velocities generated by the model and distance to the mouth. The decay rate was then calibrated such that load estimates from the

Mass Balance Model were similar to load estimates derived from observed data using LOADEST (Section 5.4.1). A calibrated exponential rate decay constant of 0.08 day^{-1} (near the middle of the range cited by Ambrose et al., 2003) results in a match between loads estimated by the Mass Balance Model (83.7 kg/yr) and those from LOADEST (83.7 kg/yr) for THg loads in the Willamette River at Portland (USGS gage 14211720).

5.4.3 Reservoir Processes

The HSPF model contains explicit representation of 11 U.S. Army Corps of Engineers reservoirs plus the PGE North Fork Dam on the Clackamas River (see Section 5.2.2). Two reservoirs are of particular interest as they receive water from mining areas with high THg concentrations and have been subjects of mercury studies. The Cottage Grove Reservoir is downstream of the former Black Butte Mine that extracted mercury ore intermittently between the 1880s and 1960s. Tailing piles and long contaminated soils in the mining area and sediment in the receiving streams have led to high THg concentrations in the tributaries that feeds Cottage Grove Reservoir, as well as in the downstream Coast Fork Willamette River. The Bohemia Mining District, where mercury amalgamation was used to recover fine gold particles, drains to Row River, a tributary to Dorena Lake.

Processes within reservoirs can affect transformations and transport of Hg in the WRB. Reservoirs trap sediment and settle out ionic Hg that is associated with sediment. Under hypoxic conditions particulate Hg can be solubilized; ionic Hg can also be converted to MeHg as a byproduct of bacterial reduction of sulfate and released from sediment storages. Within-year fluctuations in water level – which are typical for flood control reservoirs – allow replenishment of sulfate and organic carbon in exposed areas, which can be important in determining the rate of methylation and the downstream outflow (Willacker et al., 2016; Eckley et al., 2015). The THg load leaving these reservoirs depends on the influent THg, legacy THg that may have been deposited in reservoir sediments in the past, and the net balance between settling losses and regeneration from the sediment. These dynamics are complex and can be challenging to predict, so within-reservoir processes were not simulated in detail in this project (e.g., dynamics of algal blooms that may bring on anoxic conditions that stimulate production of MeHg in the sediment). While reservoirs are usually net traps of influent THg, the presence of legacy THg stores in sediment makes it difficult to predict whether a given reservoir were diminish or increase the downstream transport of THg. Studies at Cottage Grove Reservoir (Eckley et al., 2015) show that biological activity in reservoir sediment results in a significant increase in MeHg in outflow relative to inflow; however, THg decreased across the reservoir due to trapping of storm event pulses of particulate THg derived from the Black Butte Mine site. While this TMDL focuses on the sources and transport of THg, the propensity of reservoirs to convert inorganic mercury to MeHg can be an important contributor to local fish tissue contamination problems.

Limited data were available to estimate THg loads associated with outflow from Cottage Grove Reservoir and Dorena Lake for the 2006 TMDL (n = 4 in 2006 for each site); nonetheless, regressions of THg concentration against flow were developed and resulted in estimated loads from Cottage Grove Reservoir and Dorena Lake of 0.40 kg/yr and 0.36 kg/yr. Additional monitoring data are now available for the Coast Fork Willamette River downstream of Cottage Grove Reservoir (n = 91). As discussed in Section 5.4.1, these data were used to develop estimates of THg load released from Cottage Grove Reservoir using the LOADEST program. Loads from Cottage Grove Reservoir are highest during winter months, when the reservoir level is lowest and flows are high, and decrease over the spring and summer as the lake elevation rises (Figure 5-16), resulting in an estimated annual load of 2.45 kg/yr as an average over 2002-

2017. This is the net load out of the reservoir due to upstream loading and in reservoir processes (e.g., release of legacy THg, deposition and resuspension of particulate matter).

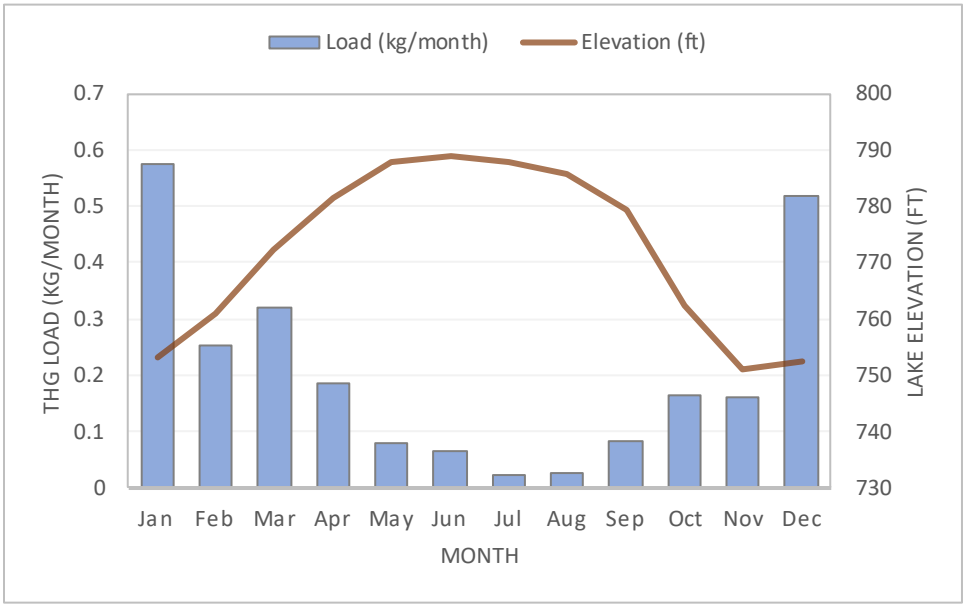

Figure 5-16. Monthly THg loads from Cottage Grove Reservoir

Monitoring of THg downstream of Dorena Lake was limited to four samples collected during 2002 – 2003, and no new data have been collected since the 2006 TMDL. Although, the lowest observed concentration was associated with the highest outflow, four data points are not sufficient to develop a reliable regression against flow. We therefore assume that the best available estimate for THg concentration in outflow from Dorena Lake is the mean of these four samples (1.84 ng/L). This concentration was combined with flow records for 2002 – 2017 to estimate an annual average THg load of 1.15 kg/yr.

For the other major reservoirs, there are no available data on THg concentrations in outflow, and only fish tissue data are available for mercury within the reservoirs. While there are mining sources upstream of several of these reservoirs, most of the mines were relatively small and did not produce large quantities of mercury. Examination of the limited data from Dorena Lake reveals that the upstream influent concentration of THg (1.78 ng/L, n =4) and within the lake (1.90 ng/L, n=4) are nearly identical to the downstream concentration of 1.84 ng/L. These observations suggest that processes within Dorena Lake have a minimal effect on the concentration of THg transported downstream, although a reduction in load proportional to evaporative losses likely occurs. Therefore, although this conclusion is based on a limited dataset, we assume that reservoirs are not sources of THg in the Mass Balance Model. Nevertheless, reservoir operations will change the timing of THg load delivery and likely result in some increase in the MeHg load due to methylation in reservoir sediments. Therefore, lacking other data, we assume that the effect of the remaining reservoirs on THg transport is accounted for in the instream modeling component (Section 5.4.2); travel times through the reservoirs (derived from the HSPF model) are longer than free-flowing reaches, and losses associated with increased travel time are represented by the exponential decay model.

5.5 Mass Balance Model Results

The Mass Balance Model results include loads from direct atmospheric deposition to water, surface runoff, groundwater, sediment erosion, MS4s and urban DMAs, mines, POTWs (including minor domestic WWTPs) and industrial dischargers. Where information was available (i.e., Portland), surface loads to combined sewer systems were excluded. Definitions for the aggregated land use categories for surface runoff, groundwater, and sediment erosion are presented in Table 5-1.

Annual average estimated THg loads are presented by HUC8 and source category (Table 5-21 - Table 5-32). These tables show at-source loads (loads prior to entering the stream network) that do not include loads from upstream HUCs. For example, the at-source loads for 17090003 include loads generated in 17090003 but not loads from upstream HUCs (17090001, 17090002, and 17090004). Predicted delivered loads at the downstream pourpoint of the HUC8, after accounting for transit losses are also included in the tables. For example, the delivered loads for 17090003 includes loads generated in upstream HUCs (17090001, 17090002, and 17090004) delivered to the outlet of 17090003 (i.e., not delivered to the mouth of the Willamette River). Results are presented in this section in units of kg/yr. The annual loads are converted to daily loads for the TMDL.

For non-headwater HUCs (17090003, 17090005, 17090007, and 17090012) the delivered loads represent the cumulative load from all upstream areas. The table for HUC 17090012 thus represents total delivered loads from the whole WRB upstream of the confluence with the Columbia River. Loads to the Multnomah Channel and Columbia Slough are not included in the HUC 17090012 tabulations and loads for these regions are presented separately in Table 5-33 and Table 5-34. Therefore, the total load delivered to the Columbia River from the study area is equal to the sum of the delivered loads from 17090012, the Multnomah Channel, and Columbia Slough. For all areas of the WRB including the Multnomah Channel and Columbia Slough, the at-source THg loads sum to approximately 132 kg/yr, while the loads delivered to the Columbia River are approximately 87.1 kg/yr.

The total load for urban DMAs across the WRB and loads for individual MS4s are presented in Table 5-35. Loads delivered to major reservoirs in the WRB are provided in separate tables (Table 5-36 - Table 5-47). At-source loads represent THg generated in the drainage area of the reservoir or lake and delivered loads represent THg loads to (not released from) the reservoir or lake.

Table 5-21. At-source and Delivered THg Load by Category for HUC 17090001 (kg/yr)

	At-source					Delivered				
	Atmospheric Deposition	Surface Runoff	Sediment Erosion	Groundwater	Total	Atmospheric Deposition	Surface Runoff	Sediment Erosion	Groundwater	Total
Agriculture		0.01	0.02	0.01	0.04		0.01	0.01	0.01	0.02
Forest		2.54	1.05	2.21	5.80		0.60	0.29	0.51	1.39
Shrub		0.67	0.38	0.33	1.38		0.14	0.14	0.06	0.33
Developed (Non MS4 and Urban DMA)		0.16	0.02	0.01	0.19		0.08	0.01	0.00	0.10
Other		0.58	0.13	0.14	0.85		0.18	0.06	0.04	0.27
Direct to streams	0.25				0.25	0.08				0.08
MS4s					0.03					0.02
Urban DMAs					0.00					0.00
POTWs					0.02					0.01
Industrial dischargers					0.00					0.00
Mines					0.00					0.00
TOTAL	0.25	3.96	1.60	2.70	8.57	0.08	1.00	0.50	0.62	2.23

Note for Table 5-21 through Table 5-34: Loads for individual MS4s and the total load for urban DMAs provided separately in Table 5-35. The Developed (Non MS4 and Urban DMA) category includes THg loads from developed land external to MS4s and urban DMAs as well as loads from open developed land and groundwater within MS4 and urban DMA boundaries. The MS4 and Urban DMAs categories include loads from atmospheric deposition, sediment erosion, and shallow interflow on developed low, medium, and high density land within their boundaries.

Table 5-22. At-source and Delivered THg Load by Category for HUC 17090002 (kg/yr)

	At-source					Delivered				
	Atmospheric Deposition	Surface Runoff	Sediment Erosion	Groundwater	Total	Atmospheric Deposition	Surface Runoff	Sediment Erosion	Groundwater	Total
Agriculture		0.04	0.22	0.01	0.28		0.03	0.12	0.01	0.17
Forest		2.75	1.06	0.46	4.27		1.28	0.55	0.24	2.08
Shrub		1.00	0.68	0.13	1.81		0.51	0.40	0.07	0.98
Developed (Non MS4 and Urban DMA)		0.22	0.07	0.01	0.30		0.16	0.06	0.01	0.22
Other		0.35	0.17	0.10	0.61		0.23	0.14	0.07	0.44
Direct to streams	0.07				0.07	0.04				0.04
MS4s					0.07					0.06
Urban DMAs					0.00					0.00
POTWs					0.00					0.00
Industrial dischargers					0.03					0.02
Mines					1.46					0.82
TOTAL	0.07	4.36	2.20	0.71	8.91	0.04	2.21	1.27	0.40	4.83

Table 5-23. At-source and Delivered THg Load by Category for HUC 17090003 (kg/yr)

	At-source					Delivered				
	Atmospheric Deposition	Surface Runoff	Sediment Erosion	Groundwater	Total	Atmospheric Deposition	Surface Runoff	Sediment Erosion	Groundwater	Total
Agriculture		0.68	2.50	0.32	3.50		0.62	2.23	0.31	3.16
Forest		1.23	5.45	0.84	7.52		4.60	6.06	3.35	14.02
Shrub		0.86	4.59	0.35	5.79		1.76	5.00	0.73	7.49
Developed (Non MS4 and Urban DMA)		1.77	0.74	0.11	2.63		1.80	0.70	0.12	2.61
Other		1.65	1.87	1.06	4.58		2.49	1.80	1.18	5.47
Direct to streams	0.42				0.42	0.56				0.56
MS4s					1.20					1.19
Urban DMAs					0.09					0.08
POTWs					0.23					0.22
Industrial dischargers					0.20					0.28
Mines					0.00					0.72
TOTAL	0.42	6.19	15.15	2.69	26.16	0.56	11.27	15.80	5.69	35.79

Note: Loads delivered to the outlet of HUC 17090003 include all sources from HUCs 17090001 [Middle Fork Willamette], 17090002 [Coast Fork Willamette], 17090003 [Upper Willamette] and 17090004 [McKenzie].

Table 5-24. At-source and Delivered THg Load by Category for HUC 17090004 (kg/yr)

	At-source					Delivered				
	Atmospheric Deposition	Surface Runoff	Sediment Erosion	Groundwater	Total	Atmospheric Deposition	Surface Runoff	Sediment Erosion	Groundwater	Total
Agriculture		0.01	0.03	0.03	0.07		0.01	0.03	0.03	0.07
Forest		3.54	1.23	3.59	8.35		2.27	1.13	2.29	5.68
Shrub		0.81	1.02	0.50	2.33		0.60	0.97	0.38	1.94
Developed (Non MS4 and Urban DMA)		0.15	0.04	0.02	0.20		0.12	0.04	0.02	0.17
Other		1.04	0.13	0.26	1.43		0.89	0.12	0.23	1.24
Direct to streams	0.12				0.12	0.09				0.09
MS4s					0.10					0.10
Urban DMAs					0.00					0.00
POTWs					0.00					0.00
Industrial dischargers					0.10					0.10
Mines					0.00					0.00
TOTAL	0.12	5.55	2.45	4.40	12.71	0.09	3.89	2.28	2.94	9.40

Table 5-25. At-source and Delivered THg Load by Category for HUC 17090005 (kg/yr)

	At-source					Delivered				
	Atmospheric Deposition	Surface Runoff	Sediment Erosion	Groundwater	Total	Atmospheric Deposition	Surface Runoff	Sediment Erosion	Groundwater	Total
Agriculture		0.06	0.14	0.05	0.25		0.12	0.34	0.10	0.56
Forest		2.35	1.18	1.65	5.18		3.93	3.15	1.69	8.77
Shrub		0.56	0.48	0.24	1.27		1.16	1.98	0.33	3.47
Developed (Non MS4 and Urban DMA)		0.20	0.05	0.01	0.26		0.32	0.11	0.02	0.45
Other		0.43	0.10	0.21	0.74		0.71	0.44	0.42	1.57
Direct to streams	0.10				0.10	0.17				0.17
MS4s					0.01					0.03
Urban DMAs					0.04					0.08
POTWs					0.03					0.06
Industrial dischargers					0.01					0.01
Mines					0.00					0.00
TOTAL	0.10	3.59	1.94	2.16	7.88	0.17	6.24	6.02	2.56	15.16

Note: Loads delivered to outlet of HUC 17090005 include all sources from HUCs 17090006 [South Santiam] and 17090005 [North Santiam].

Table 5-26. At-source and Delivered THg Load by Category for HUC 17090006 (kg/yr)

	At-source					Delivered				
	Atmospheric Deposition	Surface Runoff	Sediment Erosion	Groundwater	Total	Atmospheric Deposition	Surface Runoff	Sediment Erosion	Groundwater	Total
Agriculture		0.07	0.22	0.06	0.36		0.07	0.21	0.06	0.34
Forest		4.15	2.95	1.14	8.24		2.29	2.10	0.57	4.96
Shrub		1.33	2.01	0.28	3.62		0.76	1.57	0.16	2.49
Developed (Non MS4 and Urban DMA)		0.19	0.07	0.01	0.27		0.16	0.06	0.01	0.23
Other		0.58	0.40	0.29	1.27		0.45	0.36	0.26	1.07
Direct to streams	0.10				0.10	0.08				0.08
MS4s					0.02					0.02
Urban DMAs					0.05					0.05
POTWs					0.03					0.03
Industrial dischargers					0.00					0.00
Mines					0.00					0.00
TOTAL	0.10	6.32	5.66	1.78	13.97	0.08	3.72	4.30	1.06	9.26

Table 5-27. At-source and Delivered THg Load by Category for HUC 17090007 (kg/yr)

	At-source					Delivered				
	Atmospheric Deposition	Surface Runoff	Sediment Erosion	Groundwater	Total	Atmospheric Deposition	Surface Runoff	Sediment Erosion	Groundwater	Total
Agriculture		0.29	0.62	0.17	1.08		1.43	4.78	1.00	7.21
Forest		0.10	0.51	0.11	0.72		9.12	15.98	5.77	30.88
Shrub		0.04	0.30	0.03	0.38		3.24	11.64	1.39	16.28
Developed (Non MS4 and Urban DMA)		1.17	0.25	0.06	1.47		4.33	1.59	0.30	6.22
Other		0.34	0.28	0.30	0.92		3.69	3.52	2.47	9.69
Direct to streams	0.58				0.58	1.35				1.35
MS4s					0.65					2.62
Urban DMAs					0.22					0.68
POTWs					0.19					0.68
Industrial dischargers					0.11					0.36
Mines					0.00					0.63
TOTAL	0.58	1.94	1.95	0.67	6.33	1.35	21.82	37.52	10.94	76.59

Notes: Loads delivered to the outlet of HUC 17090007 include all sources from all HUCs in the basin except 17090011 [Clackamas] and 17090012 [Lower Willamette].

Table 5-28. At-source and Delivered THg Load by Category for HUC 17090008 (kg/yr)

	At-source					Delivered				
	Atmospheric Deposition	Surface Runoff	Sediment Erosion	Groundwater	Total	Atmospheric Deposition	Surface Runoff	Sediment Erosion	Groundwater	Total
Agriculture		0.28	1.31	0.25	1.84		0.24	1.11	0.21	1.55
Forest		0.39	3.86	0.58	4.82		0.32	3.18	0.47	3.97
Shrub		0.24	3.18	0.23	3.64		0.19	2.59	0.19	2.98
Developed (Non MS4 and Urban DMA)		0.42	0.34	0.04	0.81		0.35	0.28	0.04	0.67
Other		0.36	0.78	0.39	1.53		0.30	0.65	0.32	1.27
Direct to streams	0.07				0.07	0.06				0.06
MS4s					0.02					0.02
Urban DMAs					0.21					0.17
POTWs					0.03					0.02
Industrial dischargers					0.00					0.00
Mines					0.00					0.00
TOTAL	0.07	1.69	9.47	1.49	12.97	0.06	1.41	7.80	1.23	10.70

Table 5-29. At-source and Delivered THg Load by Category for HUC 17090009 (kg/yr)

	At-source					Delivered				
	Atmospheric Deposition	Surface Runoff	Sediment Erosion	Groundwater	Total	Atmospheric Deposition	Surface Runoff	Sediment Erosion	Groundwater	Total
Agriculture		0.17	0.55	0.21	0.92		0.14	0.47	0.18	0.79
Forest		1.16	3.55	0.71	5.42		1.08	3.06	0.64	4.79
Shrub		0.36	1.87	0.20	2.44		0.34	1.60	0.18	2.12
Developed (Non MS4 and Urban DMA)		0.41	0.27	0.04	0.72		0.36	0.23	0.03	0.62
Other		0.22	0.59	0.46	1.28		0.19	0.50	0.40	1.09
Direct to streams	0.07				0.07	0.06				0.06
MS4s					0.12					0.11
Urban DMAs					0.19					0.16
POTWs					0.05					0.04
Industrial dischargers					0.00					0.00
Mines					0.00					0.00
TOTAL	0.07	2.33	6.84	1.62	11.21	0.06	2.11	5.85	1.43	9.77

Table 5-30. At-source and Delivered THg Load by Category for HUC 17090010 (kg/yr)

	At-source					Delivered				
	Atmospheric Deposition	Surface Runoff	Sediment Erosion	Groundwater	Total	Atmospheric Deposition	Surface Runoff	Sediment Erosion	Groundwater	Total
Agriculture		0.20	0.61	0.14	0.95		0.15	0.45	0.10	0.71
Forest		0.27	1.88	0.23	2.39		0.20	1.39	0.17	1.77
Shrub		0.17	1.64	0.11	1.92		0.13	1.20	0.08	1.41
Developed (Non MS4 and Urban DMA)		0.89	0.22	0.07	1.18		0.70	0.17	0.06	0.92
Other		0.15	0.26	0.14	0.55		0.11	0.19	0.11	0.41
Direct to streams	0.08				0.08	0.07				0.07
MS4s					1.04					0.83
Urban DMAs					0.00					0.00
POTWs					0.26					0.21
Industrial dischargers					0.00					0.00
Mines					0.00					0.00
TOTAL	0.08	1.69	4.60	0.69	8.38	0.07	1.29	3.40	0.52	6.31

Table 5-31. At-source and Delivered THg Load by Category for HUC 17090011 (kg/yr)

	At-source					Delivered				
	Atmospheric Deposition	Surface Runoff	Sediment Erosion	Groundwater	Total	Atmospheric Deposition	Surface Runoff	Sediment Erosion	Groundwater	Total
Agriculture		0.03	0.11	0.04	0.18		0.03	0.10	0.04	0.18
Forest		2.16	1.28	2.38	5.82		1.72	1.20	1.88	4.79
Shrub		0.49	0.64	0.30	1.43		0.40	0.60	0.24	1.24
Developed (Non MS4 and Urban DMA)		0.27	0.13	0.02	0.42		0.26	0.12	0.02	0.40
Other		0.11	0.11	0.14	0.37		0.10	0.10	0.13	0.34
Direct to streams	0.08				0.08	0.07				0.07
MS4s					0.21					0.21
Urban DMAs					0.03					0.03
POTWs					0.09					0.08
Industrial dischargers					0.00					0.00
Mines					0.00					0.00
TOTAL	0.08	3.08	2.26	2.89	8.63	0.07	2.50	2.13	2.32	7.34

Table 5-32. At-source and Delivered THg Load by Category for HUC 17090012 (kg/yr)

	At-source					Delivered				
	Atmospheric Deposition	Surface Runoff	Sediment Erosion	Groundwater	Total	Atmospheric Deposition	Surface Runoff	Sediment Erosion	Groundwater	Total
Agriculture		0.00	0.01	0.00	0.01		1.42	4.74	1.01	7.18
Forest		0.02	0.13	0.02	0.17		10.54	16.79	7.44	34.77
Shrub		0.00	0.01	0.00	0.01		3.53	11.88	1.59	17.01
Developed (Non MS4 and Urban DMA)		0.92	0.11	0.03	1.06		5.37	1.82	0.34	7.53
Other		0.04	0.01	0.01	0.06		3.71	3.53	2.54	9.78
Direct to streams	0.18				0.18	1.54				1.54
MS4s					0.46					3.15
Urban DMAs					0.00					0.69
POTWs					0.24					0.98
Industrial dischargers					0.01					0.35
Mines					0.00					0.61
TOTAL	0.18	0.98	0.26	0.08	2.20	1.54	24.57	38.76	12.93	83.58

Notes: Loads delivered to the outlet of HUC 17090012 include all sources in the basin. Loads to the Multnomah Channel and Columbia Slough are presented separately and not included as part of HUC 17090012.

Table 5-33. At-source and Delivered THg Load by Category for Multnomah Channel (kg/yr)

	At-source					Delivered				
	Atmospheric Deposition	Surface Runoff	Sediment Erosion	Groundwater	Total	Atmospheric Deposition	Surface Runoff	Sediment Erosion	Groundwater	Total
Agriculture		0.08	0.26	0.02	0.36		0.07	0.24	0.02	0.33
Forest		0.12	0.83	0.10	1.05		0.11	0.77	0.10	0.97
Shrub		0.06	0.62	0.05	0.73		0.06	0.57	0.04	0.67
Developed (Non MS4 and Urban DMA)		0.13	0.09	0.02	0.24		0.12	0.09	0.02	0.22
Other		0.11	0.14	0.08	0.33		0.10	0.13	0.07	0.30
Direct to streams	0.02				0.02	0.02				0.02
MS4s					0.00					0.00
Urban DMAs					0.07					0.07
POTWs					0.01					0.01
Industrial dischargers					0.00					0.00
Mines					0.00					0.00
TOTAL	0.02	0.49	1.94	0.27	2.80	0.02	0.46	1.79	0.25	2.59

Table 5-34. At-source and Delivered THg Load by Category for Columbia Slough (kg/yr)

	At-source					Delivered				
	Atmospheric Deposition	Surface Runoff	Sediment Erosion	Groundwater	Total	Atmospheric Deposition	Surface Runoff	Sediment Erosion	Groundwater	Total
Agriculture		0.00	0.00	0.00	0.00		0.00	0.00	0.00	0.00
Forest		0.00	0.00	0.00	0.00		0.00	0.00	0.00	0.00
Shrub		0.00	0.00	0.00	0.00		0.00	0.00	0.00	0.00
Developed (Non MS4 and Urban DMA)		0.65	0.09	0.02	0.76		0.61	0.08	0.02	0.71
Other		0.01	0.01	0.01	0.03		0.01	0.01	0.01	0.03
Direct to streams	0.02				0.02	0.02				0.02
MS4s					0.18					0.16
Urban DMAs					0.00					0.00
POTWs					0.00					0.00
Industrial dischargers					0.00					0.00
Mines					0.00					0.00
TOTAL	0.02	0.67	0.10	0.02	0.99	0.02	0.62	0.09	0.02	0.92

Table 5-35. At-source and Delivered THg Load by MS4 (kg/yr)

MS4 Type	Jurisdiction	At-Source Load (kg/yr)	Delivered Load to Columbia River (kg/yr)
Urban DMAs	Multiple	0.92	0.77
Phase I City	Eugene	0.46	0.33
Phase I City	Fairview	0.02	0.02
Phase I City	Gladstone	0.03	0.03
Phase I City	Happy Valley	0.06	0.06
Phase I City	Johnson	0.00	0.00
Phase I City	Lake Oswego	0.07	0.07
Phase I City	Milwaukie	0.05	0.05
Phase I City	Oregon City	0.09	0.09
Phase I City	Rivergrove	0.00	0.00
Phase I City	West Linn	0.05	0.05
Phase I City	Wilsonville	0.06	0.06
Phase I City	Portland	0.22	0.20
Phase I City	Salem	0.35	0.31
Phase I City	Clean Water Services	0.93	0.72
Phase I City	Gresham	0.05	0.05
Phase I County	Washington County	0.03	0.02
Phase I County	Multnomah County	0.04	0.04
Phase I County	Clackamas County	0.28	0.27
Phase II City	Albany	0.16	0.12
Phase II City	Corvallis	0.12	0.09
Phase II City	Philomath	0.03	0.02
Phase II City	Turner	0.01	0.01
Phase II City	Wood Villa	0.01	0.01
Phase II City	Keizer	0.06	0.05
Phase II City	Millersburg	0.02	0.02
Phase II City	Springfield	0.21	0.15
Phase II County	Polk County	0.01	0.01
Phase II County	Linn County	0.03	0.02
Phase II County	Benton County	0.03	0.03
Phase II County	Marion County	0.11	0.09
Phase II County	Lane County	0.29	0.19
Basinwide	ODOT	0.24	0.19
Total		5.0	4.1

Table 5-36. At-source and Delivered THg Load by Category for North Fork Reservoir (kg/yr)

	At-source					Delivered				
	Atmospheric Deposition	Surface Runoff	Sediment Erosion	Groundwater	Total	Atmospheric Deposition	Surface Runoff	Sediment Erosion	Groundwater	Total
Agriculture		0.00	0.00	0.00	0.00		0.00	0.00	0.00	0.00
Forest		2.18	0.23	2.17	4.59		1.74	0.19	1.73	3.67
Shrub		0.44	0.10	0.25	0.79		0.35	0.08	0.20	0.63
Developed (Non MS4 and Urban DMA)		0.05	0.00	0.00	0.06		0.04	0.00	0.00	0.04
Other		0.07	0.00	0.03	0.10		0.06	0.00	0.02	0.08
Direct to streams	0.01				0.01	0.01				0.01
MS4s					0.00					0.00
Urban DMAs					0.00					0.00
POTWs					0.00					0.00
Industrial dischargers					0.00					0.00
Mines					0.00					0.00
TOTAL	0.01	2.74	0.33	2.45	5.54	0.01	2.19	0.27	1.95	4.43

Note: At-source loads include THg loads generated in the drainage area of the lake. Delivered loads represent loads to the lake (i.e., not loads released from the lake). Loads for individual MS4s and the total load for urban DMAs provided separately in Table 5 34.

Table 5-37. At-source and Delivered THg Load by Category for Cottage Grove Lake (kg/yr)

	At-source					Delivered				
	Atmospheric Deposition	Surface Runoff	Sediment Erosion	Groundwater	Total	Atmospheric Deposition	Surface Runoff	Sediment Erosion	Groundwater	Total
Agriculture		0.00	0.01	0.00	0.01		0.00	0.00	0.00	0.01
Forest		0.36	0.13	0.07	0.56		0.27	0.09	0.05	0.42
Shrub		0.21	0.12	0.03	0.37		0.16	0.09	0.02	0.27
Developed (Non MS4 and Urban DMA)		0.02	0.00	0.00	0.02		0.01	0.00	0.00	0.01
Other		0.05	0.01	0.01	0.07		0.04	0.01	0.01	0.05
Direct to streams	0.00				0.00	0.00				0.00
MS4s					0.00					0.00
Urban DMAs					0.00					0.00
POTWs					0.00					0.00
Industrial dischargers					0.00					0.00
Mines					1.34					1.00
TOTAL	0.00	0.64	0.27	0.11	2.37	0.00	0.48	0.19	0.08	1.76

Table 5-38. At-source and Delivered THg Load by Category for Cougar Reservoir (kg/yr)

	At-source					Delivered				
	Atmospheric Deposition	Surface Runoff	Sediment Erosion	Groundwater	Total	Atmospheric Deposition	Surface Runoff	Sediment Erosion	Groundwater	Total
Agriculture		0.00	0.00	0.00	0.00		0.00	0.00	0.00	0.00
Forest		1.07	0.04	0.82	1.93		0.02	0.00	0.01	0.03
Shrub		0.13	0.01	0.06	0.19		0.00	0.00	0.00	0.00
Developed (Non MS4 and Urban DMA)		0.02	0.00	0.00	0.02		0.00	0.00	0.00	0.00
Other		0.06	0.00	0.01	0.07		0.00	0.00	0.00	0.00
Direct to streams	0.00				0.00	0.00				0.00
MS4s					0.00					0.00
Urban DMAs					0.00					0.00
POTWs					0.00					0.00
Industrial dischargers					0.00					0.00
Mines					0.00					0.00
TOTAL	0.00	1.28	0.05	0.89	2.22	0.00	0.02	0.00	0.01	0.04

Table 5-39. At-source and Delivered THg Load by Category for Detroit Lake (kg/yr)

	At-source					Delivered				
	Atmospheric Deposition	Surface Runoff	Sediment Erosion	Groundwater	Total	Atmospheric Deposition	Surface Runoff	Sediment Erosion	Groundwater	Total
Agriculture		0.00	0.00	0.00	0.00		0.00	0.00	0.00	0.00
Forest		1.30	0.33	1.01	2.63		1.26	0.32	0.98	2.56
Shrub		0.27	0.10	0.13	0.50		0.26	0.10	0.12	0.49
Developed (Non MS4 and Urban DMA)		0.05	0.00	0.00	0.06		0.05	0.00	0.00	0.05
Other		0.29	0.02	0.07	0.38		0.28	0.02	0.07	0.37
Direct to streams	0.00				0.00	0.00				0.00
MS4s					0.00					0.00
Urban DMAs					0.00					0.00
POTWs					0.00					0.00
Industrial dischargers					0.00					0.00
Mines					0.00					0.00
TOTAL	0.00	1.91	0.45	1.21	3.57	0.00	1.85	0.44	1.17	3.48

Table 5-40. At-source and Delivered THg Load by Category for Dorena Lake (kg/yr)

	At-source					Delivered				
	Atmospheric Deposition	Surface Runoff	Sediment Erosion	Groundwater	Total	Atmospheric Deposition	Surface Runoff	Sediment Erosion	Groundwater	Total
Agriculture		0.00	0.07	0.00	0.07		0.00	0.05	0.00	0.05
Forest		1.32	0.54	0.23	2.09		0.93	0.38	0.16	1.48
Shrub		0.37	0.26	0.04	0.67		0.26	0.18	0.03	0.47
Developed (Non MS4 and Urban DMA)		0.01	0.00	0.00	0.01		0.00	0.00	0.00	0.01
Other		0.06	0.01	0.01	0.08		0.04	0.01	0.01	0.06
Direct to streams	0.00				0.00	0.00				0.00
MS4s					0.00					0.00
Urban DMAs					0.00					0.00
POTWs					0.00					0.00
Industrial dischargers					0.00					0.00
Mines					0.12					0.09
TOTAL	0.00	1.76	0.88	0.28	3.04	0.00	1.23	0.62	0.20	2.15

Table 5-41. At-source and Delivered THg Load by Category for Falls Creek Lake (kg/yr)

	At-source					Delivered				
	Atmospheric Deposition	Surface Runoff	Sediment Erosion	Groundwater	Total	Atmospheric Deposition	Surface Runoff	Sediment Erosion	Groundwater	Total
Agriculture		0.00	0.00	0.00	0.00		0.00	0.00	0.00	0.00
Forest		0.14	0.47	0.16	0.77		0.03	0.11	0.04	0.18
Shrub		0.04	0.13	0.02	0.18		0.01	0.03	0.00	0.04
Developed (Non MS4 and Urban DMA)		0.00	0.00	0.00	0.00		0.00	0.00	0.00	0.00
Other		0.01	0.02	0.01	0.04		0.00	0.00	0.00	0.01
Direct to streams	0.00				0.00	0.00				0.00
MS4s					0.00					0.00
Urban DMAs					0.00					0.00
POTWs					0.00					0.00
Industrial dischargers					0.00					0.00
Mines					0.00					0.00
TOTAL	0.00	0.19	0.62	0.19	0.99	0.00	0.04	0.14	0.04	0.23

Table 5-42. At-source and Delivered THg Load by Category for Fern Ridge Lake (kg/yr)

	At-source					Delivered				
	Atmospheric Deposition	Surface Runoff	Sediment Erosion	Groundwater	Total	Atmospheric Deposition	Surface Runoff	Sediment Erosion	Groundwater	Total
Agriculture		0.02	0.06	0.00	0.08		0.01	0.06	0.00	0.08
Forest		0.19	0.84	0.13	1.16		0.18	0.77	0.12	1.07
Shrub		0.11	0.61	0.05	0.77		0.10	0.56	0.04	0.71
Developed (Non MS4 and Urban DMA)		0.13	0.09	0.01	0.23		0.12	0.08	0.01	0.21
Other		0.15	0.15	0.10	0.40		0.14	0.14	0.09	0.37
Direct to streams	0.00				0.00	0.00				0.00
MS4s					0.00					0.00
Urban DMAs					0.04					0.04
POTWs					0.00					0.00
Industrial dischargers					0.00					0.00
Mines					0.00					0.00
TOTAL	0.00	0.60	1.75	0.29	2.69	0.00	0.55	1.61	0.26	2.48

Table 5-43. At-source and Delivered THg Load by Category for Foster Lake (kg/yr)

	At-source					Delivered				
	Atmospheric Deposition	Surface Runoff	Sediment Erosion	Groundwater	Total	Atmospheric Deposition	Surface Runoff	Sediment Erosion	Groundwater	Total
Agriculture		0.00	0.00	0.00	0.01		0.00	0.00	0.00	0.01
Forest		2.08	0.46	0.25	2.79		2.01	0.45	0.24	2.70
Shrub		0.49	0.22	0.04	0.75		0.47	0.21	0.04	0.73
Developed (Non MS4 and Urban DMA)		0.04	0.00	0.00	0.04		0.04	0.00	0.00	0.04
Other		0.21	0.02	0.02	0.25		0.20	0.02	0.02	0.24
Direct to streams	0.00				0.00	0.00				0.00
MS4s					0.00					0.00
Urban DMAs					0.01					0.01
POTWs					0.00					0.00
Industrial dischargers					0.00					0.00
Mines					0.00					0.00
TOTAL	0.00	2.82	0.70	0.31	3.85	0.00	2.72	0.68	0.30	3.73

Table 5-44. At-source and Delivered THg Load by Category for Green Peter Lake (kg/yr)

	At-source					Delivered				
	Atmospheric Deposition	Surface Runoff	Sediment Erosion	Groundwater	Total	Atmospheric Deposition	Surface Runoff	Sediment Erosion	Groundwater	Total
Agriculture		0.00	0.00	0.00	0.00		0.00	0.00	0.00	0.00
Forest		2.16	0.75	0.55	3.46		1.99	0.69	0.51	3.18
Shrub		0.68	0.37	0.11	1.17		0.63	0.34	0.10	1.07
Developed (Non MS4 and Urban DMA)		0.03	0.00	0.00	0.04		0.03	0.00	0.00	0.03
Other		0.17	0.02	0.02	0.21		0.15	0.02	0.02	0.19
Direct to streams	0.00				0.00	0.00				0.00
MS4s					0.00					0.00
Urban DMAs					0.00					0.00
POTWs					0.00					0.00
Industrial dischargers					0.00					0.00
Mines					0.00					0.00
TOTAL	0.00	3.04	1.14	0.68	4.88	0.00	2.80	1.05	0.63	4.49

Table 5-45. At-source and Delivered THg Load by Category for Hill Creek (kg/yr)

	At-source					Delivered				
	Atmospheric Deposition	Surface Runoff	Sediment Erosion	Groundwater	Total	Atmospheric Deposition	Surface Runoff	Sediment Erosion	Groundwater	Total
Agriculture		0.00	0.00	0.00	0.00		0.00	0.00	0.00	0.00
Forest		0.62	0.00	0.76	1.39		0.00	0.00	0.00	0.00
Shrub		0.22	0.00	0.17	0.39		0.00	0.00	0.00	0.00
Developed (Non MS4 and Urban DMA)		0.00	0.00	0.00	0.00		0.00	0.00	0.00	0.00
Other		0.09	0.00	0.05	0.14		0.00	0.00	0.00	0.00
Direct to streams	0.01				0.01	0.00				0.00
MS4s					0.00					0.00
Urban DMAs					0.00					0.00
POTWs					0.00					0.00
Industrial dischargers					0.00					0.00
Mines					0.00					0.00
TOTAL	0.01	0.93	0.00	0.98	1.93	0.00	0.00	0.00	0.00	0.00

Table 5-46. At-source and Delivered THg Load by Category for Lookout Point (kg/yr)

	At-source					Delivered				
	Atmospheric Deposition	Surface Runoff	Sediment Erosion	Groundwater	Total	Atmospheric Deposition	Surface Runoff	Sediment Erosion	Groundwater	Total
Agriculture		0.00	0.00	0.00	0.00		0.00	0.00	0.00	0.00
Forest		1.59	0.24	1.95	3.78		0.82	0.14	1.00	1.97
Shrub		0.39	0.08	0.29	0.76		0.19	0.05	0.14	0.38
Developed (Non MS4 and Urban DMA)		0.07	0.01	0.01	0.08		0.04	0.00	0.00	0.04
Other		0.36	0.04	0.09	0.49		0.19	0.02	0.04	0.26
Direct to streams	0.01				0.01	0.01				0.01
MS4s					0.00					0.00
Urban DMAs					0.01					0.01
POTWs					0.02					0.01
Industrial dischargers					0.00					0.00
Mines					0.00					0.00
TOTAL	0.01	2.41	0.37	2.34	5.16	0.01	1.24	0.21	1.18	2.68

Table 5-47. At-source and Delivered THg Load by Category for Blue River Lake (kg/yr)

	At-source					Delivered				
	Atmospheric Deposition	Surface Runoff	Sediment Erosion	Groundwater	Total	Atmospheric Deposition	Surface Runoff	Sediment Erosion	Groundwater	Total
Agriculture		0.00	0.00	0.00	0.00		0.00	0.00	0.00	0.00
Forest		0.39	0.01	0.33	0.73		0.07	0.00	0.06	0.13
Shrub		0.11	0.01	0.05	0.16		0.02	0.00	0.01	0.03
Developed (Non MS4 and Urban DMA)		0.00	0.00	0.00	0.00		0.00	0.00	0.00	0.00
Other		0.03	0.00	0.00	0.03		0.01	0.00	0.00	0.01
Direct to streams	0.00				0.00	0.00				0.00
MS4s					0.00					0.00
Urban DMAs					0.00					0.00
POTWs					0.00					0.00
Industrial dischargers					0.00					0.00
Mines					0.00					0.00
TOTAL	0.00	0.53	0.02	0.38	0.92	0.00	0.10	0.00	0.07	0.16

Figure 5-17 and Figure 5-18 show the breakdown of loads by source type, both at the point of entry to the stream network and at the confluence with the Columbia River (includes loads to the Multnomah Channel and Columbia Slough. About 3.5 kg/yr of the delivered load originates from these drainage areas). The at-source and delivered fractions shift somewhat because there are a larger proportion of MS4s and POTWs nearer the confluence with the Columbia River. Note that the MS4 load is presented separately because it is subject to NPDES permit requirements.

Figure 5-19 expands the nonpoint source types in Figure 5-17 to show their attribution to different land use categories. Sediment erosion is a major source of current THg loads. The THg in surface soils is also largely derived from atmospheric deposition of anthropogenic mercury emissions; however, the time to reach equilibrium between surface soil and atmospheric mercury concentrations is long (on the order of centuries; see USEPA, 1997), so it would be incorrect to attribute ongoing sediment-associated loads of mercury to current day atmospheric deposition. Amos et al. (2015) provide a review of evidence on global anthropogenic enrichment of mercury based on both modeling and observations from lake sediment and peat deposits. Anthropogenic mercury emissions increased significantly with the advent of large-scale mining of gold, silver, and mercury around 1550 CE and seem to have reached a peak around 1960 CE. According to Amos et al., mercury emissions during the industrial era (ca. 1880) are about 3 to 4 times greater than during the pre-industrial era (ca. 1760), but the 18th-century emission rate was about 5 times greater than in the pre-colonial era (3000 BCE to 1550 CE). Current THg concentrations in surface soils thus reflect the cumulative result of many centuries of deposition of anthropogenically derived mercury emissions.

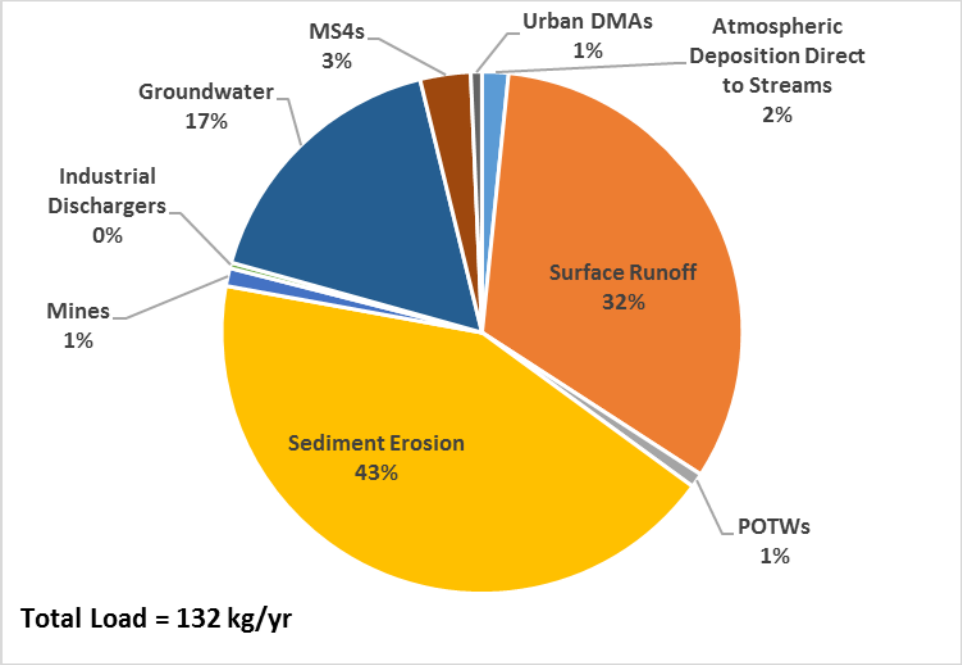

Figure 5-17. Distribution of THg Source Loads to the Stream Network

Note: Most of the sediment erosion, surface runoff, and groundwater loads originate from past atmospheric deposition of legacy emissions.

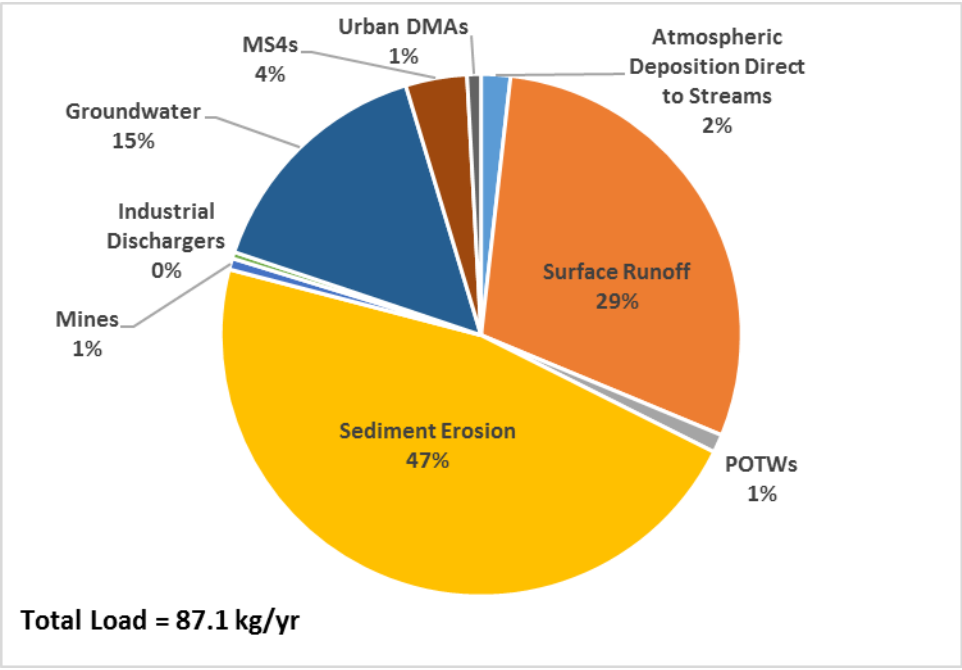

Figure 5-18. Distribution of THg Loads by Source Delivered from the WRB to the Columbia River

Note: The load delivered to the Columbia River includes THg from the Multnomah Channel and Columbia Slough direct drainage areas. A large portion of the sediment erosion and groundwater THg loads is derived from historic atmospheric deposition of global anthropogenic mercury emissions.

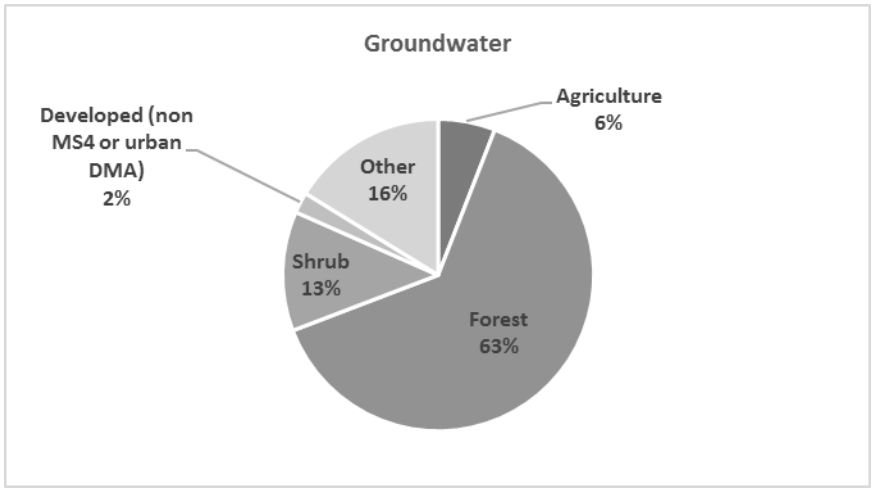

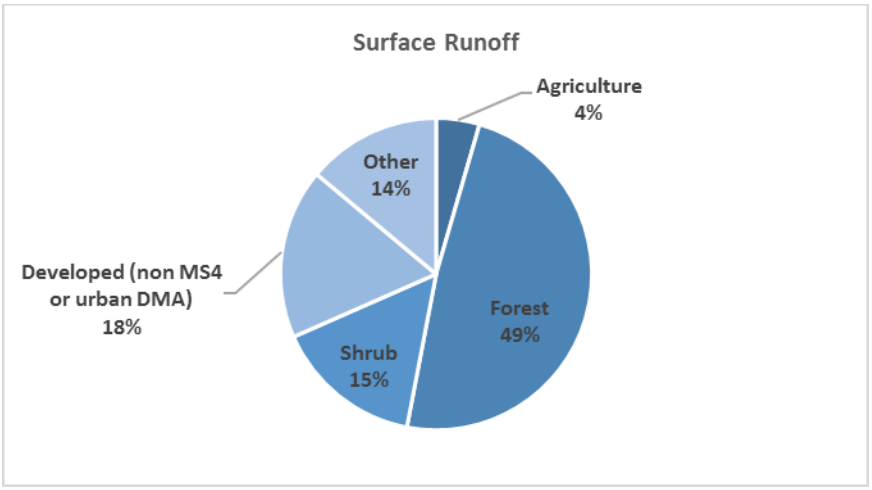

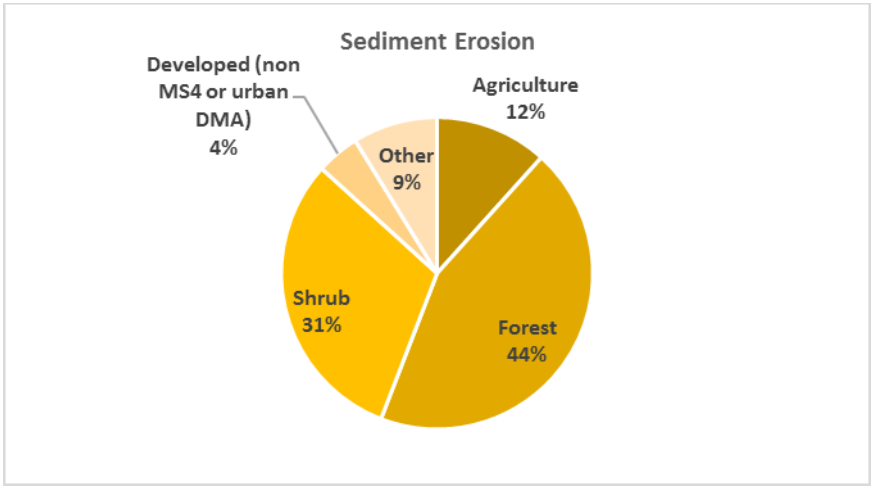

Figure 5-19. Nonpoint Sources of Mercury by Land Use Category

Note: A large portion of the surface runoff, sediment erosion, and groundwater THg loads is derived from historic atmospheric deposition of global anthropogenic mercury emissions.

REFERENCES

Alpers, C.N., J.L. Yee, J.T. Ackerman, J.L. Orlando, D.G. Slotton, and M.C. Marvin-DiPasquale. 2016. Prediction of fish and sediment mercury in streams using landscape variables and historical mining. *Science of the Total Environment,* 571:364-379.

Ambers, R.K.R., and B.N. Hygelund. 2001. Contamination of two Oregon reservoirs by cinnabar mining and mercury amalgamation. *Environmental Geology,* 40(6): 699-707.

Ambrose, R., I. Tsiros, and T. Wool. 2003. Predicting environmental concentrations of airborne pollutants in terrestrial receptors: The case of mercury. *Proceedings of the 8th International Conference on Environmental Science and Technology*, Lemnos Island, Greece.

Amos, H.M., J.E. Sonke, D. Obrist, N. Robins, N. Hagan, H.M. Horowitz, et al. 2015. Observational and modeling constraints on global anthropogenic enrichment of mercury. *Environmental Science and Technology*, 49: 4036-4047.

ATSDR (Agency for Toxic Substances and Disease Registry). 1999. ToxFAQs for Mercury (CAS# 7439-97-6).

Austin, C.M., and L.L. Smitherman. 2017. Draft Staff Report for Scientific Peer Review for the Amendment to the Water Quality Control Plan for Inland Surface Waters, Enclosed Bays, and Estuaries of California, Mercury Reservoir Provisions – Mercury TMDL and Implementation Program for Reservoirs. Statewide Mercury Control Program for Reservoirs. Report prepared for the State of California, California Environmental Protection Agency, and the State Water Resources Control Board, Sacramento, CA.

Barber, M.C. 2008. Dietary uptake models used for modeling the bioaccumulation of organic contaminants in fish. *Environmental Toxicology and Chemistry*, 27: 755-777.

Barringer, J.L., C.L. MacLeod, and R.A. Gallagher. 1997. Mercury in Ground Water, Soils, and Sediments of the Kirkwood-Cohansey Aquifer System in the New Jersey Coastal Plain. U.S. Geological Survey Open-File Report 95-475. 271 pp.

Bertalanffy, L. von. 1938. A quantitative theory of organic growth (Inquiries on growth laws. II). *Human Biology*, 10: 181-213.

Bicknell, B.R., J.C. Imhoff, J.L. Kittle Jr., T.H. Jobes, P. Duda, and A. Donigian, Jr. 2005. HSPF Version 12.2 User's Manual. U.S. Environmental Protection Agency, National Exposure Research Laboratory, Office of Research and Development, Athens, GA.

Bolks, A., A. DeWire, and J.B. Harcum. 2014. Baseline Assessment of Left-Censored Environmental Data Using R. Tech Notes 10. National Nonpoint Source Monitoring Program, U.S. Environmental Protection Agency.

Brooks, H.C. 1963. Quicksilver in Oregon (Bulletin No. 55). State of Oregon Department of Geology and Mineral Industries, Portland, Oregon.

Brooks, H.C. 1971. Quicksilver Deposits in Oregon (Miscellaneous Paper 15). State of Oregon Department of Geology and Mineral Industries, Portland, Oregon.

Butcher, J., A. Parker, S. Sarkar, S. Job, M. Faizullabhoy, P. Cada, et al. 2013. Model Configuration, Calibration and Validation; Basin: Willamette River. Appendix H to Watershed Modeling to Assess the Sensitivity of Streamflow, Nutrient, and Sediment Loads to Potential Climate Change and Urban Development in 20 U.S. Watersheds. National Center for Environmental Assessment, Office of Research and Development, U.S. Environmental Protection Agency, Washington, DC. http://cfpub.epa.gov/ncea/global/recordisplay.cfm?deid=256912.

Canty, A., and B. Ripley. 2017. boot: Bootstrap R (S-Plus) Functions. https://cran.r-project.org/package=boot.

CDMSmith. 2018. Draft Remedial Investigation Report, Operable Unit 1, Black Butte Mine Superfund Site, Cottage Grove, Oregon. Prepared for U.S. Environmental Protection Agency, Region 10, Seattle, WA.

Cleveland, W.S., and S.J. Devlin. 1988. Locally-weighted regression: an approach to regression analysis by local fitting. *Journal of the American Statistical Association*. 83 (403): 596–610.

Corbitt, E.S., D.J. Jacob, C.D. Holmes, D.G, Streets, and E.M. Sunderland. 2011. Global source-receptor relationships for mercury deposition under present-day and 2050 emissions scenarios. *Environmental Science and Technology*, 45(24): 10477-10484.

Dang, F., and W.-X. Wang. 2011. Why mercury concentration increases with fish size? Biokinetic explanation. *Environmental Pollution*, 163: 192-198.

Davison, A.C., and D.V. Hinkley. 1997. *Bootstrap Methods and Their Applications*. Cambridge University Press, Cambridge. ISBN 0-521-57391-2.

Delignette-Muller, M.L., and C. Dutang. 2015. fitdistrplus: An R Package for Fitting Distributions. *Journal of Statistical Software*, 64, Issue 4. Doi:10.18637/jss.v064.i04

Domagalski, J., M.S. Majewski, C.N. Alpers, C.S. Eckley, C.A. Eagles-Smith, L. Schenk, and S. Wherry. 2016. Comparison of mercury mass loading in streams to atmospheric deposition in watersheds of Western North America: Evidence for non-atmospheric mercury sources. *Science of the Total Environment,* 568: 638-650.

Eagles-Smith, C.A., J.G. Wiener, C.S. Eckley, J.J. Willacker, D.C. Evers, M. Marvin-DiPasquale, et al. 2016a. Mercury in western North America: A synthesis of environmental contamination, fluxes, bioaccumulation, and risk to fish and wildlife. *Science of the Total Environmen*t, 568: 1213-1226. doi:10.1016/j.scitotenv.2016.05.094.

Eagles-Smith, C.A., J.T. Ackerman, J.J. Willacker, M.T. Tate, M.A. Lutz, J.A.Fleck, et al. 2016b. Spatial and temporal patterns of mercury concentrations in freshwater fish across the Western United States and Canada. *Science of the Total Environment,* 568:1171-1184.

Eckley, C.S., and B. Branfireun. 2008. Gaseous mercury emissions from urban surfaces: controls. *Applied Geochemistry,* 23: 369-383.

Eckley, C.S., C. Eagles-Smith, M.T. Tate, B. Kowalski, R. Danehy, S.L. Johnson, and D.P. Krabbenhoft. 2018. Stream mercury export in response to contemporary timber harvesting methods (Pacific coastal mountains, Oregon, USA). *Environmental Science and Technology*, 52(4):1971-1980.

Eckley, C.S., M.T. Tate, C.-J. Lin, M. Gustin, S. Dent, C. Eagles-Smith, et al. 2016. Surface-air mercury fluxes across Western North America: A synthesis of spatial trends and controlling variables. *Science of the Total Environmen*t, 568: 651-665.

Eckley, C.S., T.P.Luxton, J.L.McKernan, J.Goetz, and J.Goulet. 2015. Influence of reservoir water level fluctuations on sediment methylmercury concentrations downstream of the historical Black Butte mercury mine, OR. *Applied Geochemistry,* 61: 284-293.

Efron, B. 1987. Better bootstrap confidence intervals (with discussion). *Journal of the American Statistical Association,* 82, 171–200.

FERC. 2006. Draft Environmental Impact Statement, Clackamas River Hydroelectric Project, Clackamas County, Oregon, FERC Project No. 2195. FERC/DEIS – 0187D. Federal Energy Regulatory Commission, Office of Energy Projects, Washington, DC. Available on Google Books.

Fernandez, M. 2017. Willamette Hg Food Web Model (DRAFT). Memorandum from Mark Ferndandez to Jayshika Ramrakha, Leigh Woodruff, Alan Henning (USEPA), and Paula Calvert (Oregon DEQ), Sept. 22, 2017. Tetra Tech, Inc., Research Triangle Park, NC.

Fordham, C.L., and D.P. Reagan. 1990. Pathways analysis method for estimating water and sediment criteria at hazardous waste sites. *Environmental Toxicology and Chemistry*, 10: 949-960.

Gilbert, R.O. 1987. *Statistical Methods for Environmental Pollution Monitoring.* Van Nostrand Reinhold, New York.

Gobas, F.A.P.C. 1993. A model for predicting bioaccumulation of hydrophobic organic chemicals in aquatic food webs: Application to Lake Ontario. *Ecological Modelling*, 69: 1-17.

Grigal, D.F. 2002. Inputs and outputs of mercury from terrestrial watersheds: A review. *Environmental Reviews*, 10(1): 1-39.

Grigal, D.F., R.K. Kolka,, J.A. Fleck, and E.A. Nater. 2000. Mercury budget of an upland-peatland watershed. *Biogeochemistry*, 50: 95–109.

Hankin, D., and J. Richards. 2000. The Northern Pikeminnow Management Program. An Independent Review of Program Justification, Performance, and Cost-Effectiveness. https://www.salmonrecovery.gov/Files/APR/Section%202%20Literature%20Cited/Hankin%20and%20Richards%202000_NPMP.pdf (accessed 7/6/2018).

HDR. 2013. Treatment Technology Review and Assessment. Prepared for Association of Washington Business, Association of Washington Cities, and Washington State Association of Counties by HDR, Bellevue, Washington.

Helsel, D. 2005. *Nondetects and Data Analysis, Statistics for Censored Environmental Data*. John Wiley & Sons, Hoboken, NJ.

Helsel, D.L., and R.M. Hirsch. 2002. *Statistical Methods in Water Resources*. Chapter A3, Techniques of Water-Resources Investigations of the United States Geological Survey Book 4, Hydrologic Analysis and Interpretation. U.S. Geological Survey. http://water.usgs.gov/pubs/twri/twri4a3/.

Henny, C.J., J.L. Kaiser, H.A. Packard, R.A. Grove, and M.R. Taft. 2005. Assessing mercury exposure and effects to American dippers in headwater streams near mining sites. *Ecotoxicology*, 14:709-725.

Hinkle, S.R., K.E. Bencala, D.A. Wentz, and D.P. Krabbenhoft. 2013. Mercury and methylmercury dynamics in the hyporheic zone of an Oregon stream. *Water, Air, and Soil Pollution*, 225:1694.

Homer, C.G., J.A. Dewitz, L. Yang, S. Jin, P. Danielson, G. Xian, et al. 2015. Completion of the 2011 National Land Cover Database for the conterminous United States-Representing a decade of land cover change information. *Photogrammetric Engineering and Remote Sensing*, 81(5): 345-354.

Hope, B. 2003. A basin-specific aquatic food web biomagnification model for estimation of mercury target levels. *Environmental Toxicology and Chemistry,* 22 (10): 2525-2537.

Hope, B. 2005. Revised Estimate of a Mercury Mass Balance for the Willamette River Basin. Appendix B in Willamette Basin TMDL, Portland, OR: Oregon Dept. of Environmental Quality, B-83 - B-127. Accessed August 28, 2017. http://www.oregon.gov/deq/wq/tmdls/Pages/TMDLs-Willamette-Basin.aspx.

Hope, B. 2006. ODEQ Food Web Model. Appendix B in Willamette Basin TMDL, Portland, OR: Oregon Dept. of Environmental Quality, B-5 - B-82. Accessed August 28, 2017. http://www.oregon.gov/deq/wq/tmdls/Pages/TMDLs-Willamette-Basin.aspx.

Hsu-Kim, H., C.S. Eckley, D. Achá, X. Feng, C.C. Gilmour, S. Jonsson, and C.P.J. Mitchell. 2018. Challenges and opportunities for managing aquatic mercury pollution in altered landscapes. *Ambio,* 47(2): 141-169.

Hygelund,B.N., R.K. Ambers, and C.P. Ambers. 2001. Tracing the source of mercury contamination in the Dorena Lake watershed, western Oregon. *Environmental Geology*, 40:853-859.

Krabbenhoft, D.P. and C.L. Babiaz. 1992. The role of groundwater transport in aquatic mercury cycling. *Water Resources Research*, 28(12): 3119-3128.

MacDonald, D.F. 1908. Notes on the Bohemia Mining District, Oregon. *Contributions to Economic Geology,* 1908, Part I.

McBain and Trush, Inc. 2002. Sediment yield analysis for the Oak Grove Fork and upper mainstem Clackamas River above North Fork Reservoir. Technical report prepared for Clackamas River Hydroelectric Project Relicensing Fish and Aquatics Workgroup. McBain and Trush, Inc., Arcata, CA. (cited in FERC, 2006)

MPCA. 2007. Minnesota Statewide Mercury Total Maximum Daily Load. Report No. wq-iw4-01b. Minnesota Pollution Control Agency, St. Paul, MN.

Naughton, G.P., and D.H. Bennett. 2003. Diet composition of northern pikeminnow in the Lower Granite Reservoir system. *Northwest Science*, 77: 19-24.

NEIWPCC. 2007. Northeast Regional Mercury Total Maximum Daily Load. Connecticut, Maine, Massachusetts, New Hampshire, New York State, Rhode Island, and Vermont Departments of Environmental Protection and New England Interstate Water Pollution Control Commission.

Northwest Environmental Advocates vs. U.S. Environmental Protection Agency, State of Oregon, Oregon Water Standards Group, and The Freshwater Trust. 2017. 3:12-cv-01751-AC (US District Court for the District of Oregon, April 11).

Obrist, D., C. Pearson, J. Webster, T. Kane, C.-J. Lin, G. R. Aiken, and C.N. Alpers. 2016. A synthesis of terrestrial mercury in the western United States: Spatial distribution defined by land cover and plant productivity. *Science of the Total Environment,* 568: 522-535.

ODEQ (Oregon Dept. of Environmental Quality). 2006. Willamette Basin Mercury TMDL. Chapter 3 in Willamette Basin TMDL, Portland, OR: Oregon Dept. of Environmental Quality. Accessed August 28, 2017. http://www.oregon.gov/deq/wq/tmdls/Pages/TMDLs-Willamette-Basin.aspx.

O'Leary, M. 2004. Mercury Mines along the Oak Grove Fork of the Clackamas River. Paper HC 441: Willamette River Health, Clark Honors College, University of Oregon.

Oregon Health Authority. 2013. Public Health Assessment, Black Butte Mine, Cottage Grove, Oregon, EPA Facility ID: OR0000515759. Environmental Health Assessment Program. http://www.oregon.gov/oha/PH/HEALTHYENVIRONMENTS/TRACKINGASSESSMENT/ENVIRONMENTALHEALTHASSESSMENT/Documents/Black%20Butte%20Mine_PHA-Final_03-13-2013.pdf.

Park, J.-G., and L.R. Curtis. 1997. Mercury distribution in sediments and bioaccumulation by fish in two Oregon reservoirs: Point-source and nonpoint-source impacted systems. *Archives of Environmental Contamination and Toxicology,* 33: 423-429.

Portland Environmental Services. 2017. Annual CSO and CMOM Report, FY 2017, Required by NPDES Permit #101505. City of Portland Bureau of Environmental Services, Portland, OR. https://www.portlandoregon.gov/bes/31002.

Pouillot, R., and M.-L. Delignette-Muller. 2010. Evaluating Variability and Uncertainty in Microbial Quantitative Risk Assessment using two R packages. *International Journal of Food Microbiology,* 142(3):330-40.

R Core Team. 2017. R: A Language and Environment for Statistical Computing. R Foundation for Statistical Computing, Vienna, Austria. https://www.R-project.org/.

Riva-Murray, K., P.M. Bradley, B.C. Scudder Eikenberry, C.D. Knightes, C.A. Journey, M.E. Brigham, and D.T. Button. 2013. Optimizing stream water mercury sampling for calculation of fish bioaccumulation factors. *Environmental Science & Technology,* 47(11): 5904–5912.

Runkel, R.L., Crawford, C.G., and Cohn, T.A. 2004. Load Estimator (LOADEST): A FORTRAN Program for Estimating Constituent Loads in Streams and Rivers. U.S. Geological Survey Techniques and Methods Book 4, Chapter A5.

Schmidt, M. 2018. Willamette River Basin Mercury Data Summary (DRAFT). Memorandum from Michelle Schmidt to Jayshika Ramrakha, Leigh Woodruff, Alan Henning (USEPA), and Paula Calvert (ODEQ), March 6, 2018. Tetra Tech, Inc., Research Triangle Park, NC.

Seigneur, C., K. Vijayraghavan, K. Lohman, P. Karamchandani, and C. Scott. 2004. Global source attribution for mercury deposition in the United States. *Environmental Science and Technology*, 38: 555-569.

Smith, D.B., W.F. Cannon, L.G. Woodruff, F. Solano, J.E. Kilburn, and D.L. Fey. 2013. Geochemical and Mineralogical Data for Soils of the Conterminous United States. U.S. Geological Survey Data Series 801.

Tetra Tech. 2008. Quality Assurance Project Plan for Watershed Modeling to Evaluate Potential Impacts of Climate and Land Use Change on the Hydrology and Water Quality of Major U.S. Drainage Basins. Contract No. EP-C-05-61, Task Order Control No. STREAMS-83. QAPP No. 178. Prepared for U.S. Environmental Protection Agency, Office of Research and Development, Global Change Research Program by Tetra Tech, Inc., Fairfax, VA.

Tetra Tech. 2017. Modeling Quality Assurance Project Plan for Mercury TMDL Development for Willamette River Basin (Oregon). Contract EP-C-12-055, Task 10; QAPP 491. Prepared for USEPA Region 10, Seattle, WA by Tetra Tech, Inc., Research Triangle Park, NC.

Trudel, M., and J.B. Rasmussen. 1997. Modeling the elimination of mercury by fish. *Environmental Science and Technology*, 31: 1716-1722.

Trudel, M., and J.B. Rasmussen. 2006. Bionergetics and mercury dynamics in fish, a modeling perspective. *Canadian Journal of Fisheries and Aquatic Science,* 63: 1890-1902*.*

Ullrich, S.M., T.W. Tanton, and S.A. Abdrashitova. 2001. Mercury in the aquatic environment: A review of factors affecting methylation. *Critical Reviews in Environmental Science and Technology*, 31(3): 241-293.

USEPA (United States Environmental Protection Agency). 1991. Guidance for Water Quality-Based Decisions: The TMDL Process. EPA 440/4-91-001. U.S. Environmental Protection Agency, Office of Water, Washington, DC.

USEPA (United States Environmental Protection Agency). 1997. Mercury Study Report to Congress, Vol. 3: Fate and Transport of Mercury in the Environment. EPA-452-R/97-005. Washington, DC: U.S. Environmental Protection Agency, Office of Air Quality Planning and Standards, and Office of Research and Development.

USEPA (United States Environmental Protection Agency). 2001a. Methyl mercury Fact Sheet. EPA-823-F-01-001

USEPA (United States Environmental Protection Agency). 2001b. Water Quality Criterion for the Protection of Human Health: Methyl mercury. EPA-823-R-01-001.

USEPA (United States Environmental Protection Agency). 2005. Technical Support Document for the Final Clean Air Mercury Rule – Air Quality Modeling. US Environmental Protection Agency, Office of Air Quality Planning and Standards, Research Triangle Park, NC. March 2005. http://www.epa.gov/ttn/atw/utility/agm_oar-2002-0056-6130.pdf

USEPA (United States Environmental Protection Agency) Region 3. 2006. IDL- MDL- PQL: What the "L" is Going On? What Does All This Alphabet Soup Really Mean? https://www.epa.gov/sites/production/files/2015-06/documents/whatthel.pdf.

USEPA (United States Environmental Protection Agency). 2008. Final Removal Action Report for Black Butte Mine, Cottage Grove, Oregon. U.S. Environmental Protection Agency Region 10, Seattle, Washington, July 20, 2008.

USEPA (United States Environmental Protection Agency). 2010. Guidance for Implementing the January 2001 Methylmercury Water Quality Criterion. Office of Science and Technology, U.S. Environmental Protection Agency, Washington, DC.

USEPA (United States Environmental Protection Agency). 2012. Optimization Review Black Butte Mine Superfund Site, Lane County, Oregon. EPA-542-R-12-003. U.S. Environmental Protection Agency, Office of Superfund Remediation and Technology Innovation, July 13, 2012.

USEPA (United States Environmental Protection Agency). 2018. Fact Sheet: EPA Cleans up Furnace Creek Area at Black Butte. US Environmental Protection Agency. November 2018. https://semspub.epa.gov/work/10/100125983.pdf.

Watras, C.J., N.S. Bloom, R.J.M. Hudson, S. Gherini, R, Munson, S.A. Claas, et al. 1994. Sources and fates of mercury and methylmercury in Wisconsin lakes. In *Mercury Pollution: Integration and Synthesis* (C.J. Watras and J.W. Huckabee, eds.) Lewis Publishers, Chelsea, MI.

Willacker, J.J., C.A. Eagles-Smith, M.A. Lutz, M.T. Tate, J.M. Lepak, and J.T. Ackerman. 2016. Reservoirs and water management influence fish mercury concentrations in the western United States and Canada. *Science of the Total Environment,* 568: 739-748.

Xian, G., C. Homer, J. Dewitz, J. Fry, N. Hossain, and J. Wickham. 2011. The change of impervious surface area between 2001 and 2006 in the conterminous United States. *Photogrammetric Engineering and Remote Sensing*, 77(8): 758-762.

Zimmerman, M.P. 1999. Food habits of smallmouth bass, walleyes, and northern pikeminnow in the Lower Columbia River Basin during outmigration of juvenile andadromous salmonids. *Transactions of the American Fisheries Society*, 128: 1036-1054.